Transient Response Analysis and Design of Current-Controlled Grid-Tied Converters

Author: *Ana Vidal González*

Supervisors: *Jesús Doval Gandoy & Francisco D. Freijedo Fernández*

Applied Power Electronics Research Group,
University of Vigo

15th May 2015

Dissertation submitted for the degree of Doctor of Philosophy at the University of Vigo
"International Doctor Mention"

APET Applied Power Electronics Technology Research Group

Universidade Vigo

Outline

APET Universida de Vigo

Outline

1. Introduction
   - Background
   - Objectives
   - Review of Previous Research
2. Equivalent Loss Resistance Estimation of Grid-Tied Converters for Current Control Analysis and Design
3. A Method for Identification of the Equivalent Inductance and Resistance in the Plant Model of Current-Controlled Grid-Tied Converters
4. Assessment and Optimization of the Transient Response of Proportional-Resonant Current Controllers for Distributed Power Generation Systems
5. Transient Response Evaluation of Stationary-Frame Resonant Current Controllers for Grid-Connected Applications
6. Conclusions and Future Research

APET
Universidade Vigo

Current Electric Grid

- ✓ Flexibility
- ✓ Bidirectionality
- × Problems to guarantee stability ➡ Grid codes

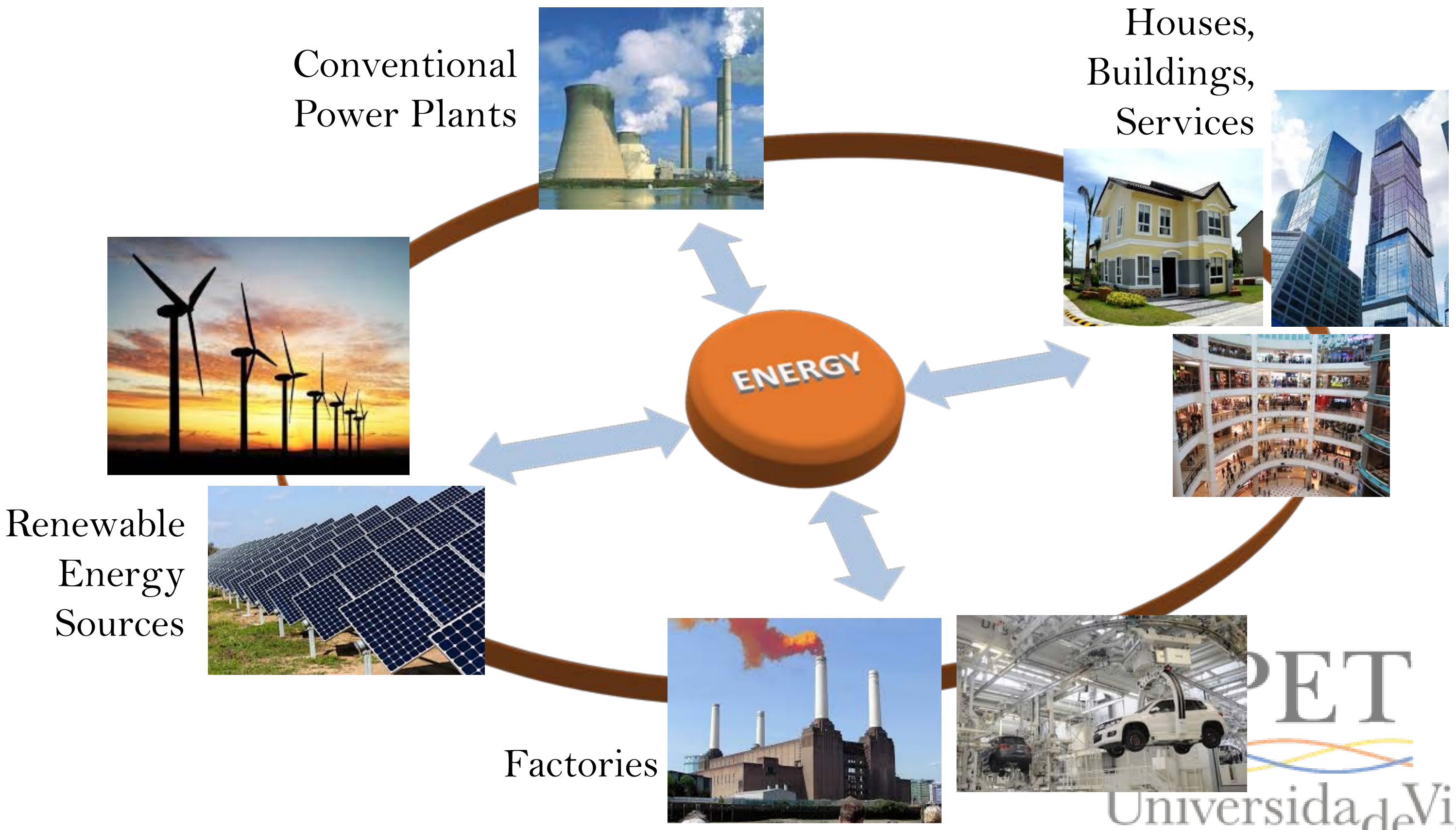

Pag.
2

Current Electric Grid

- ✓ Flexibility
- ✓ Bidirectionality
- × Problems to guarantee stability ➡ Grid codes

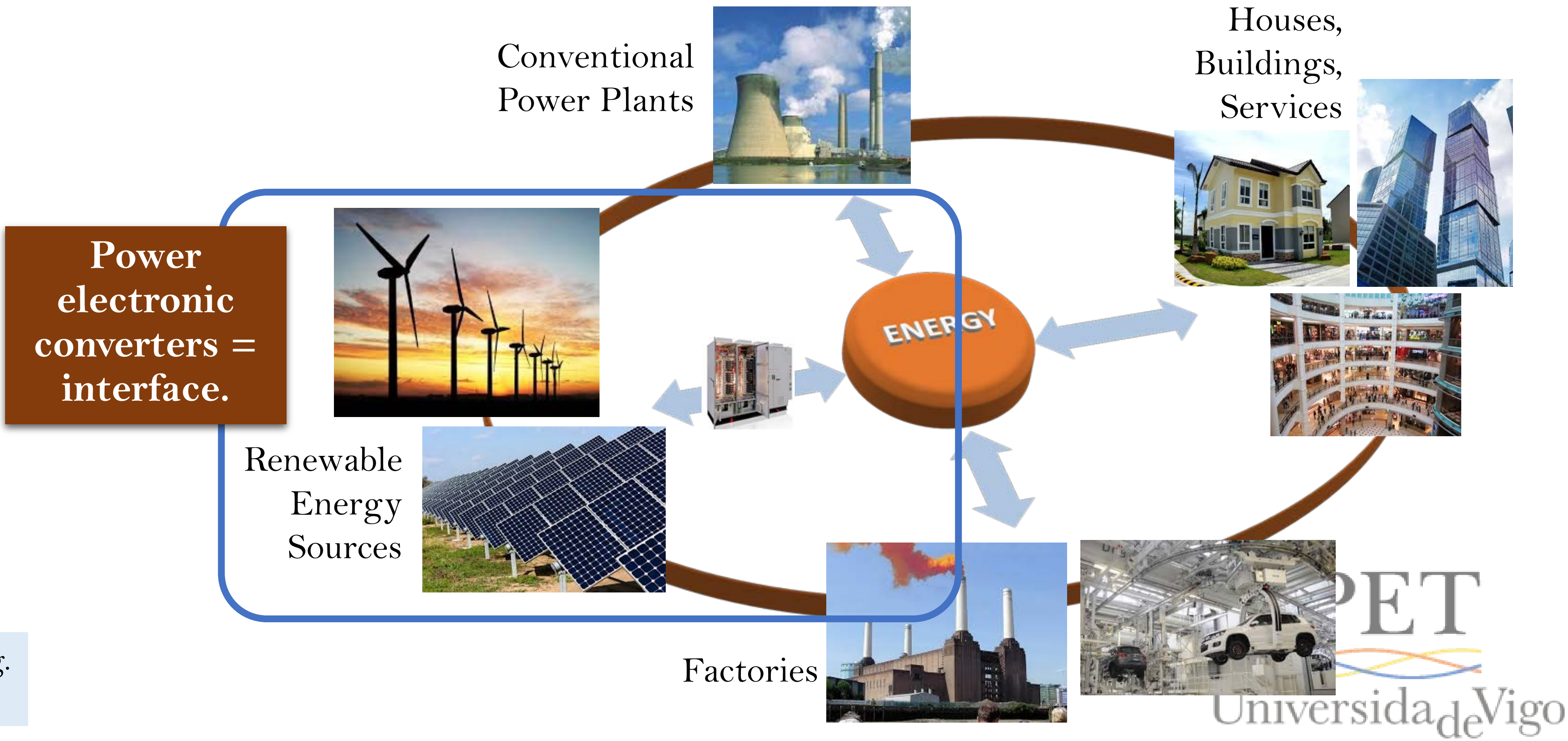

Pag. 2

Grid-Side VSC

- Tasks
  - Maintaining the dc link constant
  - Interaction with the grid (*P* & *Q*)
- Implementation
  - Modulation stage
  - Multiple cascaded loops of linear controllers
    - Outer power/ dc-link voltage controllers
    - Inner current controllers
      - Appropriate power factor
      - Harmonic rejection
      - Disturbance rejection (faults)
      - Fast transient response

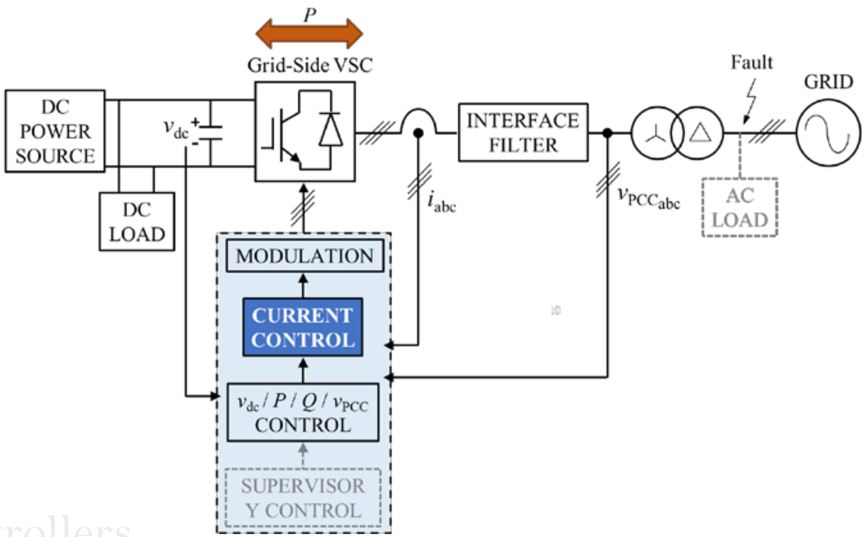

Accurate tuning of the regulators

Grid-Side VSC

- Tasks
  - Maintaining the dc link constant
  - Interaction with the grid (P & Q)
- Implementation
  - Modulation stage
  - Multiple cascaded loops of linear controllers
    - Outer power/ dc-link voltage controllers
    - **Inner current controllers**
      - **Appropriate power factor**
      - **Harmonic rejection**
      - **Disturbance rejection (faults)**
      - **Fast transient response**

Accurate tuning of the regulators

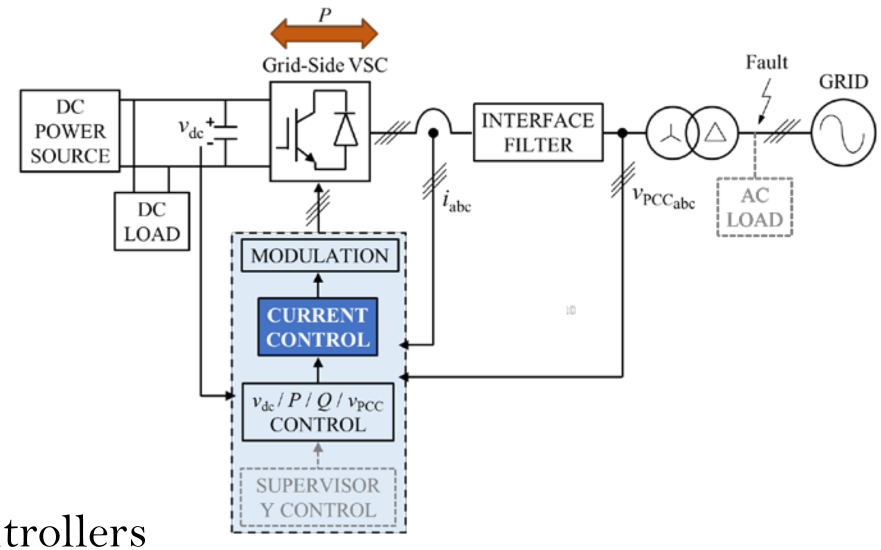

Pag. 2-4

Main Objective of this Thesis

- A thorough analysis and design of the current control closed loop, oriented to an accurate tuning of the regulators is developed.

Precise plant model.

Accurate plant parameters.

Appropriate controller structure.

Rigorous regulator tuning.

Pag. 1, 4

APET Universidade Vigo

Main Objective of this Thesis

- A thorough analysis and design of the current control closed loop, oriented to an accurate tuning of the regulators is developed.

Precise plant model.

Chapters 2 & 3

Accurate plant parameters.

Appropriate controller structure.

Chapters 4 & 5

Rigorous regulator tuning.

Chapter 1: Introduction

APET
Universidade Vigo

Plant Model for Current-Controlled Grid-Tied VSCs

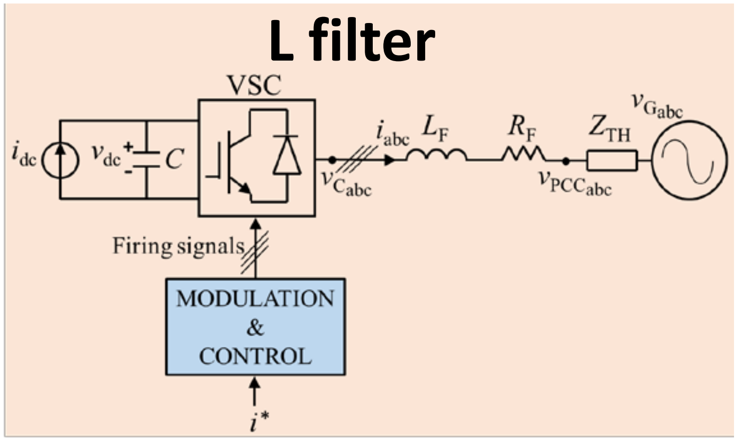

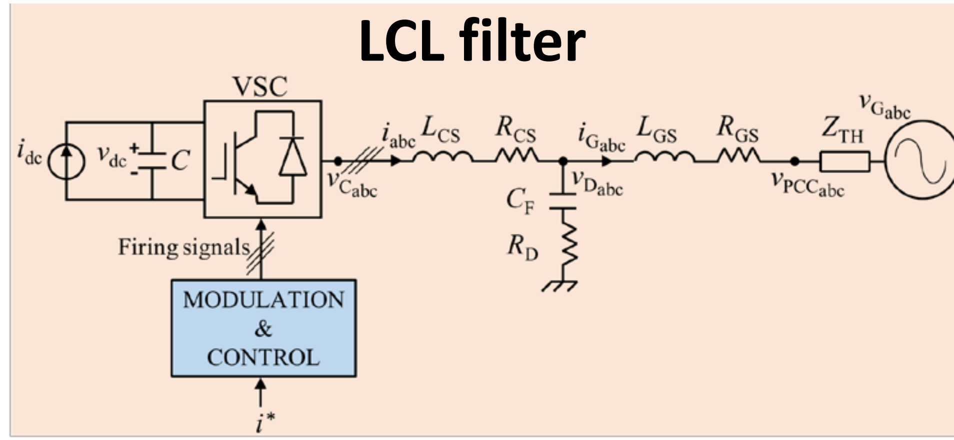

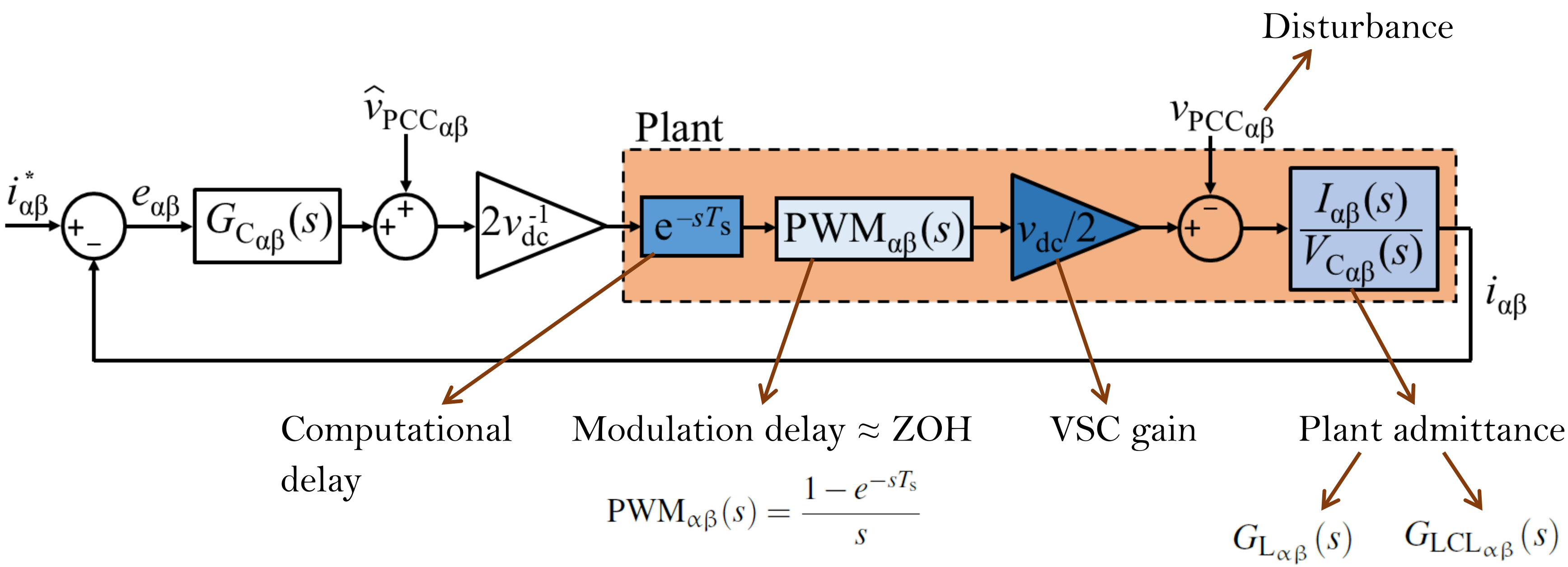

$$\mathrm{PWM}_{\alpha\beta}(s) = \frac{1-e^{-sT_s}}{s}$$

Pag. 5-11

Plant Admittance

L filter

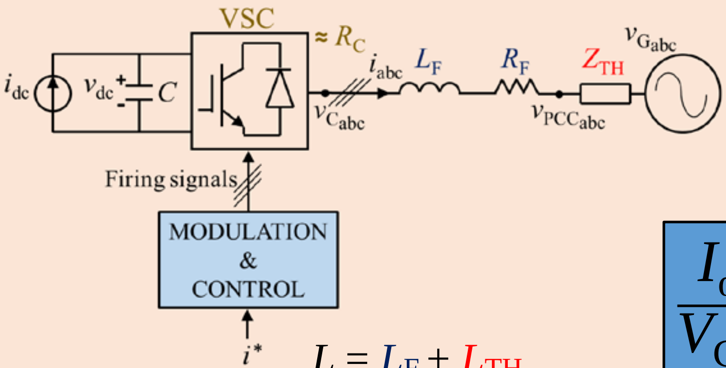

$L = L_F + L_{TH}$

$R = R_F + R_{TH} + R_C$

$$G_{L_{\alpha\beta}}(s) = \frac{I_{\alpha\beta}(s)}{V_{C_{\alpha\beta}}(s)} = \frac{1}{sL+R}$$

$$\frac{I_{\alpha\beta}(s)}{V_{C\alpha\beta}(s)}$$

LCL filter

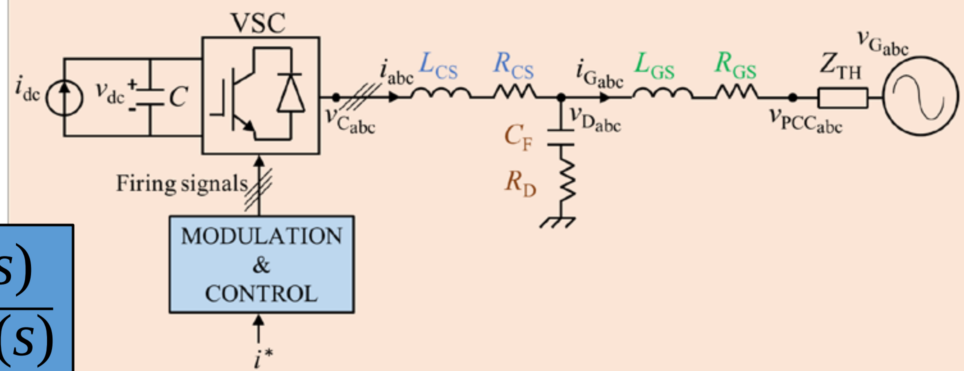

$$G_{LCL_{\alpha\beta}}(s) = \frac{I_{\alpha\beta}(s)}{V_{C_{\alpha\beta}}(s)} = \frac{Y_{CS}(s)\,[1+Y_{GS}(s)\,Z_D(s)]}{1+Y_{CS}(s)\,Z_D(s)+Y_{GS}(s)\,Z_D(s)}$$

Pag. 5-11

APET Universida de Vigo

Equivalence Between L and LCL Filters

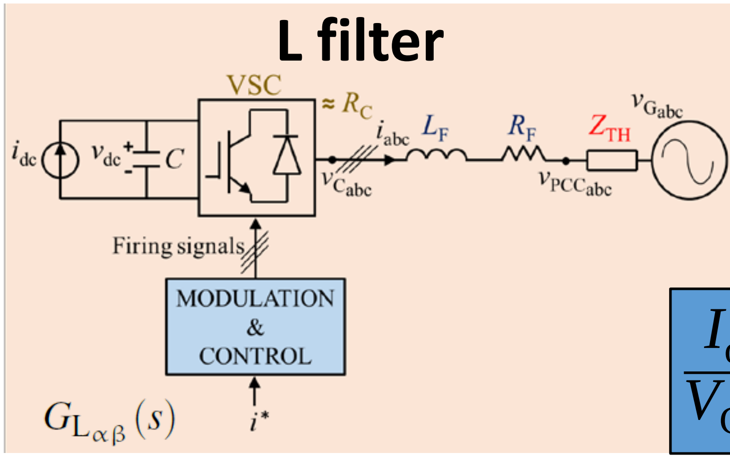

$$\frac{I_{\alpha\beta}(s)}{V_{C\alpha\beta}(s)}$$

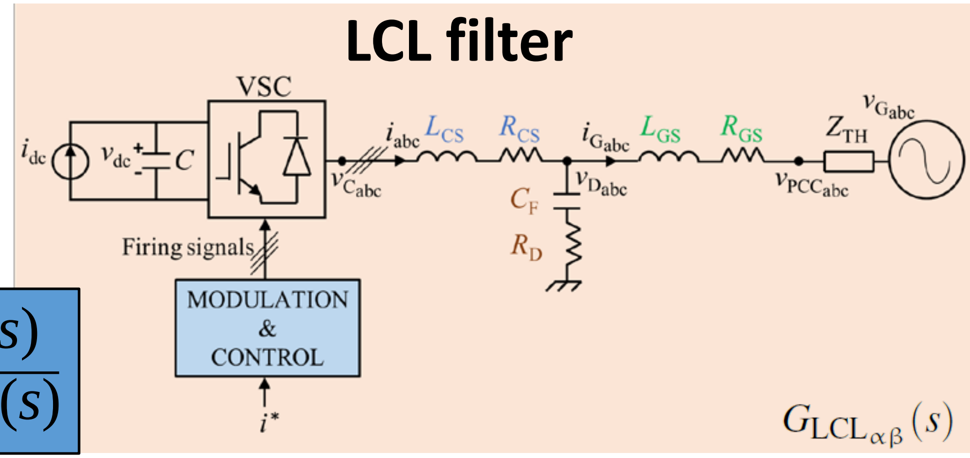

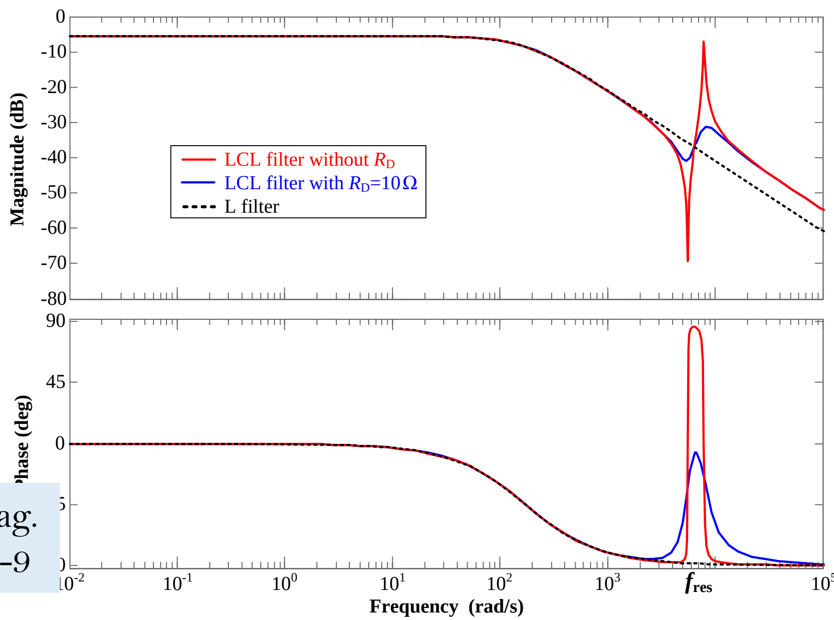

If $L_F = L_{CS} + L_{GS}$ and $R_F = R_{CS} + R_{GS}$

LCL filters behave as L ones at frequencies lower than approx. f_{res}.

$$G_{L_{\alpha\beta}}(s) \approx G_{LCL_{\alpha\beta}}(s)$$

Pag. 7-9

APET Universida de Vigo

Plant Model for Current-Controlled Grid-Tied VSCs

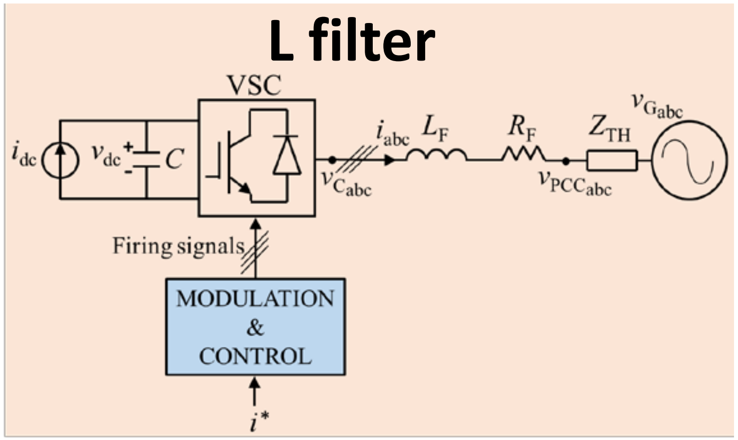

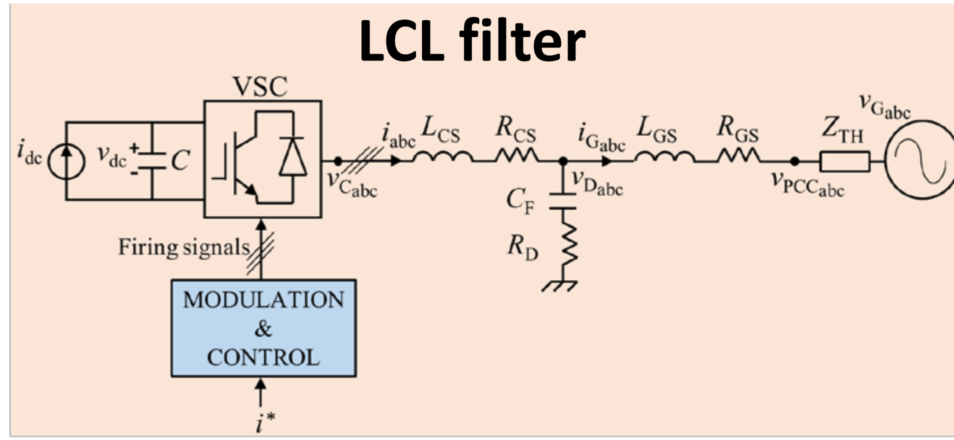

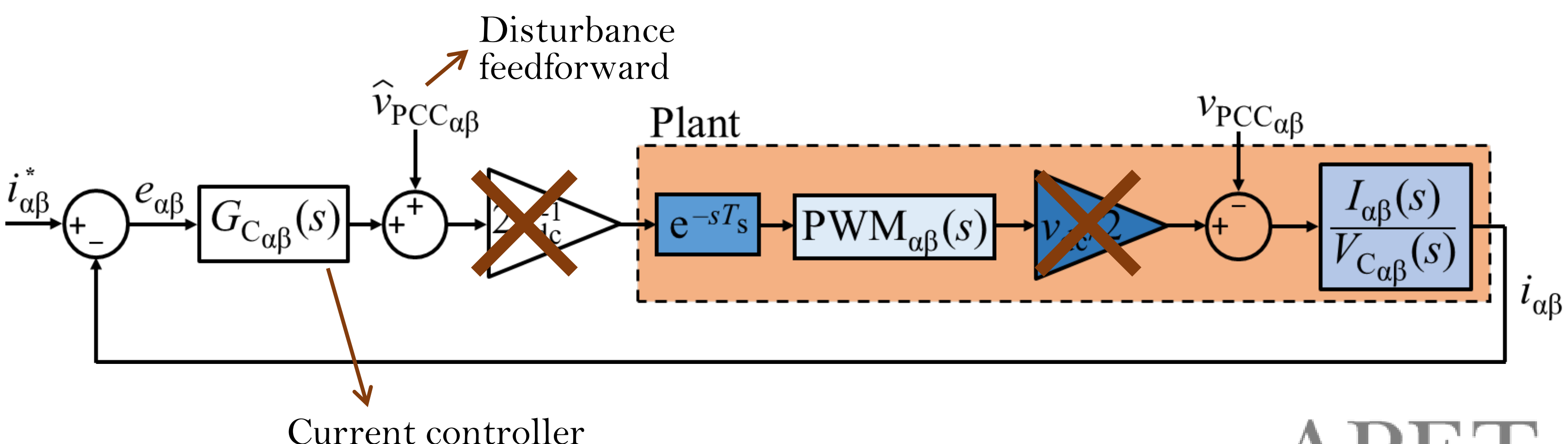

Pag.
5-11

Parameter Identification

- **Precise knowledge** of L and R is **essential** to guarantee the **performance** of the **current loop** (particularly when **specifications** are stablished in terms of **transient response**).
- Parameter uncertainties.
  - Non negligible impedance at the PCC.
  - Variation in the value of the different components with the working conditions.
    - Particularly significant in the parameters employed to model the losses (e.g., R_C).
  - Errors in the measurements.

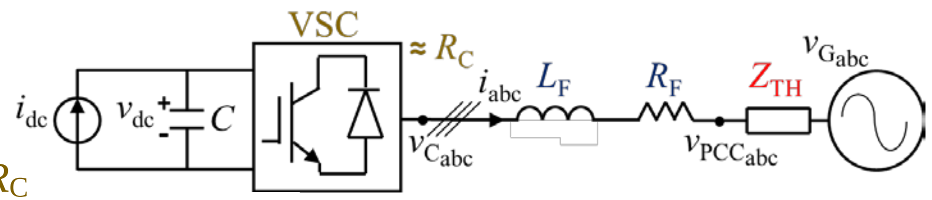

$L = L_F + L_{TH}$

$R = R_F + R_{TH} + R_C$

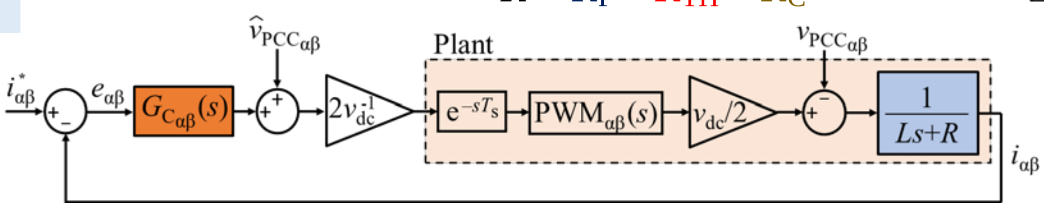

Pag. 11

Parameter Identification

- **Precise knowledge** of ***L*** and ***R*** is **essential** to guarantee the **performance** of the **current loop** (particularly when **specifications** are stablished in terms of **transient response**).
- **Parameter uncertainties**.
  - **Non negligible impedance at the PCC**.
  - **Variation** in the value of the different components **with the working conditions.**
    - Particularly significant in the **parameters** employed to **model the losses** (e.g., R_C).
  - Errors in the measurements.

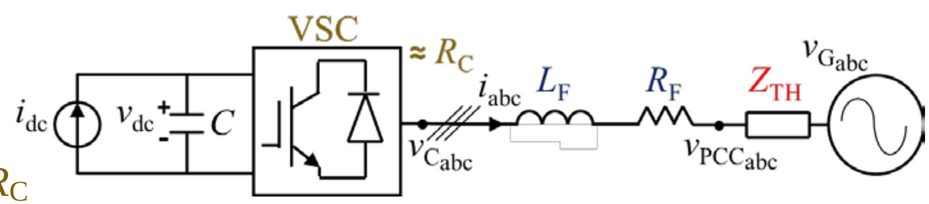

$L = L_F + L_{TH}$

$R = R_F + R_{TH} + R_C$

Pag.
11

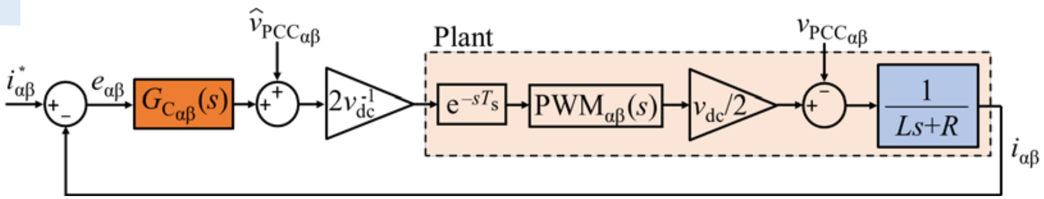

APET
Universida de Vigo

Parameter Identification Methods

They can be classified attending to different criteria.

- How they are executed:
  - **online**
  - **offline**

MRAS

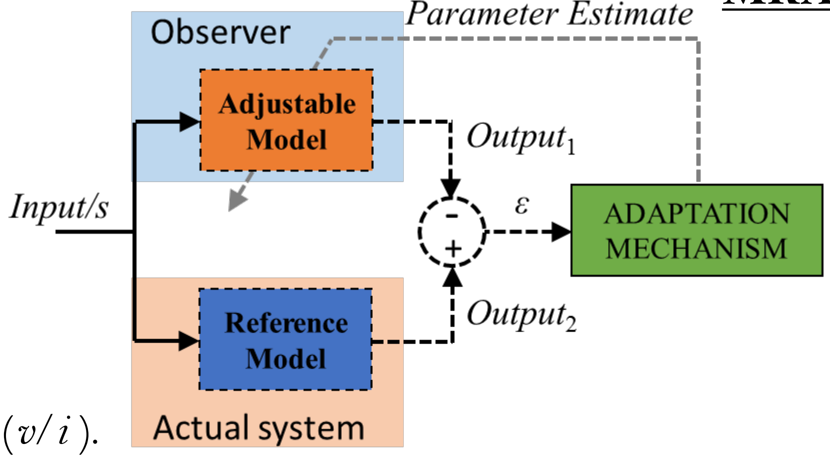

- How they calculate the impedance:
  - **directly** from the **measurements** (v/i).
  - **iteratively**, by means of an **adaptive observer**.
    - Iterative minimization of the error (RLS, GPA, EKF, custom-made options….)
    - E.g., recursive closed-loop methods such as MRAS-based solutions.
- Whether they need a source of excitation:
  - NO → **passive**
  - YES → **active** (signal injection, change in the operating conditions…)

Pag. 11-14

Parameter Identification Methods

The following observations can be drawn from the available bibliography.

- There is **no previous technique aimed at the converter equivalent loss resistance estimation**.
- **None** of these methods is **oriented to** exactly the same objective as the one sought in this thesis: **an accurate analysis and design of current loop transient response in grid-tied VSCs**.

Pag.
12-14

APET
Universidade Vigo

PI Controllers in SRF

- One of the most extended solutions.

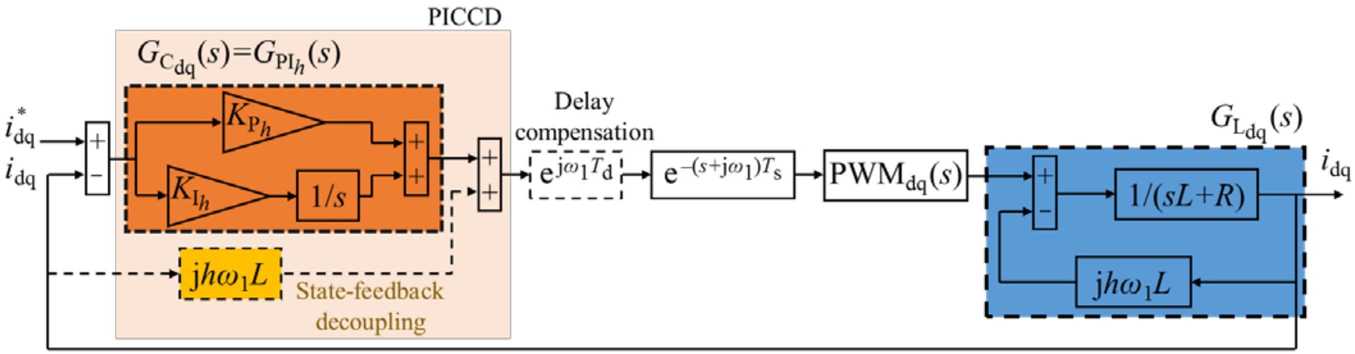

Classical PI controller with cross-coupling decoupling (PICCD)

Tuned according to **IMC**

Pag. 14-18

PI Controllers in SRF

- One of the most extended solutions.

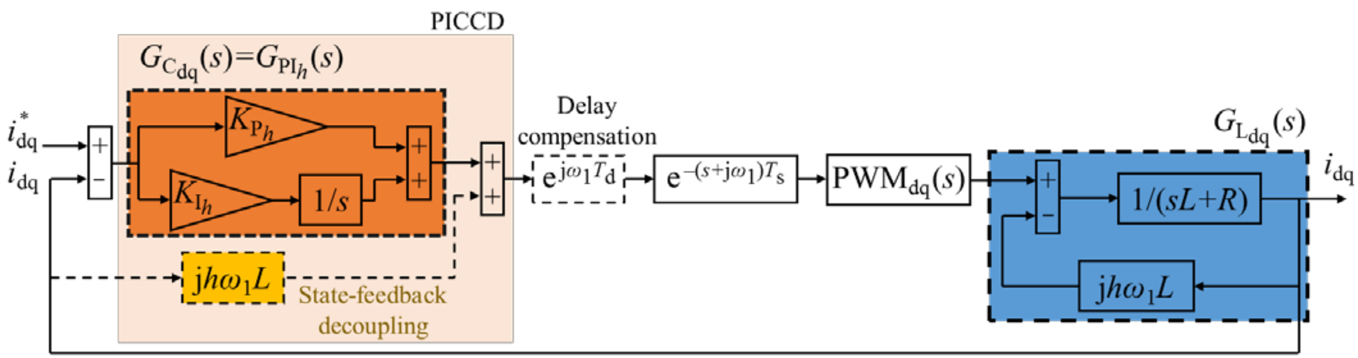

Classical PI controller with cross-coupling decoupling (PICCD)

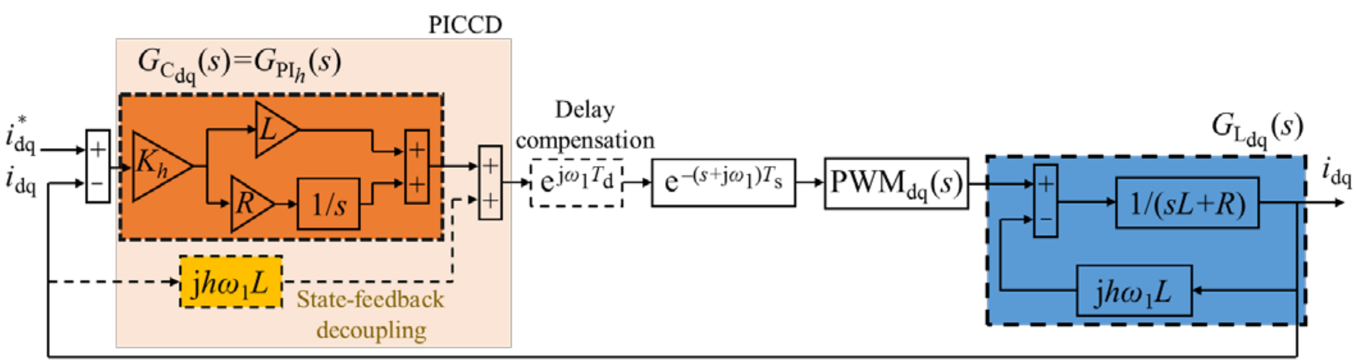

Tuned according to **IMC**

Pag. 14-18

APET Universida de Vigo

Resonant Controllers in Stationary Frame (Vs PI Controllers in SRF)

- ✓ Open-loop **infinite gain** at the **resonant frequency** → ac currents can be regulated **in stationary frame** with **zero steady-state error**,
  - ✓ **reducing the computational burden** (Park transformations can be avoided),
  - ✓ showing **lower sensitiveness to errors and noise in synchronization**.
- ✓ Ability to **regulate positive- and negative-sequence components of the same harmonic order** ← equivalence to two identical PI regulators implemented in two SRFs simultaneously (one positive and one negative).
- × **Complex schemes for distortion-free saturation.**
- × Great **sensitiveness** of their **resonant frequency** to **the discretization technique.**

APET
Universida de Vigo

Resonant Controllers in Stationary Frame (Vs PI Controllers in SRF)

- ✓ Open-loop **infinite gain** at the **resonant frequency** → ac currents can be regulated **in stationary frame** with **zero steady-state error**,
  - ✓ **reducing the computational burden** (Park transformations can be avoided),
  - ✓ showing **lower sensitiveness to errors and noise in synchronization**.

- ✓ Ability to **regulate positive- and negative-sequence components of the same harmonic order** ← equivalence to two identical PI regulators implemented in two SRFs simultaneously (one positive and one negative).

- × **Complex schemes for distortion-free saturation**.

- × Great **sensitiveness** of their **resonant frequency** to **the discretization technique.**

PR Controllers

$$G_{PR}(s) = K_{P_T} + \sum_{h=1,5,7\ldots} K_{I_h} \frac{s}{s^2 + h^2\omega_1^2}$$

Proportional gain:

- Influences: phase margin and $f_{crossover}$.
- Selection: well-stablished rules.

Integral gain:

- Influences: bandwidth around hf_1.
- Selection: guidelines (selectivity Vs fast dynamics).
  - × Qualitative guidelines.
  - × Ignoring the delay.
  - × Not aimed at the optimization of the disturbance rejection transient response.

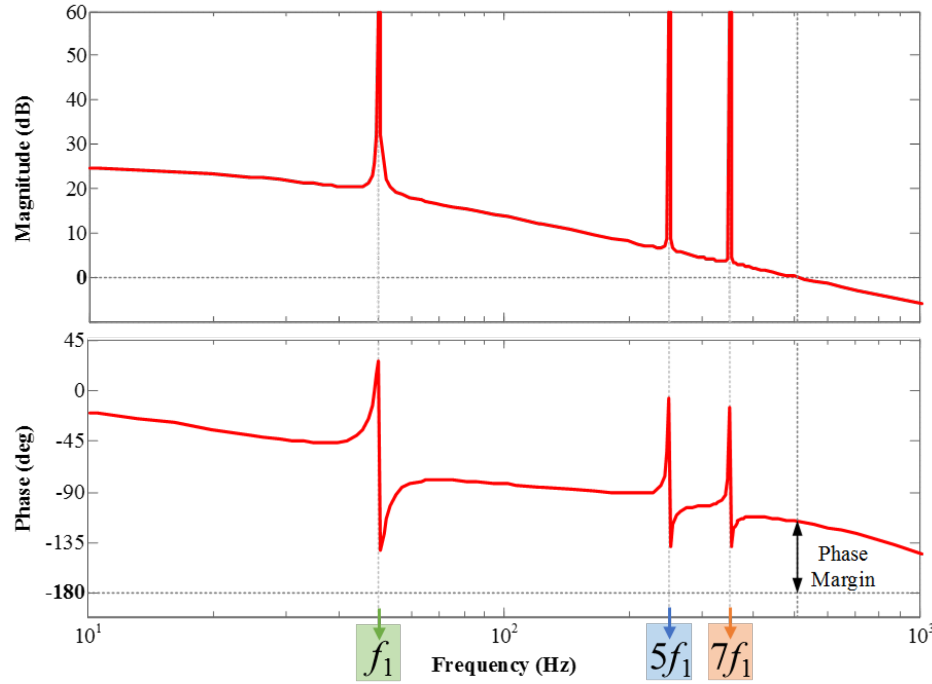

Pag.
18-21

PR Controllers

Proportional gain:
- Influences: phase margin and $f_{crossover.}$
- Selection: well-stablished rules.

Integral gain:
- Influences: bandwidth around hf_1.
- Selection: guidelines (selectivity Vs fast dynamics).

  - × Qualitative guidelines.
  - × Ignoring the delay.
  - × Not aimed at the optimization of the disturbance rejection transient response.

$$G_{PR}(s) = K_{P_T} + \sum_{h=1,5,7\ldots} K_{I_h} \frac{s}{s^2 + h^2\omega_1^2}$$

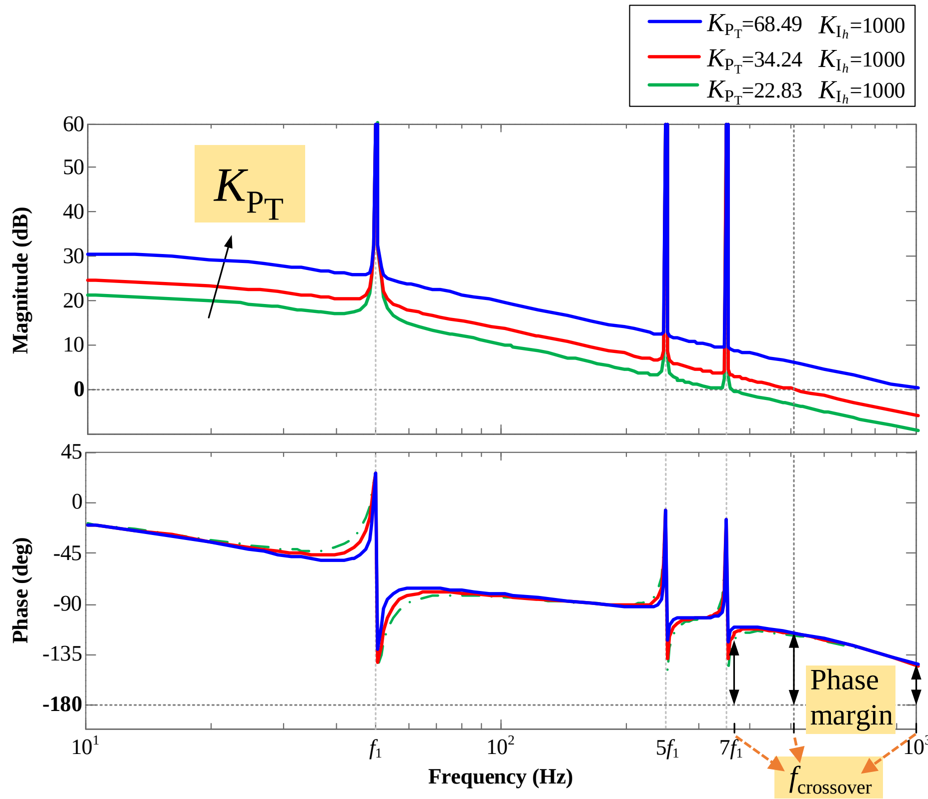

Pag. 18-21

PR Controllers

$$G_{PR}(s) = K_{P_T} + \sum_{h=1,5,7\ldots} K_{I_h} \frac{s}{s^2 + h^2\omega_1^2}$$

Proportional gain:
- Influences: phase margin and $f_{crossover.}$
- Selection: well-stablished rules.

Integral gain:
- Influences: bandwidth around $hf_{1.}$
- Selection: guidelines (**selectivity Vs fast dynamics**).

  - × **Qualitative guidelines.**
  - × **Ignoring the delay.**
  - × **Not aimed at** the **optimization** of the **disturbance rejection** transient response.

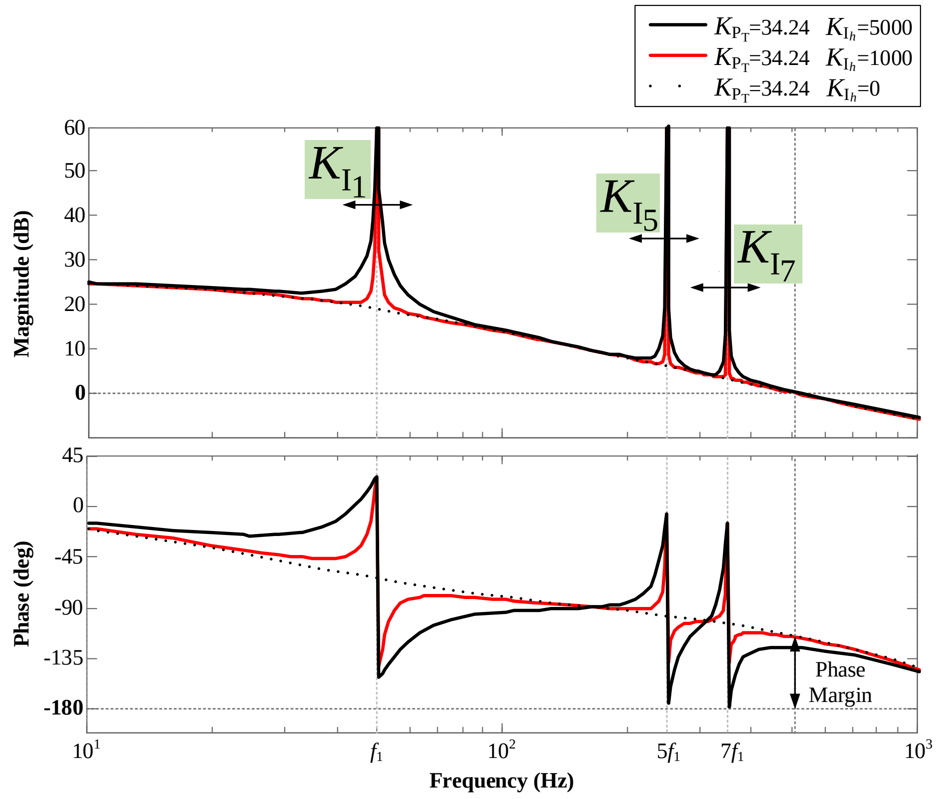

Pag. 18-21

Universidade de Vigo

VPI Controllers

$$G_{\mathrm{VPI}_h}(s) = \frac{s^2 K_{\mathrm{P}h} + s K_{\mathrm{I}h}}{s^2 + h^2\omega_1^2}$$

IMC

$$G_{\mathrm{VPI}_h}(s) = K_h \frac{s(sL+R)}{s^2 + h^2\omega_1^2}$$

K_h:

- Influences: bandwidth around hf_1.
- Selection: guidelines (selectivity Vs fast dynamics).

× Qualitative guidelines.
× Ignoring the delay.
× Not aimed at the optimization of the disturbance rejection transient response.

Pag. 21-24

APET Universida de Vigo

VPI Controllers

$$G_{\mathrm{VPI}_h}(s) = \frac{s^2 K_{\mathrm{P}h} + s K_{\mathrm{I}h}}{s^2 + h^2\omega_1^2} \quad \xrightarrow{\text{IMC}} \quad G_{\mathrm{VPI}_h}(s) = K_h \frac{s(sL+R)}{s^2 + h^2\omega_1^2}$$

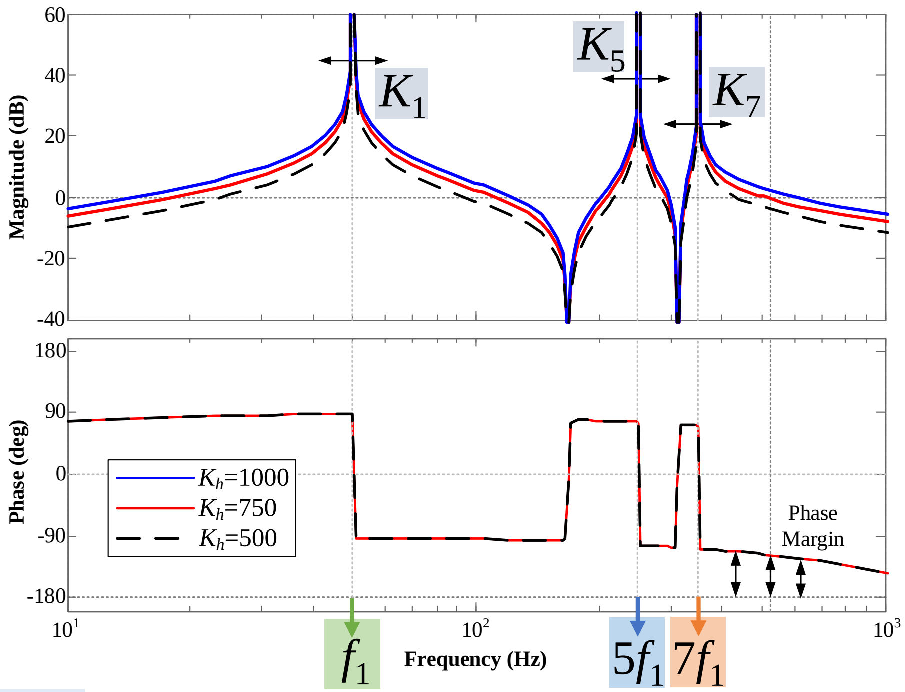

***K_h*:**

- Influences: bandwidth around hf_1.
- Selection: guidelines (**selectivity Vs fast dynamics**).

× **Qualitative guidelines.**
× **Ignoring the delay**.
× **Not aimed at** the **optimization** of the **disturbance rejection** transient response.

Pag. 21-24

APET Universida de Vigo

Main Objective of this Thesis

- A thorough analysis and design of the current control closed loop, oriented to a precise tuning of the regulators is developed.

Precise plant model.

Accurate plant parameters.

Appropriate controller structure.

Rigorous regulator tuning.

Chapters 2 & 3

- Plant **parameter identification methods** oriented to transient response optimization.

Chapters 4 & 5

- Accurate **tuning methods** for resonant controllers oriented to transient response optimization (command tracking and disturbance rejection).
- **Comparison** between **PR** and **VPI** controllers (transient response and THD).

Outline

Open-Loop Transfer Function

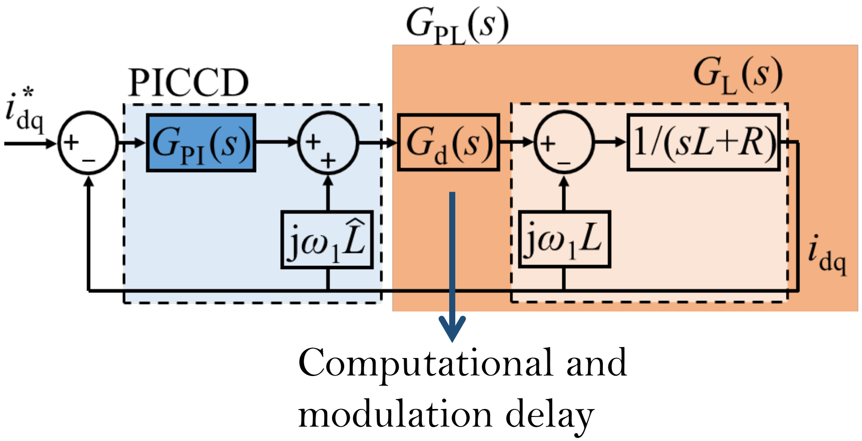

Neglecting $G_d(s)$ & assuming $\hat{L}=L$

$$G_{OL}(s)=G_{PI}(s)\frac{1}{sL+R}=\frac{sK_P+K_I}{s}\frac{1}{sL+R}$$

where $\begin{cases} R=R_F+R_C \\ L=L_F \end{cases}$

IMC
$K_P/K_I=\hat{L}/\hat{R}$
$K_P=K\hat{L}$

If $\begin{cases} \hat{R}=R \\ \& \\ \hat{L}=L \end{cases}$ ⇒ $G'_{OL}(s)=K\frac{1}{s}$

If $\begin{cases} \hat{R}\neq R \\ \& \\ \hat{L}=L \end{cases}$ ⇒ $G''_{OL}(s)=K\frac{sL+\hat{R}}{s}\frac{1}{sL+R}$

Pag.
29-34

Open-Loop Transfer Function

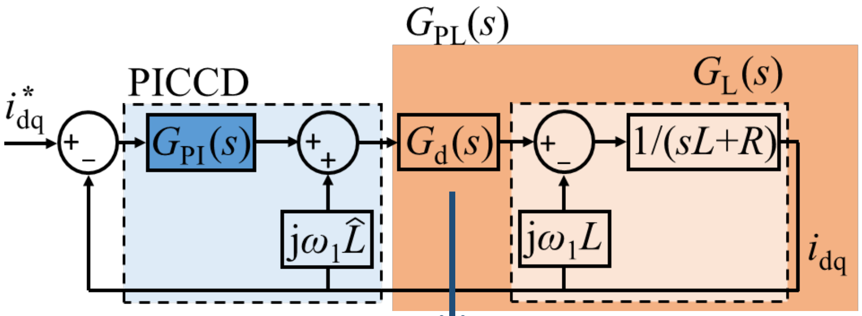

Neglecting $G_d(s)$ & assuming $\hat{L} = L$

$$G_{OL}(s) = G_{PI}(s)\frac{1}{sL+R} = \frac{sK_P + K_I}{s}\frac{1}{sL+R}$$

where $\begin{cases} R = R_F + R_C \\ L = L_F \end{cases}$

IMC

$K_P/K_I = \hat{L}/\hat{R}$

$K_P = K\hat{L}$

If $\begin{cases} \hat{R} = R \\ \& \\ \hat{L} = L \end{cases}$ $\Rightarrow$ $G'_{OL}(s) = K\frac{1}{s}$

If $\begin{cases} \hat{R} \neq R \\ \& \\ \hat{L} = L \end{cases}$ $\Rightarrow$ $G''_{OL}(s) = K\frac{sL+\hat{R}}{s}\frac{1}{sL+R}$

Pag. 29-34

Open-Loop Transfer Function

Including $G_d(s)$

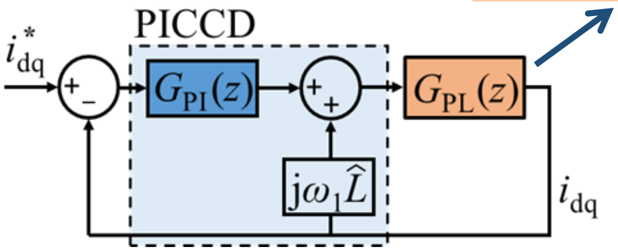

Correct identification of R

If $\begin{cases} \hat{R} = R \\ \& \\ \hat{L} = L \end{cases}$

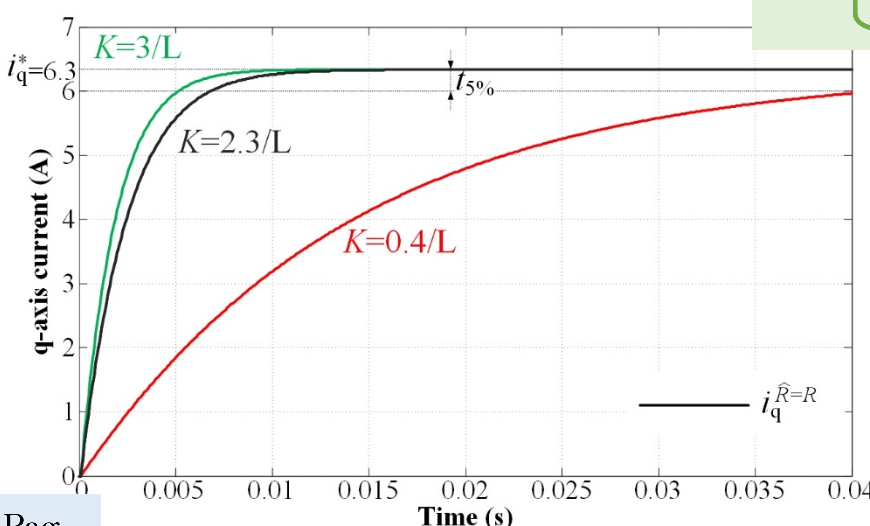

Neglecting $G_d(s)$ & assuming $\hat{L} = L$

$$G_{OL}(s) = G_{PI}(s)\frac{1}{sL+R} = \frac{sK_P + K_I}{s}\frac{1}{sL+R}$$

where $\begin{cases} R = R_F + R_C \\ L = L_F \end{cases}$

IMC

$K_P/K_I = \hat{L}/\hat{R}$

$K_P = K\hat{L}$

$$G'_{OL}(s) = K\frac{1}{s}$$

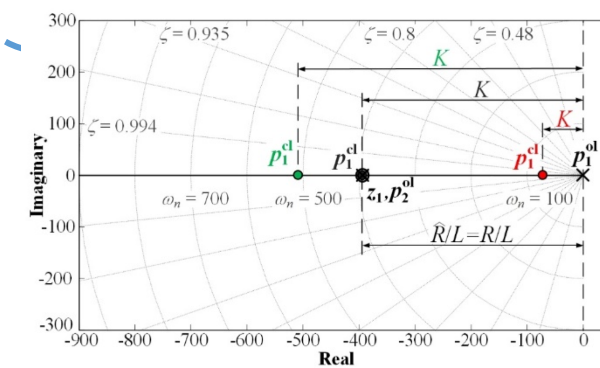

Pag. 29-34

Open-Loop Transfer Function

Including $G_d(s)$

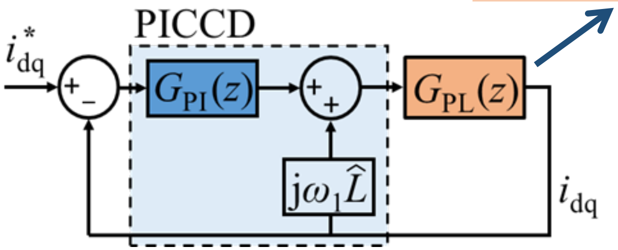

Underestimation of R

If $\begin{cases} \hat{R} = R_F < R \\ \& \\ \hat{L} = L \end{cases}$

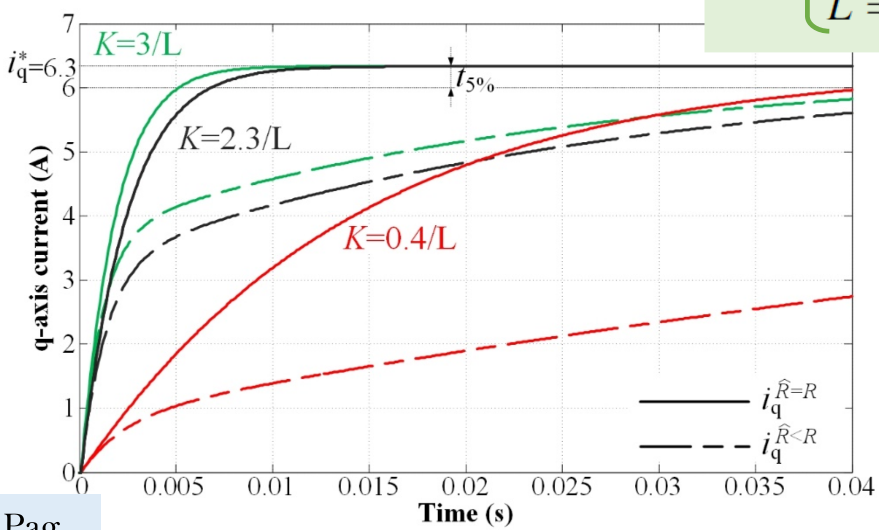

Neglecting $G_d(s)$ & assuming $\hat{L} = L$

$$G_{OL}(s) = G_{PI}(s)\frac{1}{sL+R} = \frac{sK_P + K_I}{s}\frac{1}{sL+R}$$

where $\begin{cases} R = R_F + R_C \\ L = L_F \end{cases}$

IMC

$K_P/K_I = \hat{L}/\hat{R}$

$K_P = K\hat{L}$

$$G''_{OL}(s) = K\frac{sL+\hat{R}}{s}\frac{1}{sL+R}$$

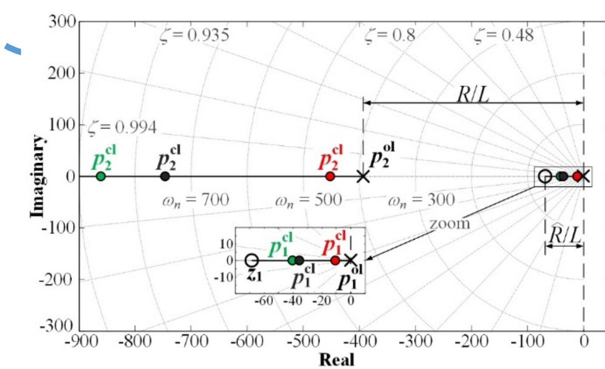

Pag. 29-34

Open-Loop Transfer Function

Including $G_d(s)$

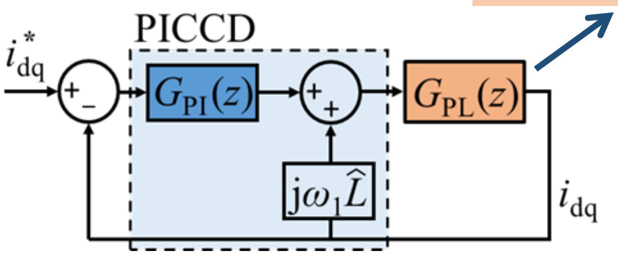

Overestimation of R

If $\begin{cases} \hat{R} > R \\ \& \\ \hat{L} = L \end{cases}$

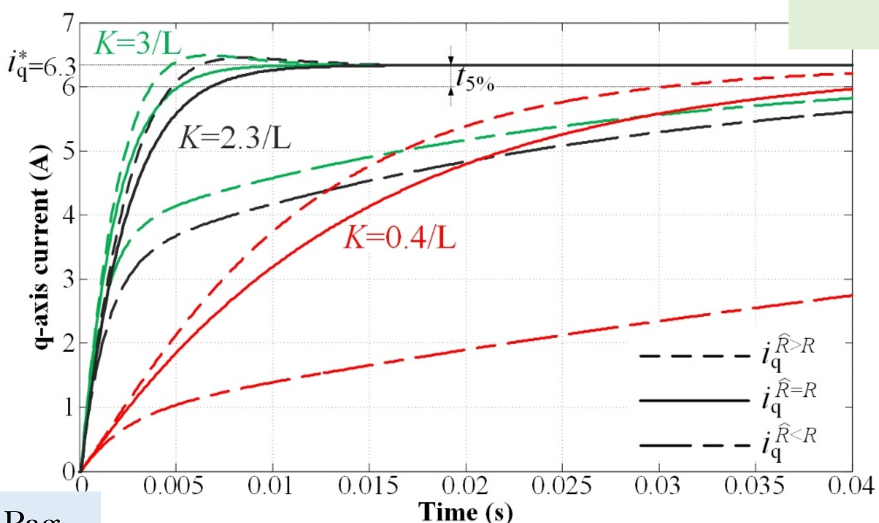

Neglecting $G_d(s)$ & assuming $\hat{L} = L$

$$G_{OL}(s) = G_{PI}(s)\frac{1}{sL+R} = \frac{sK_P + K_I}{s}\frac{1}{sL+R}$$

where $\begin{cases} R = R_F + R_C \\ L = L_F \end{cases}$

IMC
$K_P/K_I = \hat{L}/\hat{R}$
$K_P = K\hat{L}$

$$G''_{OL}(s) = K\frac{sL+\hat{R}}{s}\frac{1}{sL+R}$$

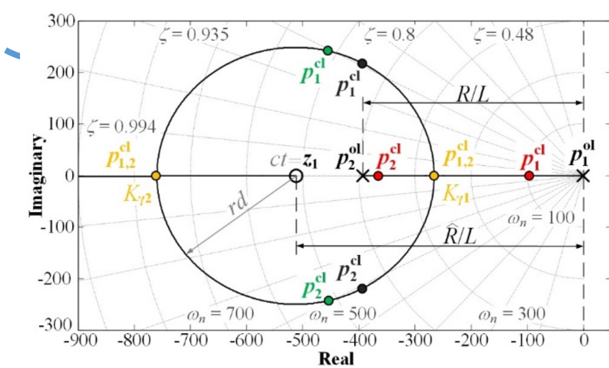

Pag. 29-34

Current Step Response in the Discrete-Time Domain

From the step response, having $i_q^{\widehat{R}=R}$ as a target, **two indicators** can be used to identify the actual R:

- the sign of the error area (**IE**) → whether R is **under** or **overestimated**,
- the area (**IAE**) → **how large** is the R **mismatch**

needs to be modified to weight the underestimate and overestimate cases → **WIAE**.

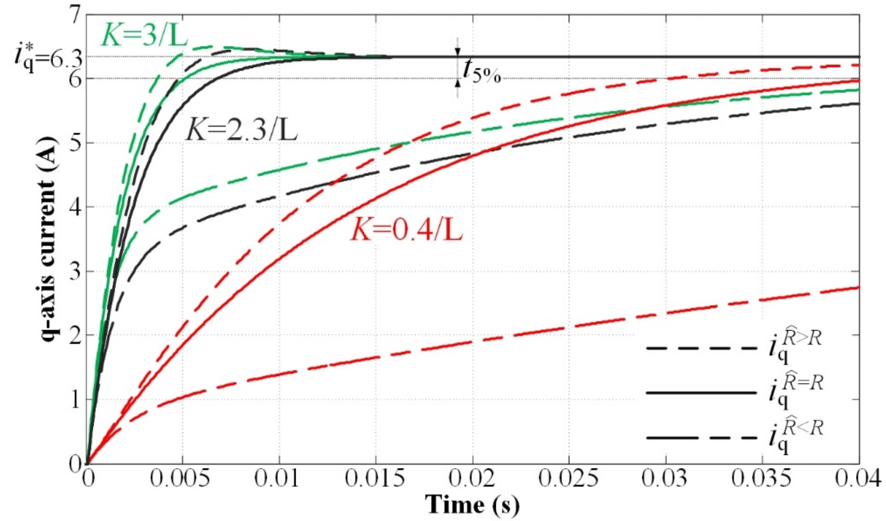

Pag. 39-40

Developed Method

- **MRAS-based** technique. Iterative process.
- If $\widehat{R} \approx R \Longleftrightarrow i_q^{\widehat{R}=R} \approx i_q$

Adjustable Model (AM)

Reference Model (RM)

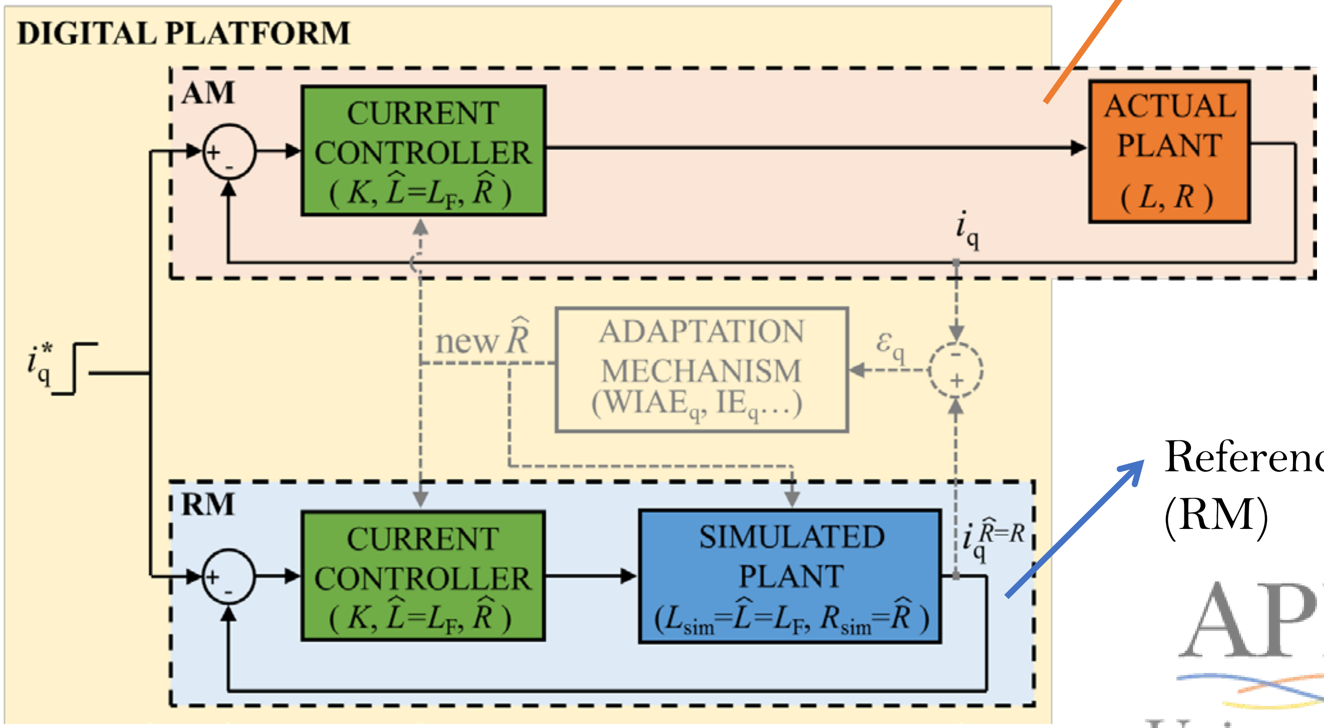

Pag. 35, 36

Developed Method

1. Initialization
   - Auxiliary variables
   - Controller parameters

$$\hat{R}(1),\ \hat{L}=L_F,\ K(k)=\hat{R}(k)/L_F$$

   - Simulated plant parameters

$$L_{sim}=L_F,\ R_{sim}(k)=\hat{R}(k)$$

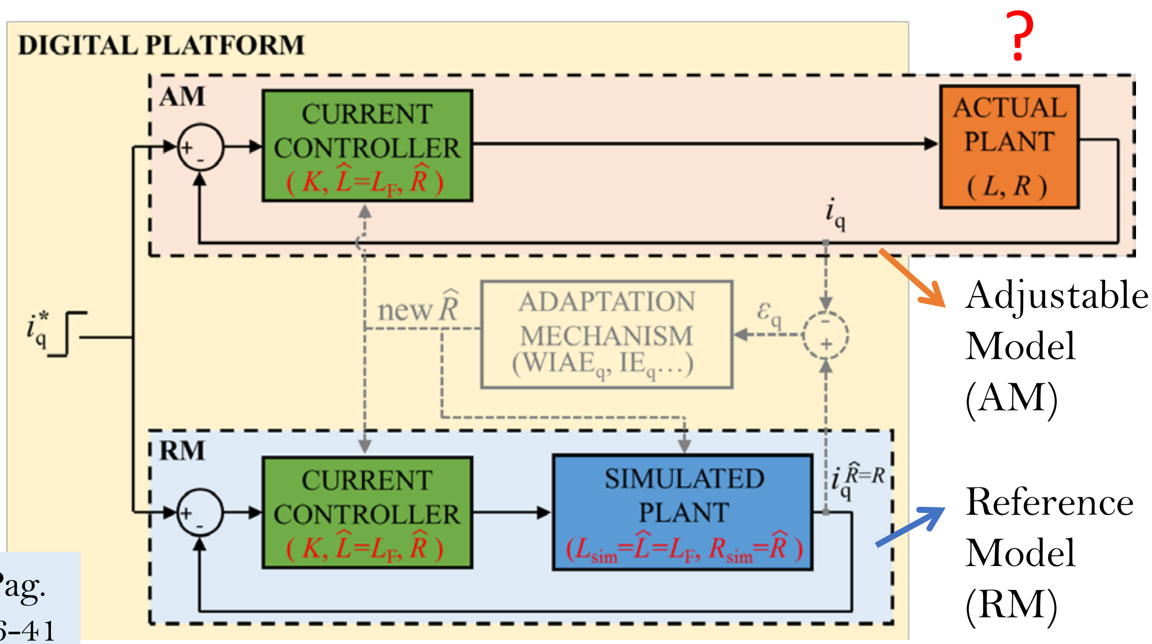

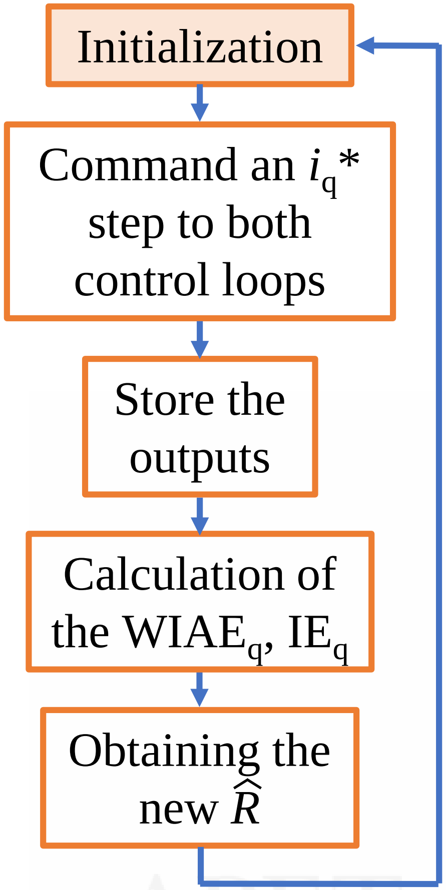

Pag. 36-41

Developed Method

2. Command an i_q^* step to both loops at the same time.
3. Store the outputs i_q and $i_q^{\hat{R}=R}$.

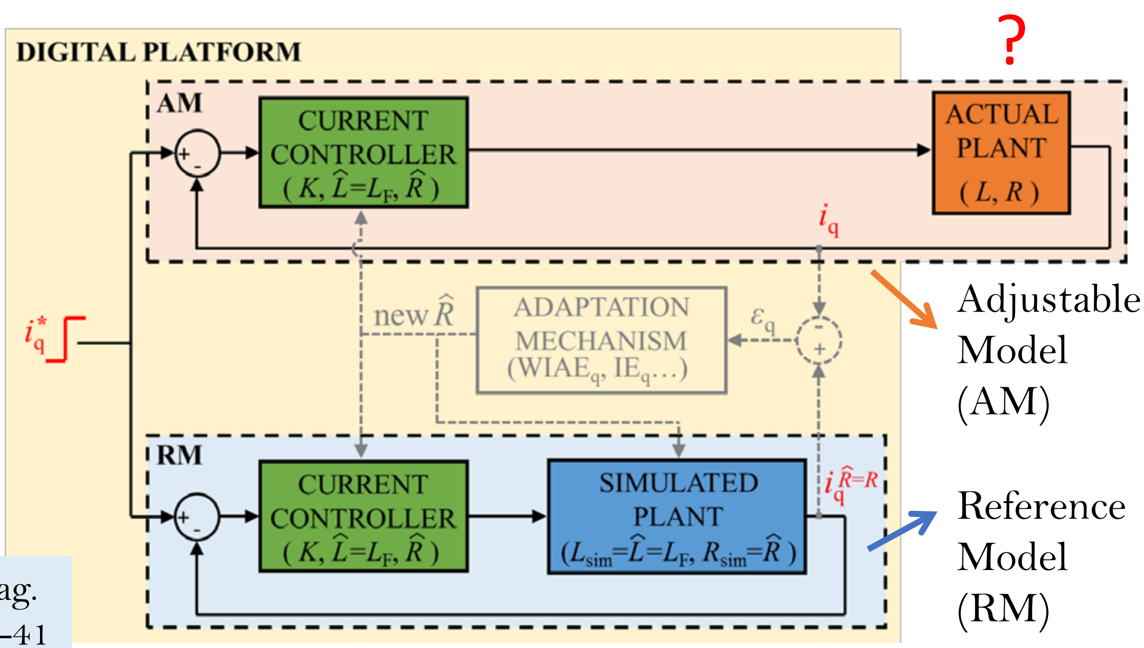

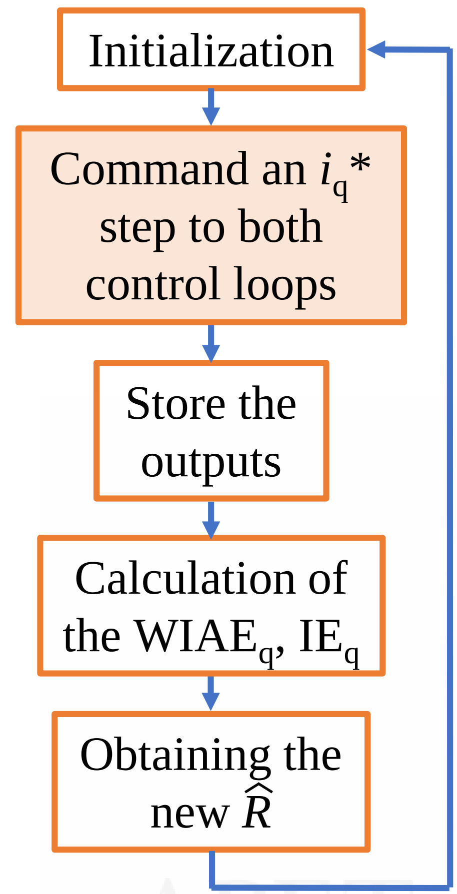

Pag. 36-41

Developed Method

2. Command an i_q^* step to both loops at the same time.
3. Store the outputs i_q and $i_q^{\hat{R}=R}$.

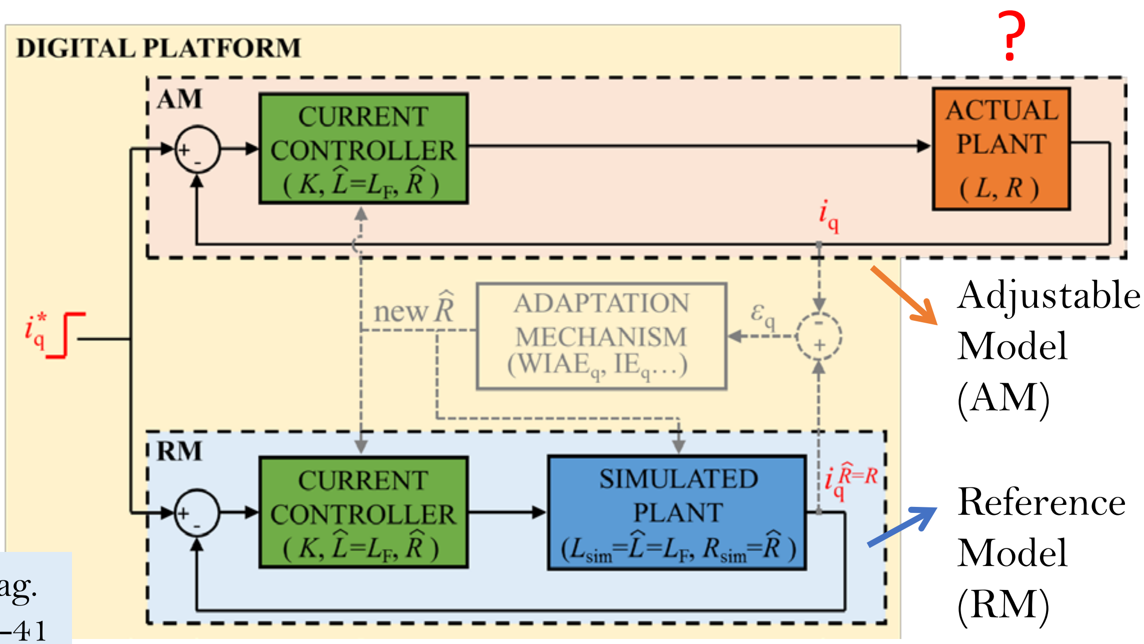

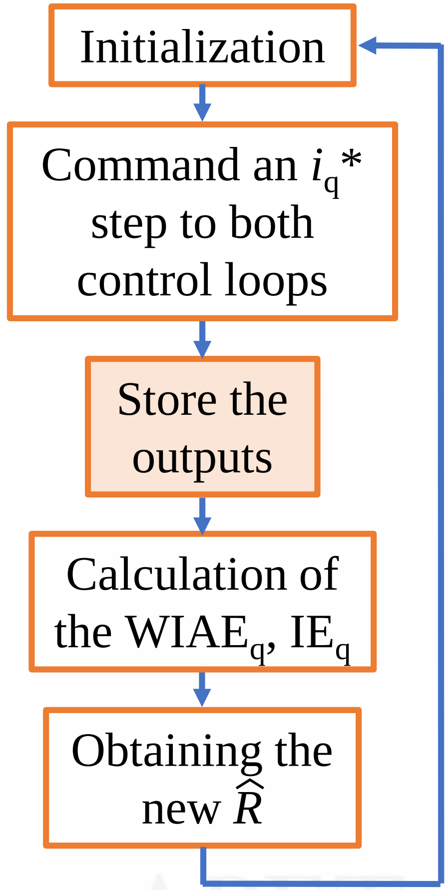

Pag. 36-41

Developed Method

4. Calculation of two indicators ($WIAE_q$, IE_q) from the error between the two curves.

5. Obtaining the new R estimate:
   - $WIAE_q$, IE_q → $\hat{R}$

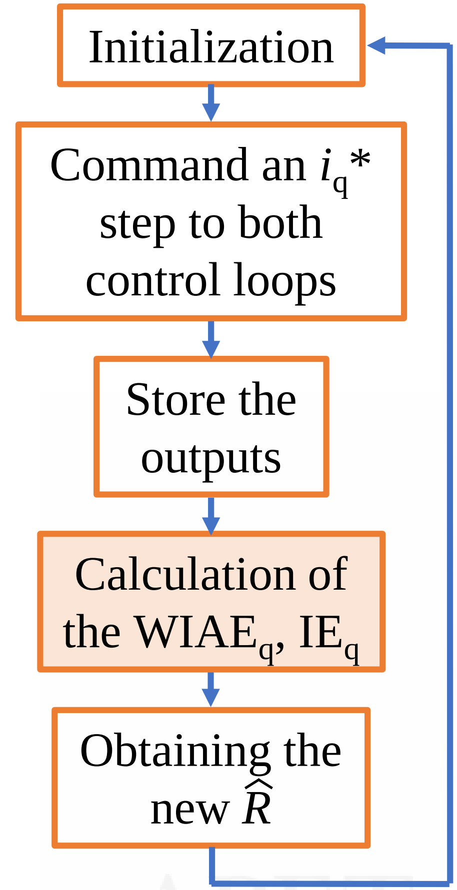

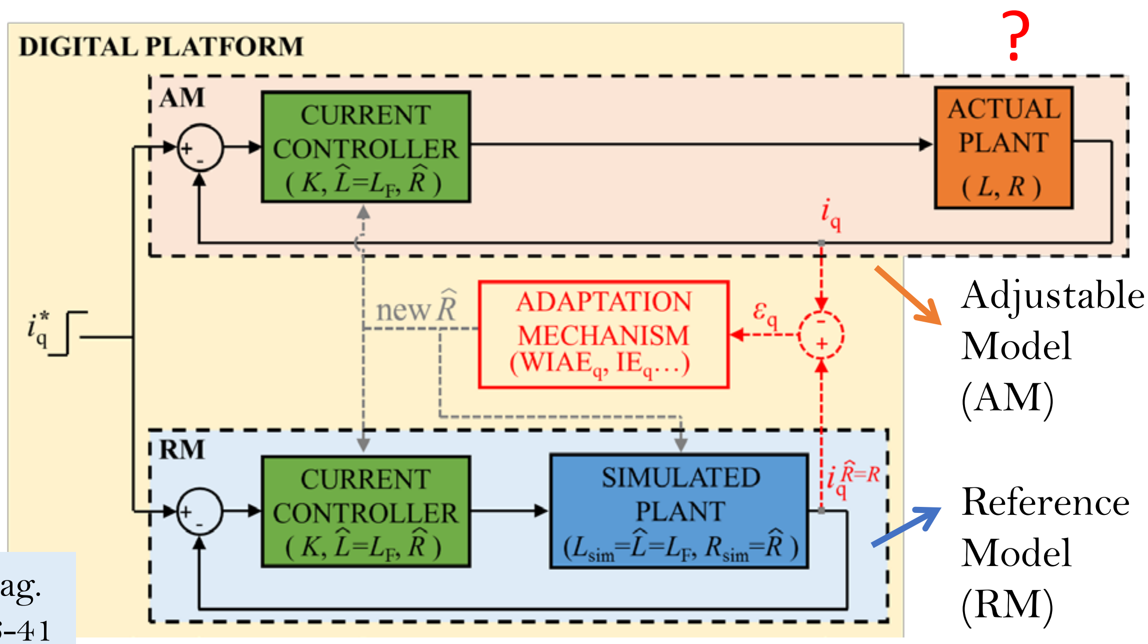

Pag. 36-41

Developed Method

4. Calculation of two indicators ($WIAE_q$, IE_q) from the error between the two curves.
5. Obtaining the new R estimate:
   - $WIAE_q$, IE_q → $\hat{R}$

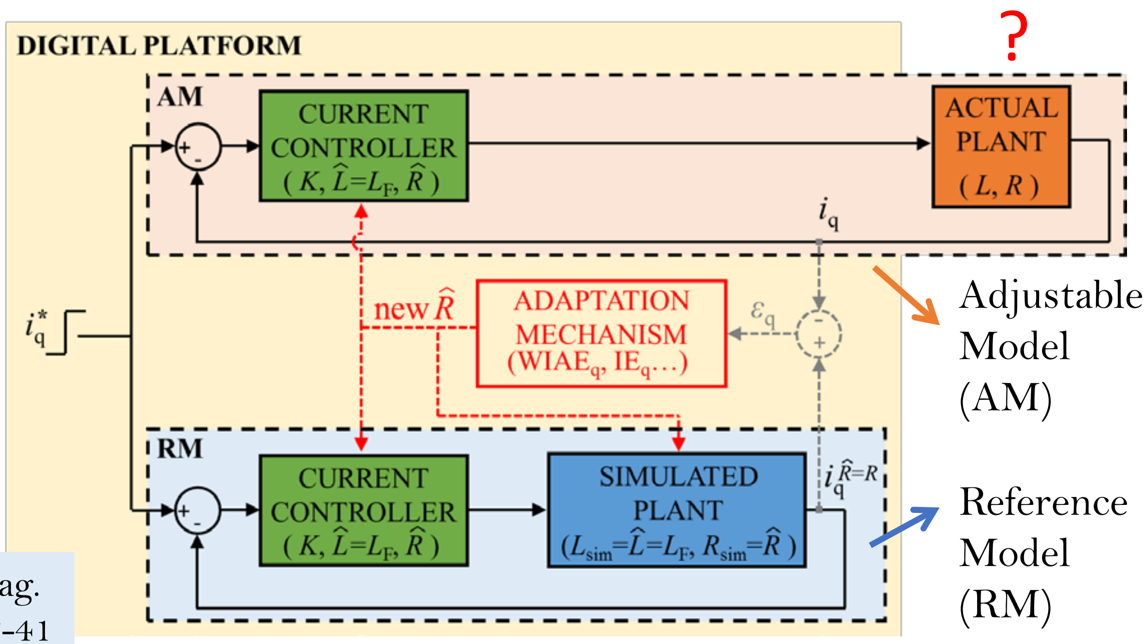

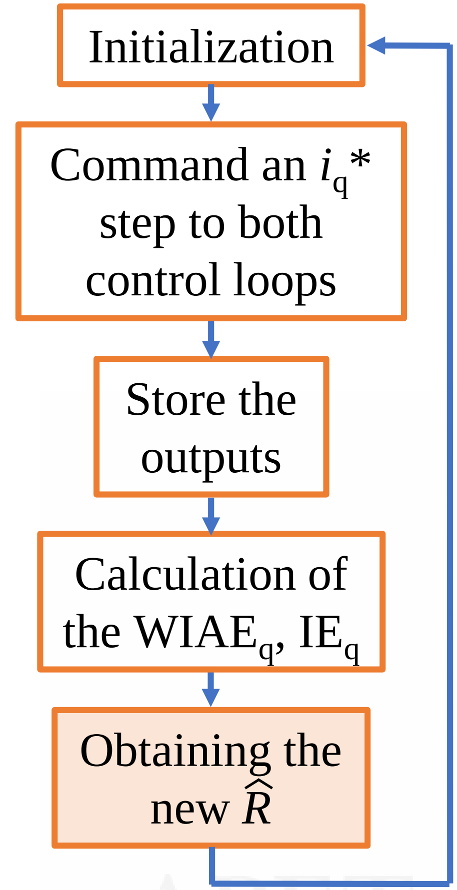

Pag. 36-41

Developed Method

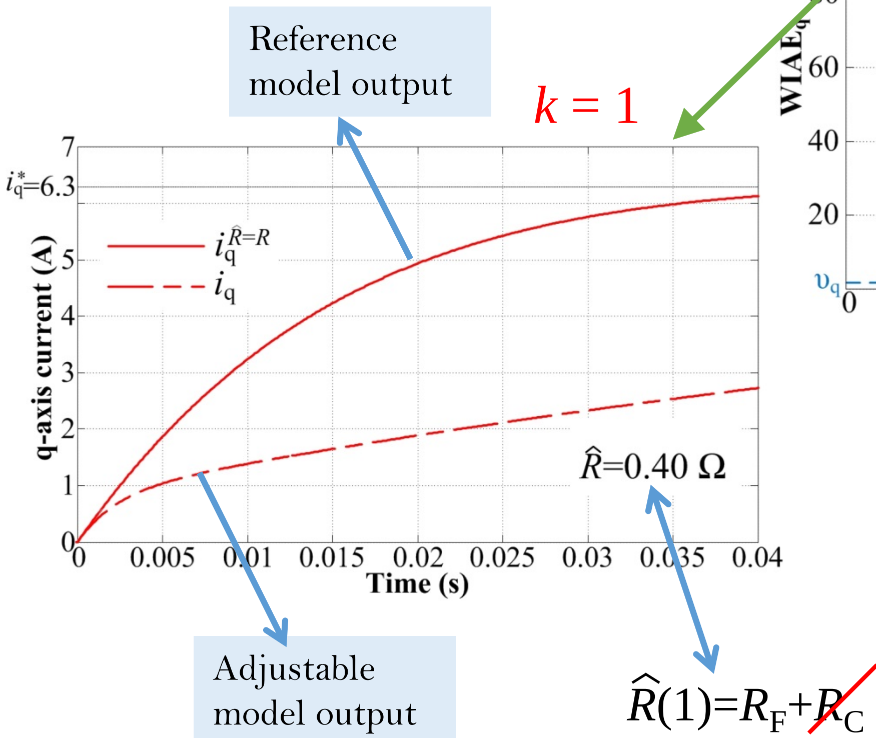

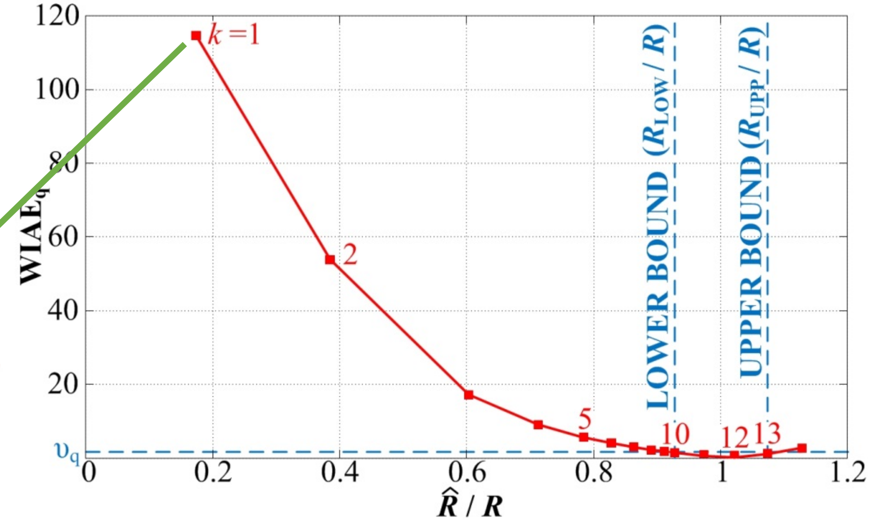

CASE A

P_{dc}	4.3 kW
$f_{sw} = f_s$	10 kHz
i_d	9 A
i_q*	6.3 A
$\hat{L} = L_F$	5.9 mH
R (R_F+R_C)	2.3 Ω
$\hat{R}(1) = R_F$	0.4 Ω

Pag. 36-41

Developed Method

- **Main idea:** using the area between both curves to correct the *R* mismatch.
  - $WIAE_q$,
  - IE_q

Reference model output

$k = 1$

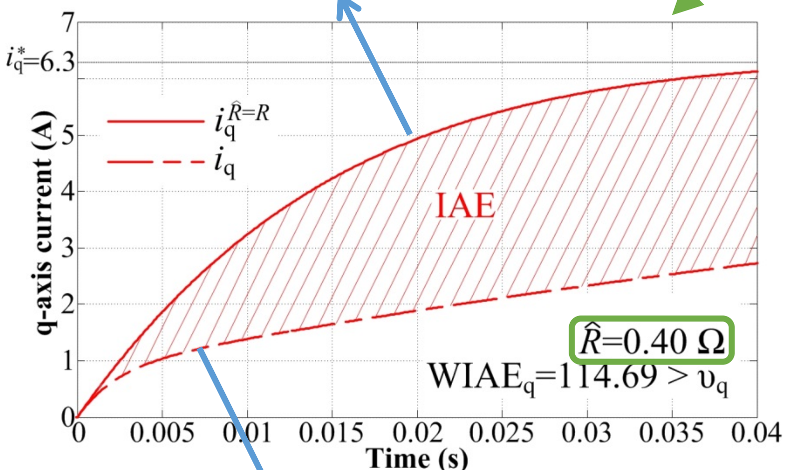

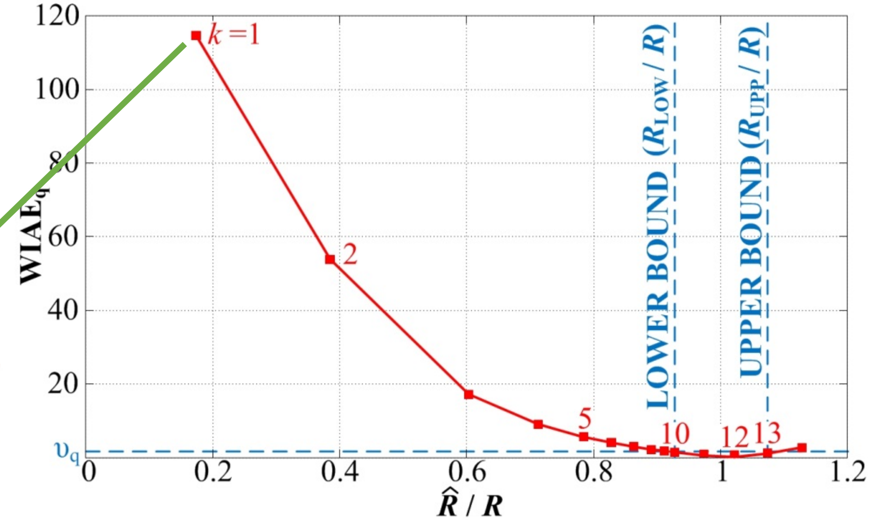

R	2.3 Ω

Adjustable model output

Pag. 36-41

Developed Method

- **Main idea:** using the area between both curves to correct the *R* mismatch.
  - $WIAE_q$,
  - IE_q

Reference model output

$k = 1$

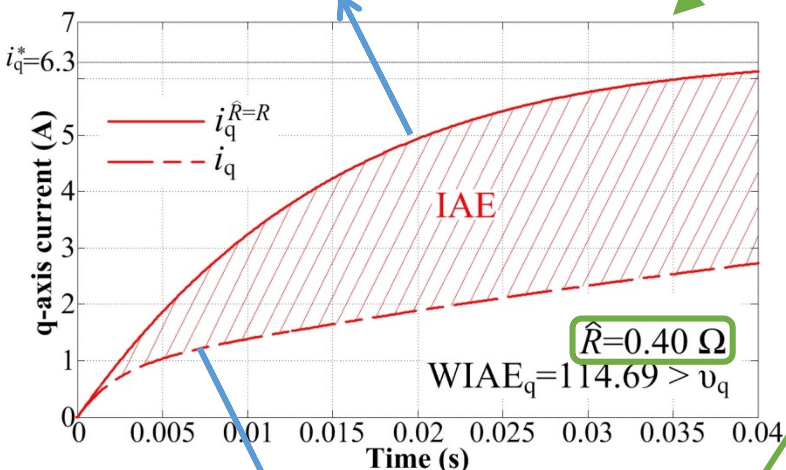

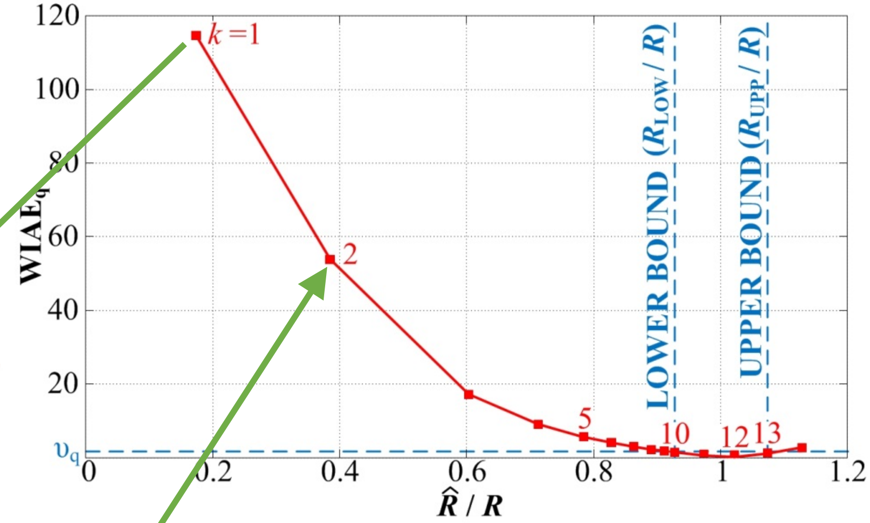

R	2.3 Ω

Adjustable model output

$$\hat{R}(k+1) = [1+\Delta_q(k)]\cdot\hat{R}(k)$$

$$\Delta_q(k) = f\,(WIAE_q(k), i_q^*)$$

Pag. 36-41

APET Universida de Vigo

Developed Method

- **Main idea:** using the area between both curves to correct the *R* mismatch.
  - WIAE_q,
  - IE_q

Reference model output

$k = 1$

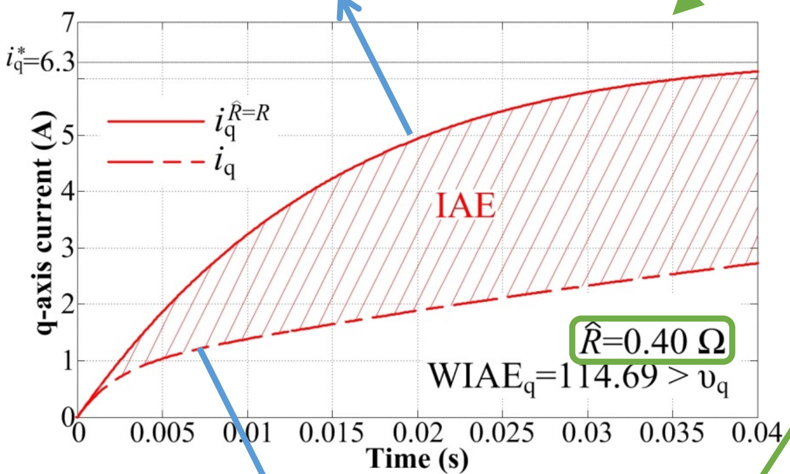

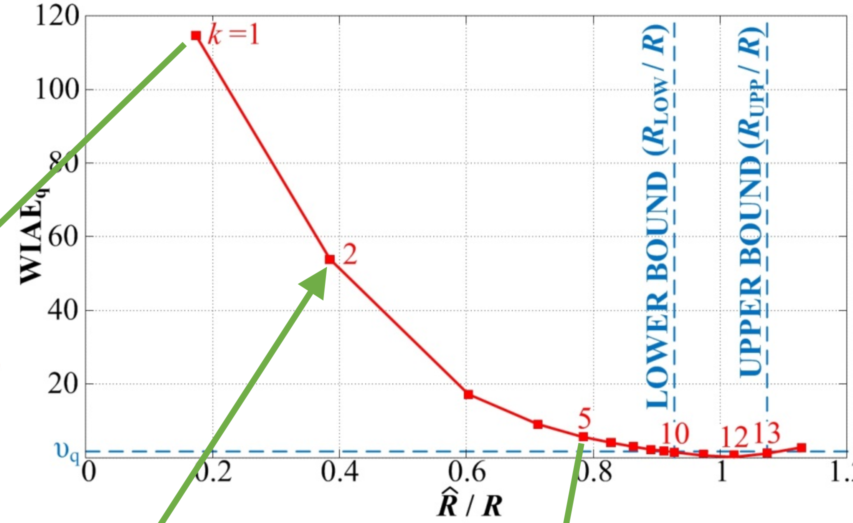

R	2.3 Ω

Adjustable model output

$k = 5$

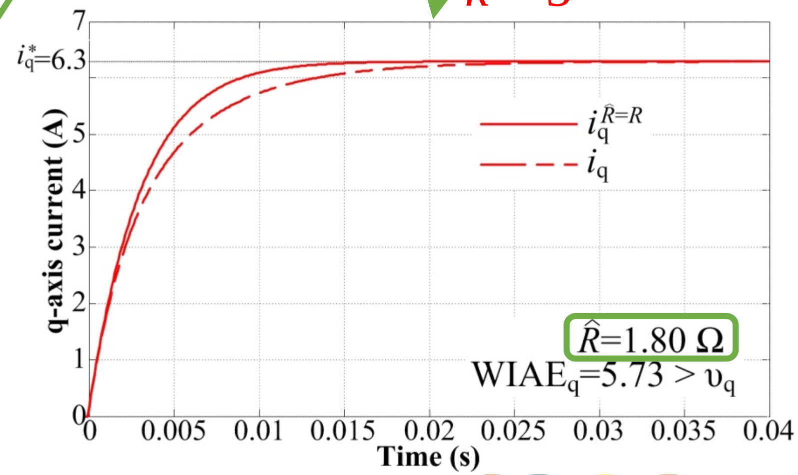

$$\hat{R}(k+1) = [1+\Delta_q(k)]\cdot\hat{R}(k)$$

$$\Delta_q(k) = f\,(\text{WIAE}_q(k), i_q^*)$$

Pag. 36-41

Universidade Vigo

Developed Method

Approach to *R* lower bound

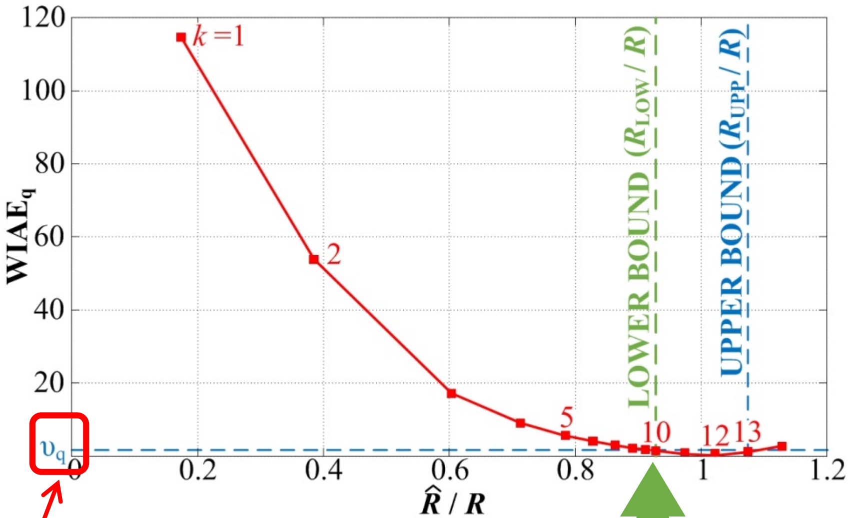

Threshold

Lower Bound

R_{LOW}

$k = 10$

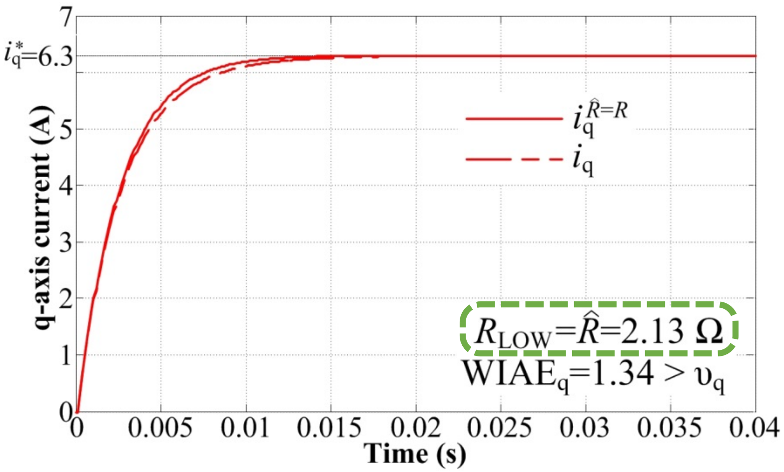

Pag.
36-41

Developed Method

Approach to *R* lower bound

Refinement

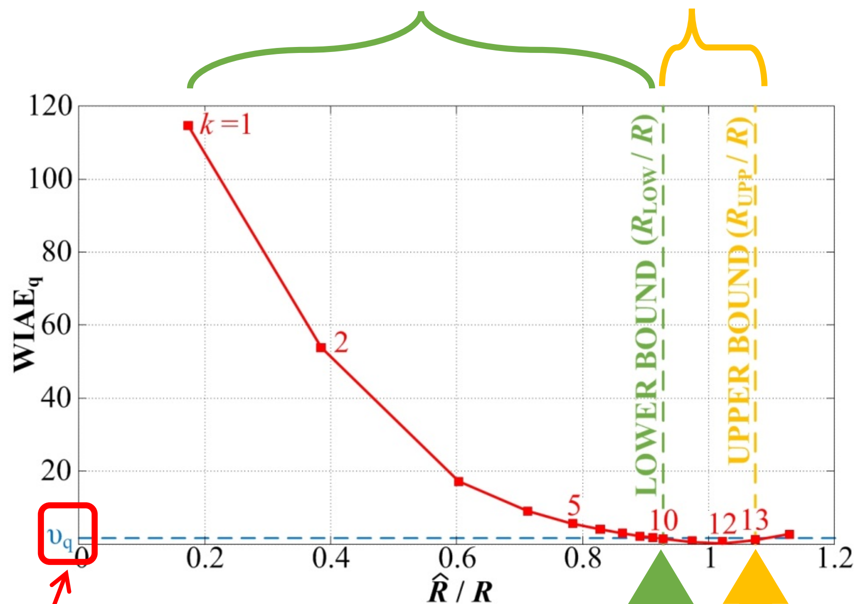

Threshold

Lower Bound → R_{LOW}

Upper Bound → R_{UPP}

k = 13

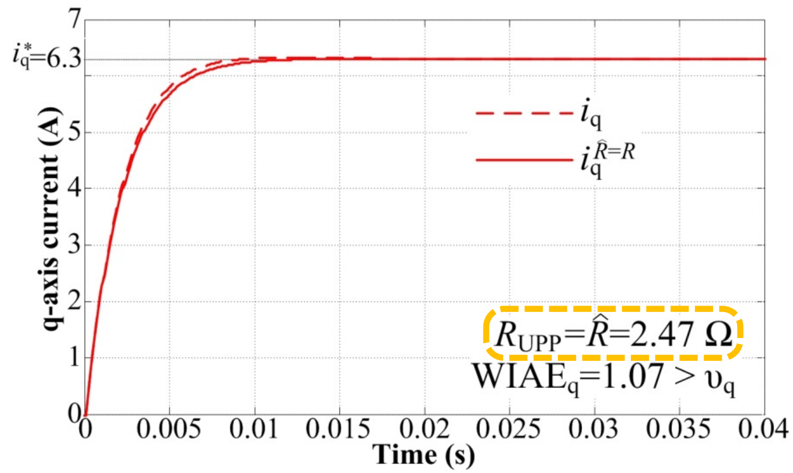

Pag. 36-41

APET Universida de Vigo

Developed Method

Approach to *R* lower bound

Refinement

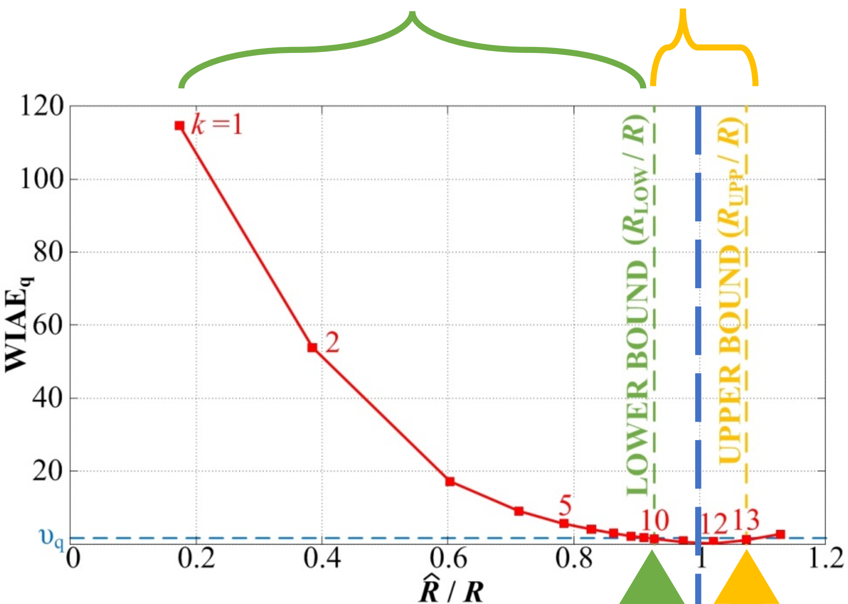

k = 14

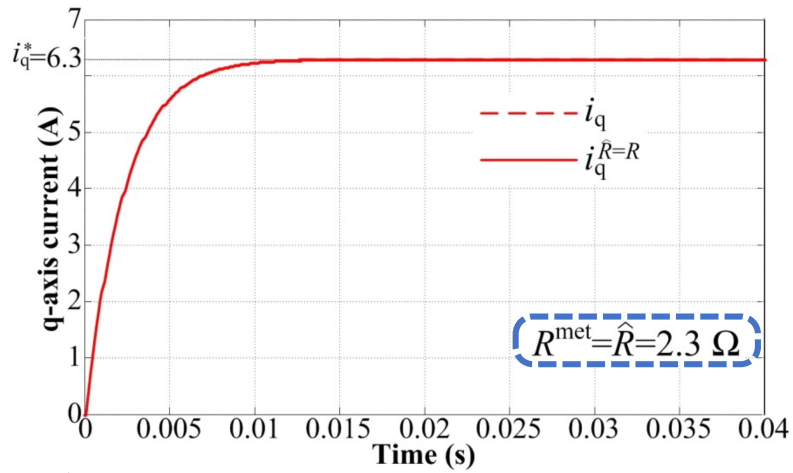

Lower Bound

Upper Bound

$$i_q^{\hat{R}=R} \approx i_q$$

***R* estimation end**

$$R^{met} = (R_{LOW} + R_{UPP})/2$$

$$R_C^{met} = R^{met} - R_F$$

Pag.
36-41

Other contents of Chapter 2

- **Theoretical examples** of **representative situations** with L and with LCL filters (P_{rated}, $V_{LLrated}$, P_{level}, f_{sw}, f_s, i_q*, L_F, R_F, R_C).
  - For all the cases, R_C matches quite well R_C^{met} in few iterations.

Pag. 41-42

- **Implementation options**:
  - **Offline**, during a precommissioning stage.
  - **Online** → PICCD must be adopted to regulate the positive-sequence fundamental component of the current.

Pag. 41-43

- **Effect** on the resistance estimate **of uncertainties in the inductance** value.
  - The error made in $\widehat{R}$ is **irrelevant**, even for $\widehat{L}/L$=1.20 and $\widehat{L}/L$=0.80.

Pag. 44

- 2DOF PI controller case ("active resistance").
  - Although including an "**active resistance**" **lowers** to a certain point the **sensitivity** of the current loop response in the presence of ***R*** **uncertainties**, **knowing** ***R*** permits to **further enhance the transient response**, especially as R grows.

Pag. 45-48

Experimental Setup

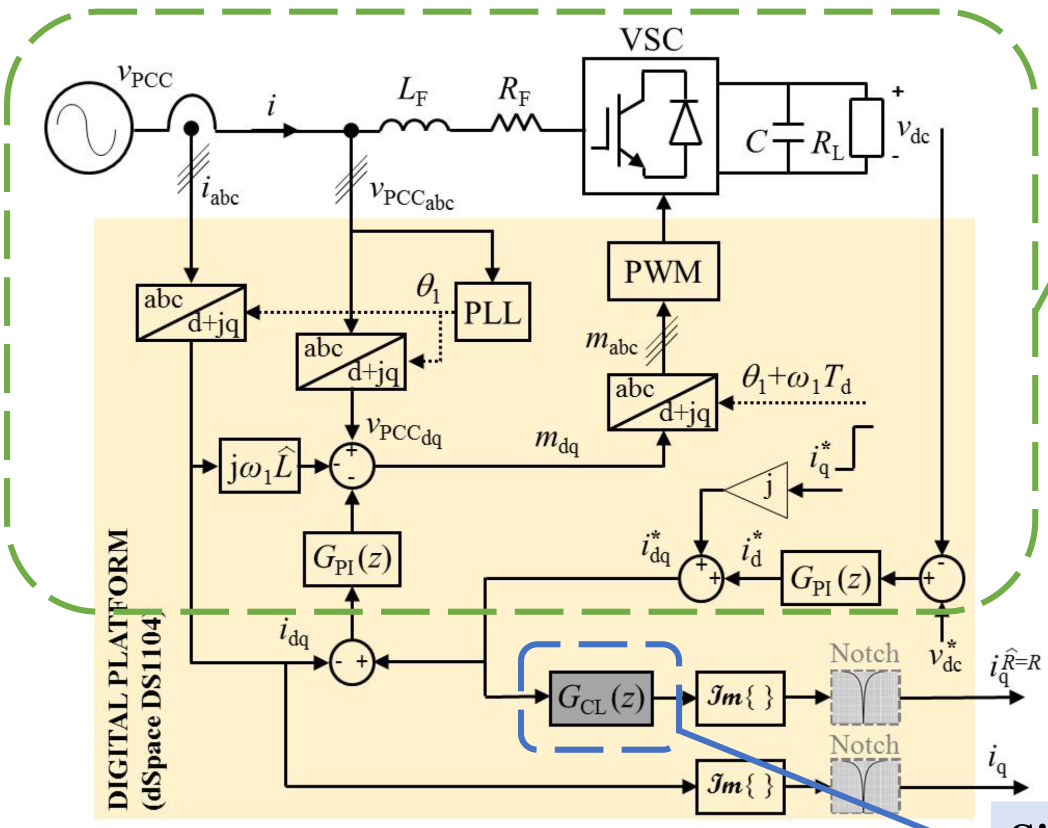

Actual control loop:

- plant → a 3-ph grid-tied VSC
- control → dSpace.

Simulated control loop:

- simulated plant + control → dSpace.

Pag. 48-50

Experimental Tests

Case	P_{dc}	$f_{sw}=f_s$	L_F	R_F	i_d	i_q*	v_{dc}	v_{PCC}	R_C^{met}	k_{max}
A	4.3 kW	10 kHz	5.9 mH	0.4 Ω	9.7 A	6.3 A	750 V	230 V	1.9 Ω	14
B	2.8 kW	10 kHz	5.9 mH	0.4 Ω	6.3 A	6.3 A	750 V	230 V	2.6 Ω	16
C	1.8 kW	10 kHz	5.9 mH	0.4 Ω	4.3 A	4.3 A	750 V	230 V	3.8 Ω	22
D	1.8 kW	5 kHz	9.6 mH	0.4 Ω	4.3 A	4.3 A	750 V	230 V	2.7 Ω	13
E	1.8 kW	2.5 kHz	11.7 mH	0.4 Ω	4.3 A	4.3 A	750 V	230 V	1.3 Ω	9

Pag.
50-54

APET
Universidade Vigo

Experimental Test A

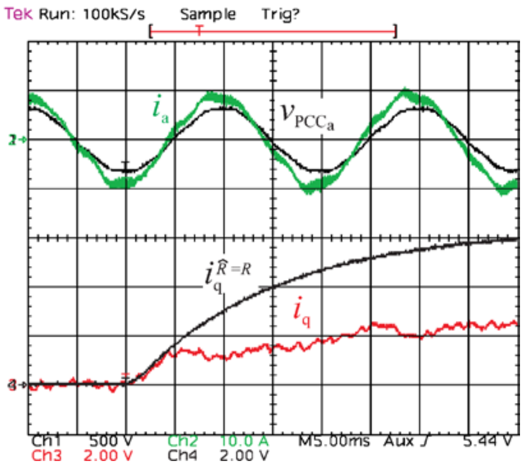

$k = 1;\ \hat{R} = 0.40\ \Omega;$

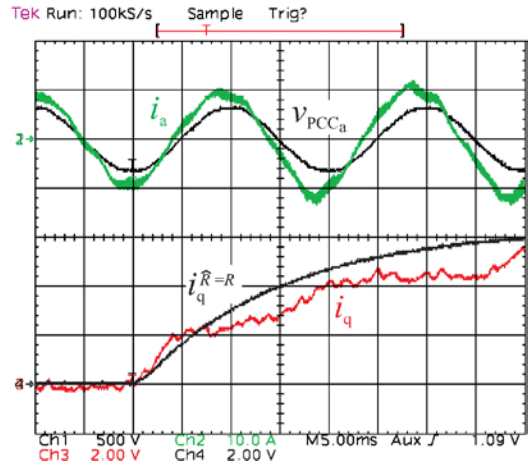

$k = 2;\ \hat{R} = 0.89\ \Omega;$

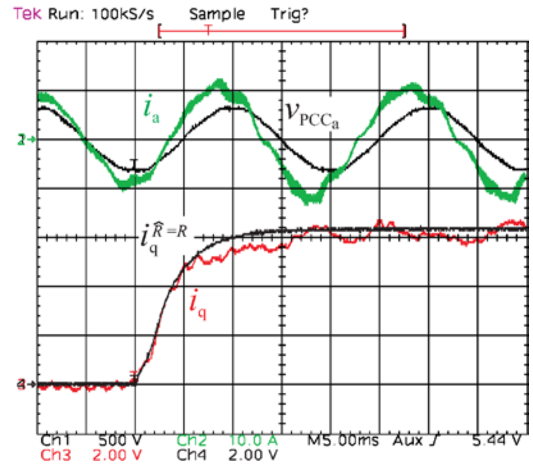

$k = 5;\ \hat{R} = 1.80\ \Omega;$

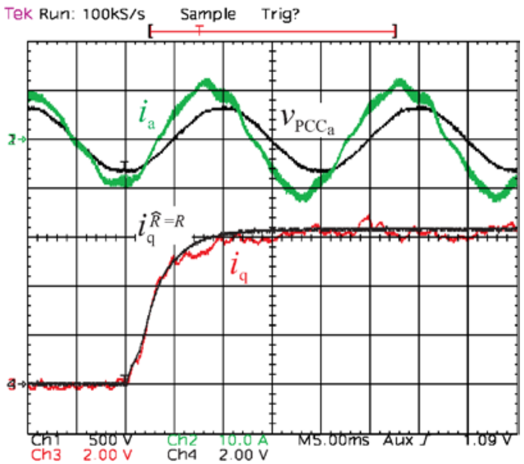

$k = 10;\ R_{LOW}=\hat{R} = 2.13\ \Omega;$

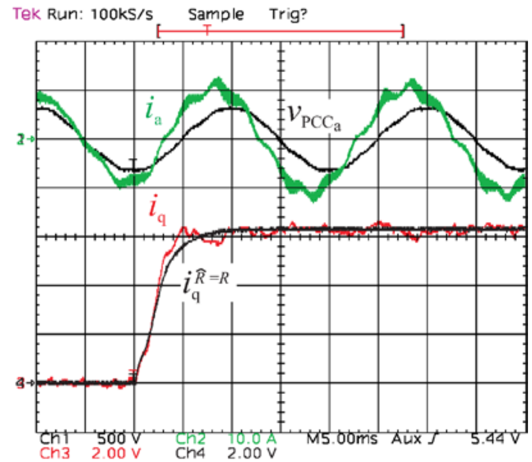

$k = 13;\ R_{UPP}=\hat{R} = 2.47\ \Omega;$

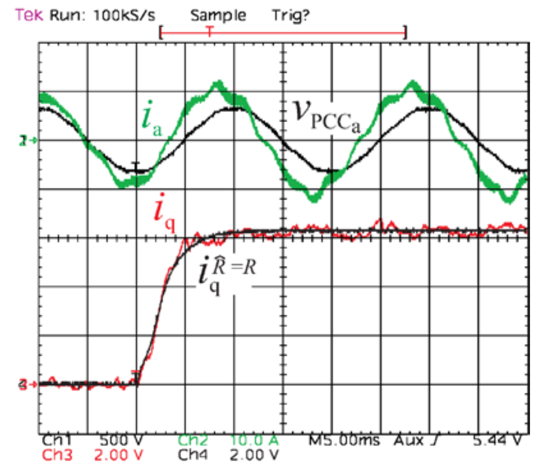

$k = 14;$ $\mathbf{R^{met} = 2.30\ \Omega}$

Conclusions of Chapter 2

- An **incorrect estimation** of the **equivalent resistance** in the plant model of the **current control closed loop** leads to a **degraded behavior** of it, different from the theoretical one (e.g., in terms of settling time and overshoot). Hence, its **identification** is **essential** for a **rigorous analysis** and **design** of this loop.
- A **method** to **estimate** the **VSC equivalent loss resistance** in specific working conditions has been proposed. Such resistance reflects the influence of the power losses on the plant model.
- The developed algorithm is based on the **iterative minimization** of a **cost function that quantifies the error between the current control closed-loop step responses of the actual and the one including a simulated plant**, with the current controllers tuned according to IMC. Thus, it is **particularly oriented** to the fulfillment of **transient response constraints**.

APET Universidade Vigo

Outline

APET
UniversidadeVigo

Current Loop

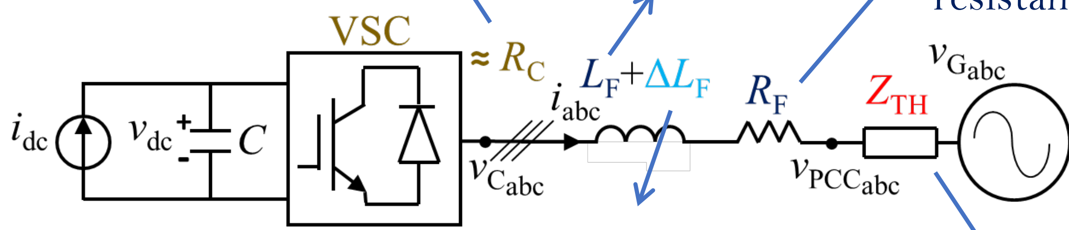

$L = L_F + \Delta L_F + L_{TH}$

$R = R_F + R_C + R_{TH}$

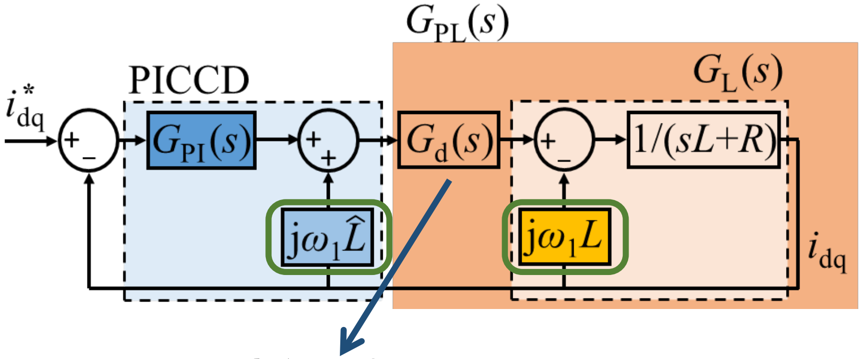

Remaining delay after applying delay compensation in SRF.

To study the **impact** of the ***L* uncertainties on** the **current closed loop**, it is important **not to neglect the delay** (even for a first approach).

Pag. 59, 60

Influence of Mismatches on the Time-Domain Step Responses

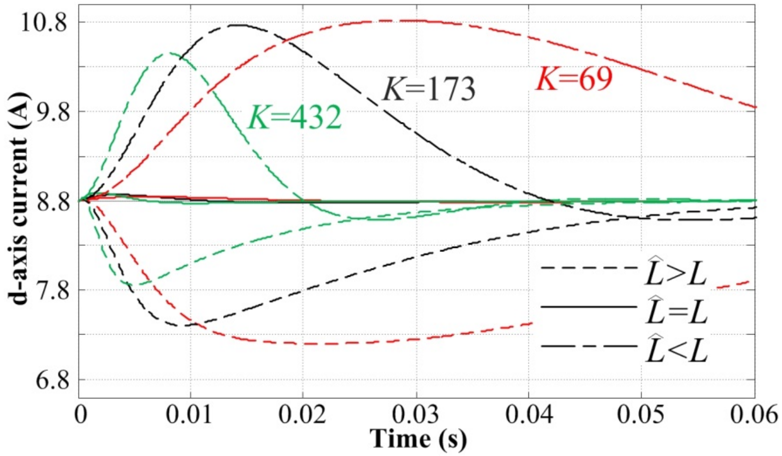

Effect of $\hat{L}$ on i_d.

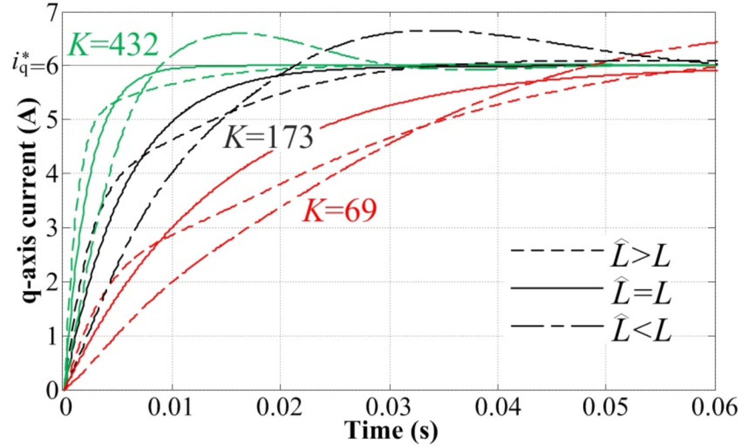

Effect of $\hat{L}$ on i_q.

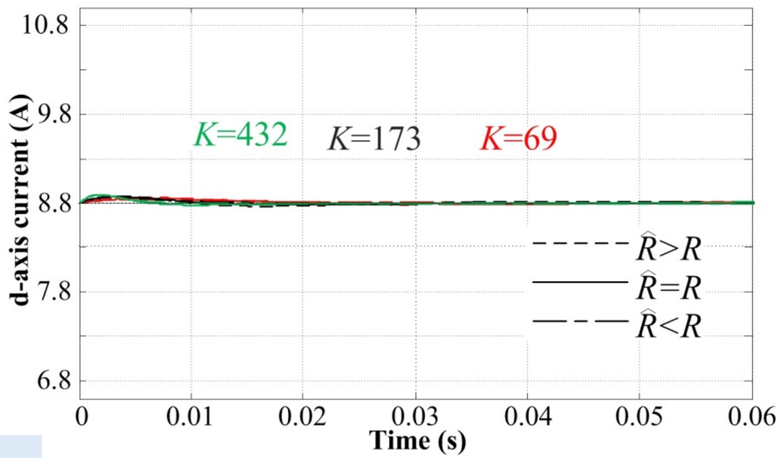

Effect of $\hat{R}$ on i_d.

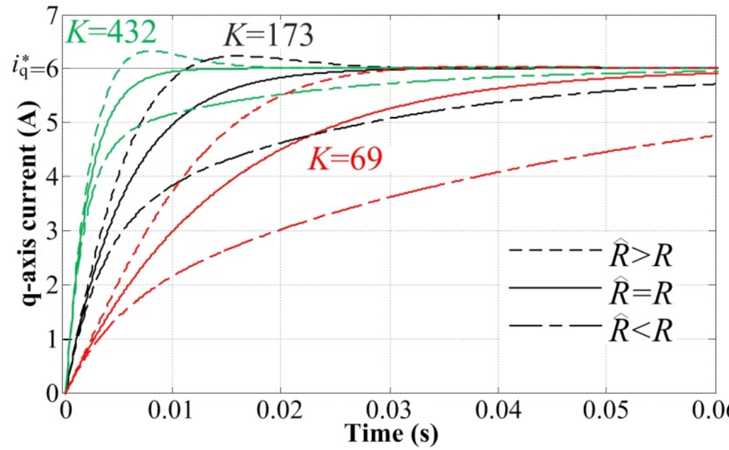

Effect of $\hat{R}$ on i_q.

Pag. 64-66

Influence of Mismatches on the Time-Domain Step Responses

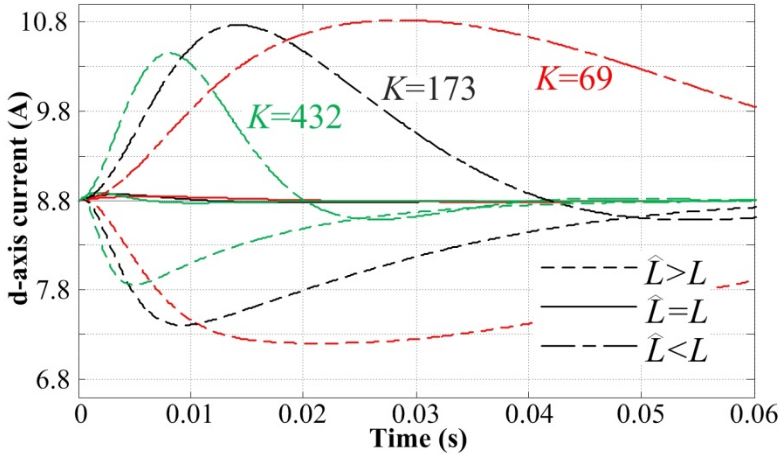

Effect of $\widehat{L}$ on i_d.

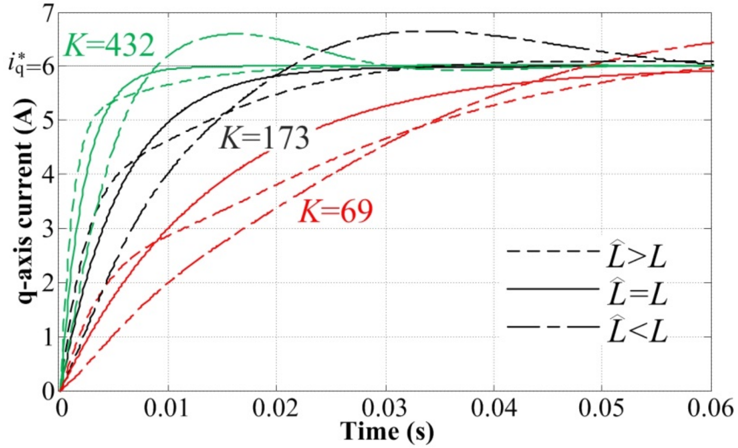

Effect of $\widehat{L}$ on i_q.

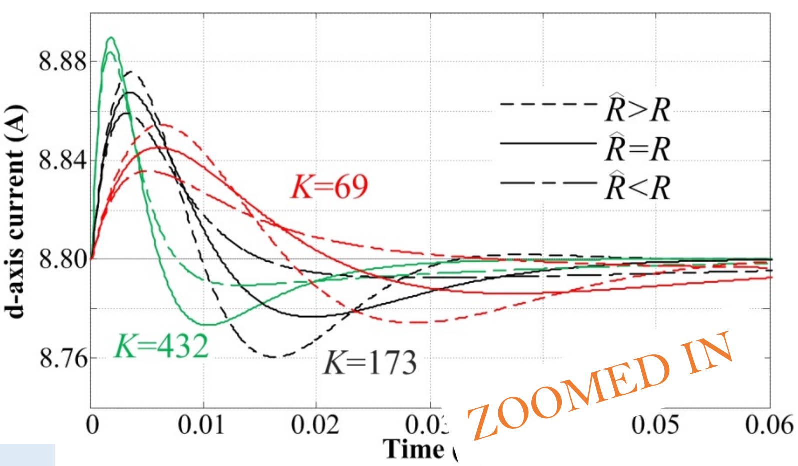

Effect of $\widehat{R}$ on i_d.

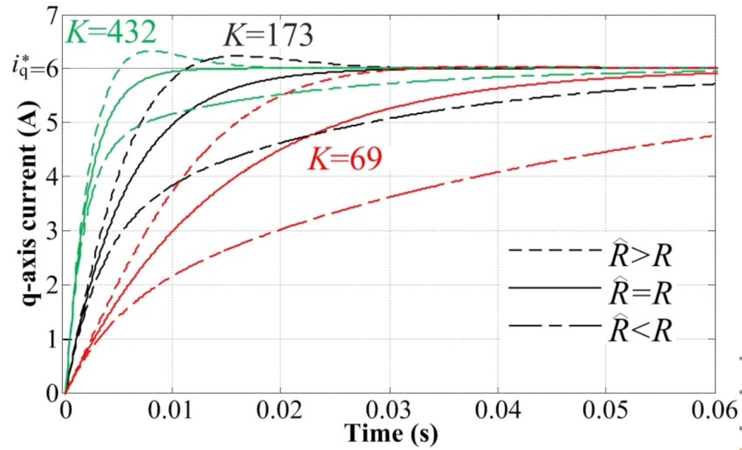

Effect of $\widehat{R}$ on i_q.

Pag. 64-66

Influence of Mismatches on the Time-Domain Step Responses

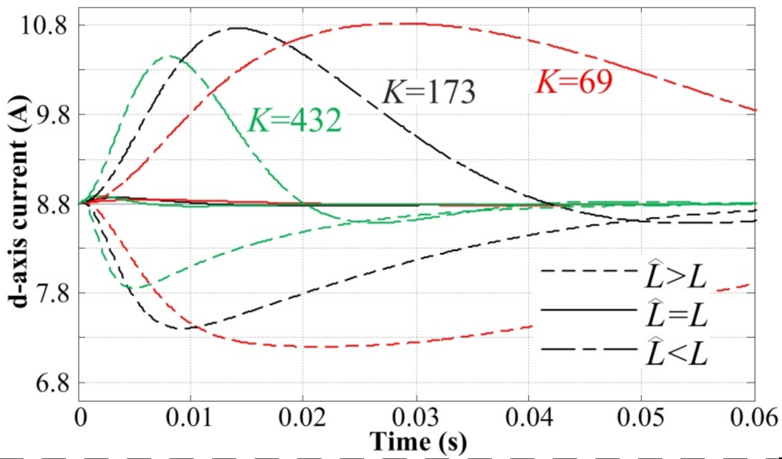

Effect of $\hat{L}$ on i_d.

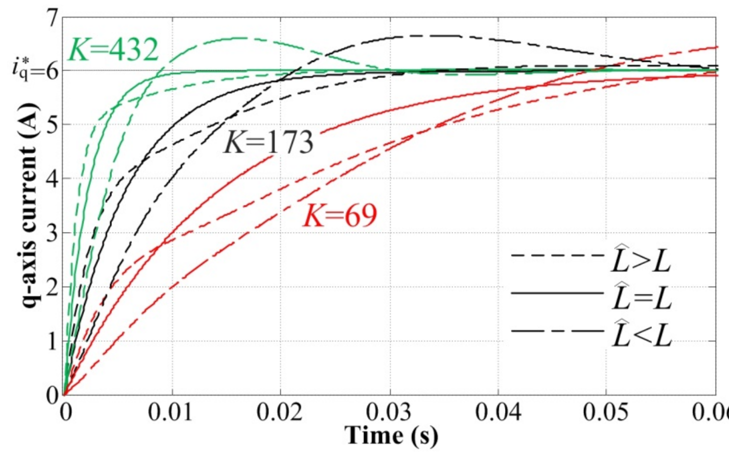

Effect of $\hat{L}$ on i_q.

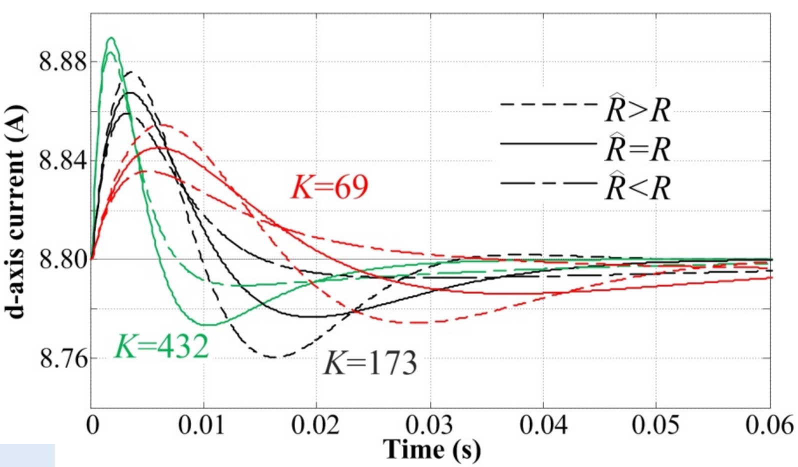

Effect of $\hat{R}$ on i_d.

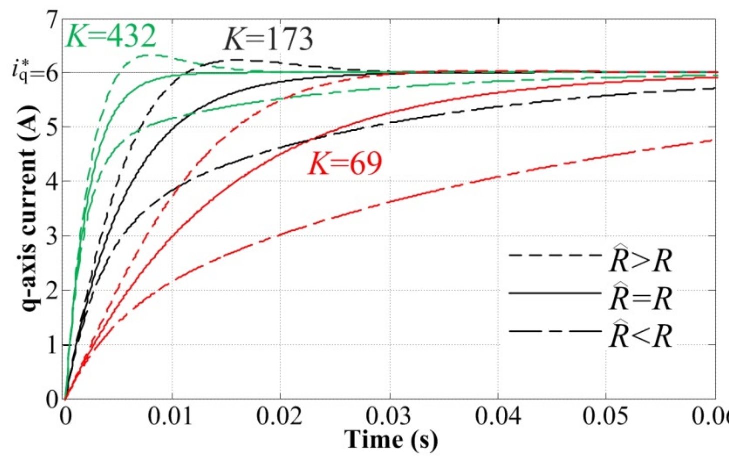

Effect of $\hat{R}$ on i_q.

Pag. 64-66

Influence of Mismatches on the Time-Domain Step Responses

Pag. 64-67

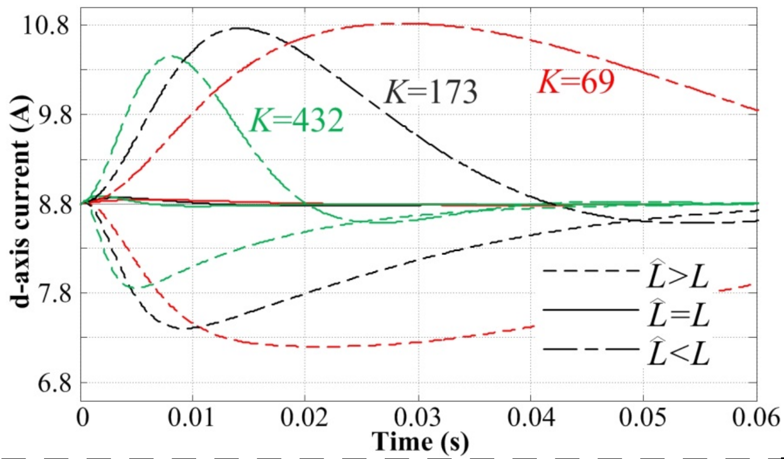

Effect of $\hat{L}$ on i_d.

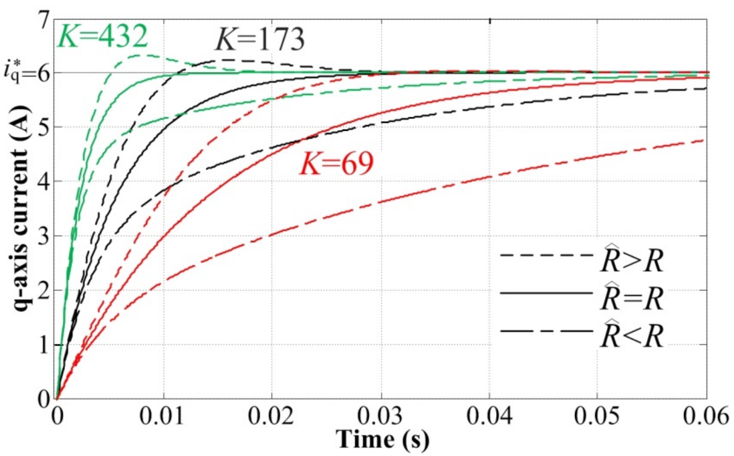

Effect of $\hat{R}$ on i_q.

Two indicators:

- the sign of the error area (**IE**) → whether the parameter is **under** or **overestimated**,
- the area (**IAE**) → **how large** is the **parameter mismatch**.

Developed Method

- Able to estimate **both parameters**: $L = L_F + \Delta L_F + L_{TH}$ and $R = R_F + R_C + R_{TH}$.
- **Both orthogonal components** of the plant output are considered.
- The **inability** of the **axes decoupling** to perform properly **in the presence of parameter mismatches** is exploited.
- If $\hat{R} \approx R$ and $\hat{L} \approx L$

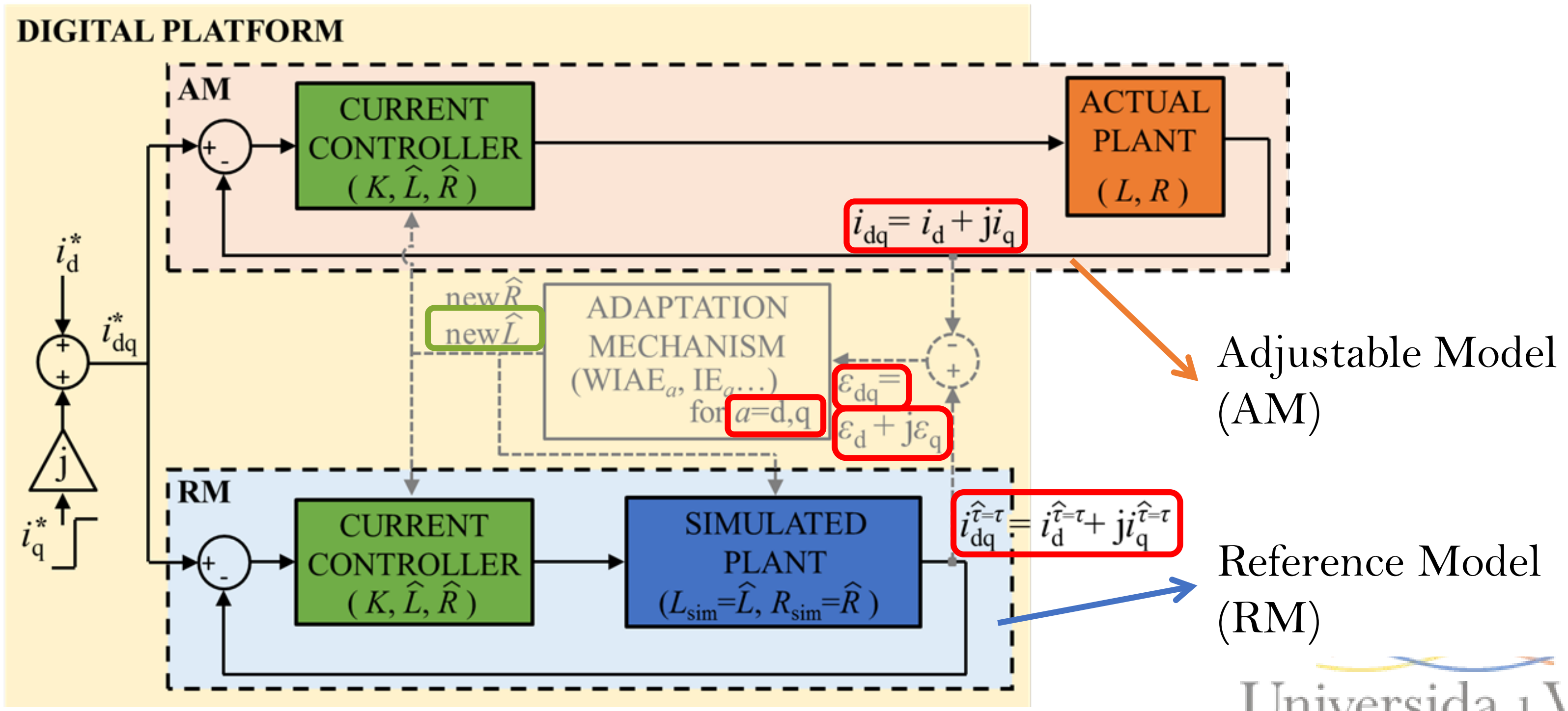

Pag. 66, 67

Developed Method

1. Initialization → extra variables
   - Auxiliary variables
   - Controller parameters

$$\widehat{R}(1),\ \widehat{L}(1),\ K(k)=\widehat{R}(k)/\widehat{L}(k)$$

   - Simulated plant parameters

$$L_{sim}=\widehat{L}(k),\ R_{sim}(k)=\widehat{R}(k)$$

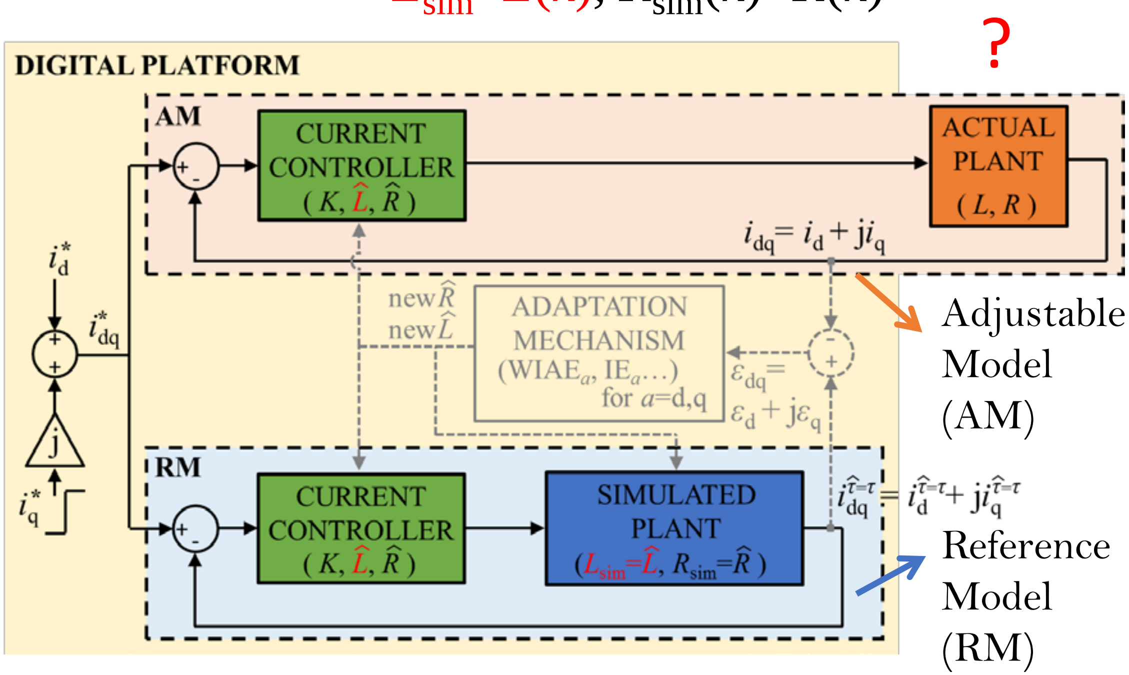

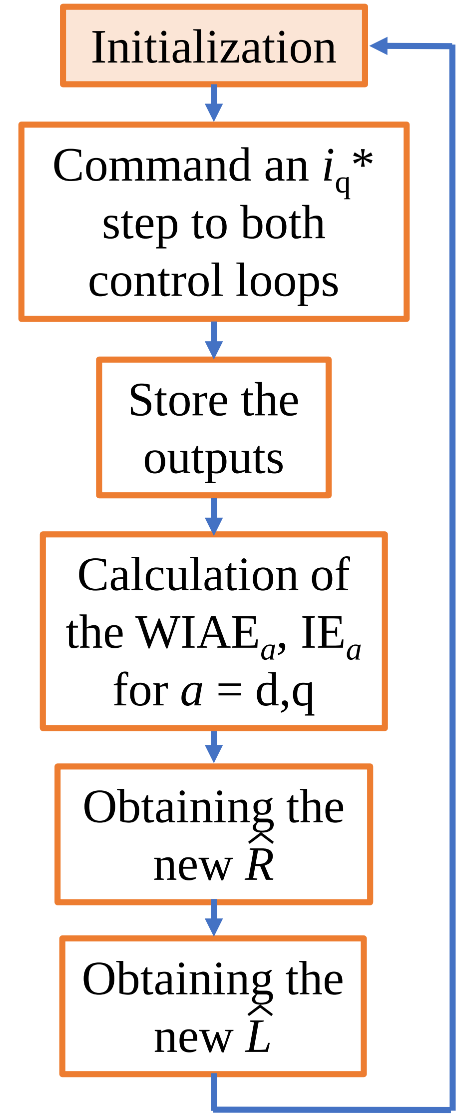

Pag. 67-73

Developed Method

$k = 1$

Coupling

Step

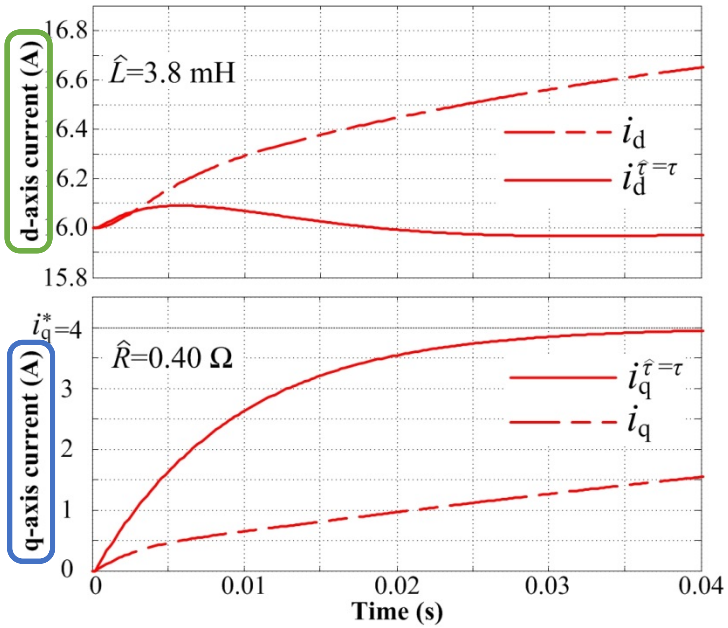

Pag.
67-73

?

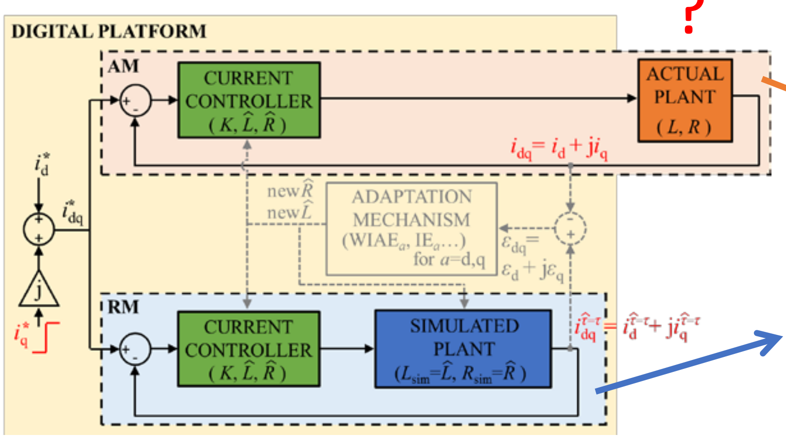

Adjustable Model (AM)

Reference Model (RM)

CASE C

$f_{sw} = f_s$	5 kHz
L	9.9 mH
$\hat{L}(1) = L_F$	3.8 mH
R	3 Ω
$\hat{R}(1) = R_F$	0.4 Ω

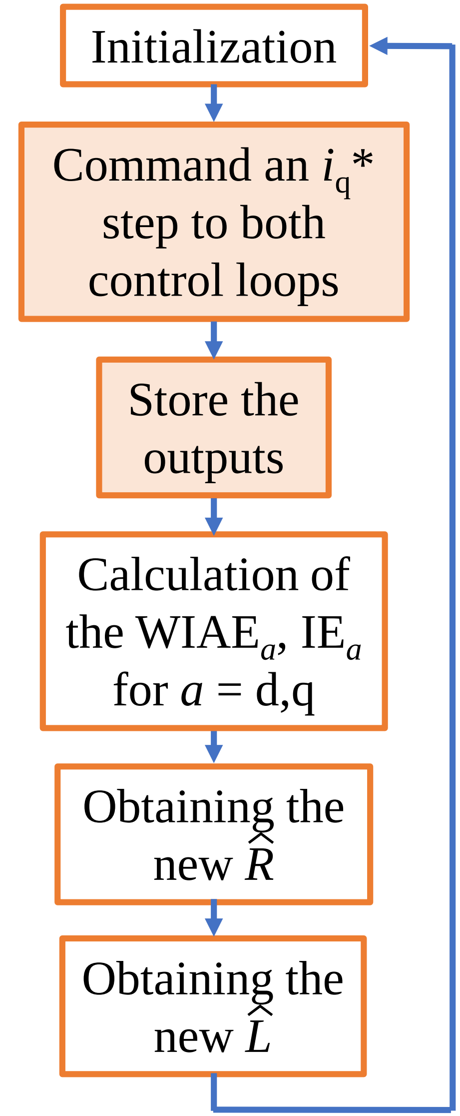

Developed Method

At each iteration (within each commanded step), **a correct estimate of both parameters is aimed.**

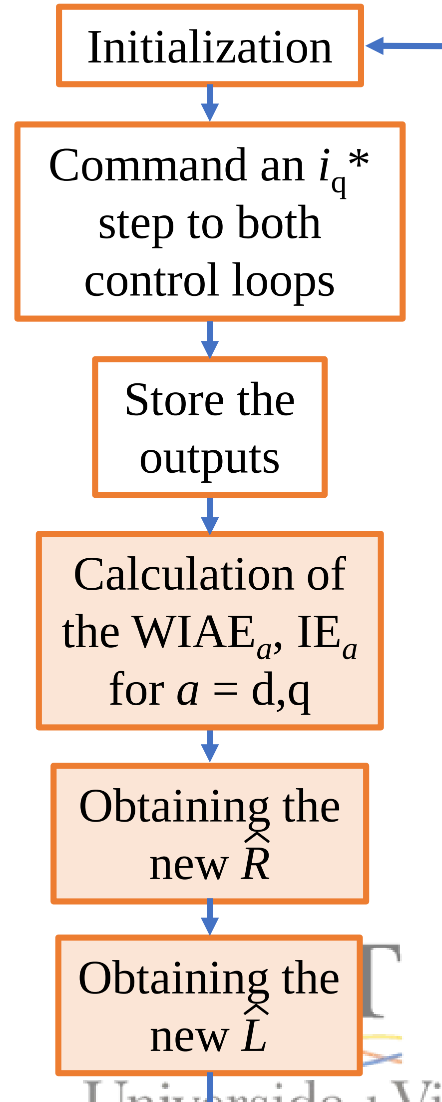

_L_ identification Vs _R_ identification:

- **$WIAE_d$ = IAE_d** for **under and overestimate cases**.
- **Initial overestimation** is also regarded.
- As the **delay** has an **important influence on the axis cross coupling**, T_s should be also considered when **updating** the new ***L* estimate**.

$$WIAE_d = IAE_d$$

$$WIAE_q \begin{cases} IAE_q & \text{if } IE_q \geq 0 \\ (IAE_q)^2 & \text{if } IE_q < 0 \end{cases}$$

$$\hat{L}(k+1) = [1+L_{F\_under} \cdot \Delta_d(k)] \cdot \hat{L}(k)$$

$$\Delta_d(k) = f\,(WIAE_d(k), i_q^*, T_s)$$

Developed Method

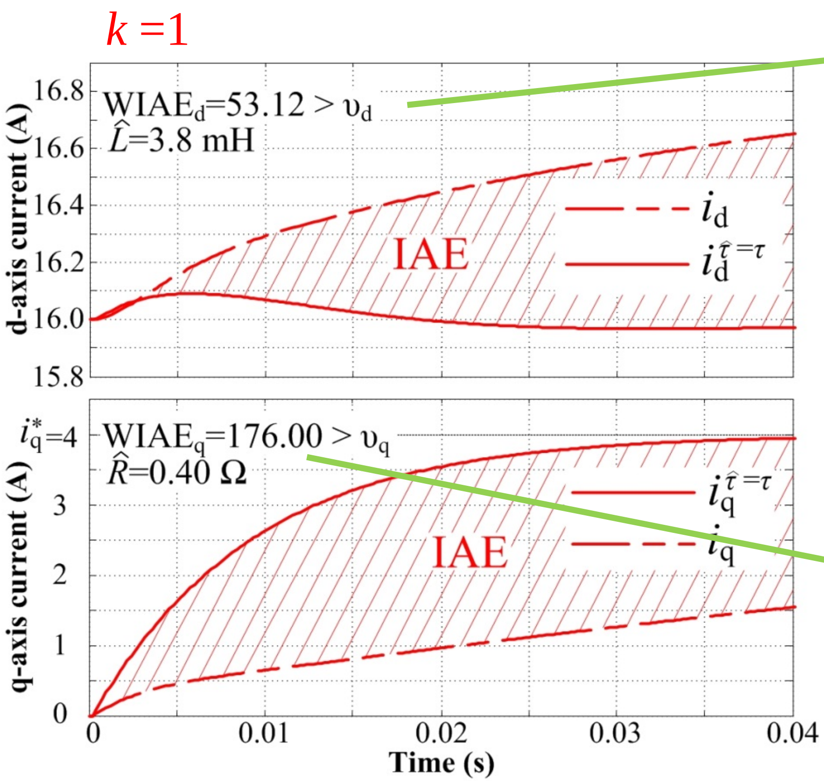

Approach to L 1st bound

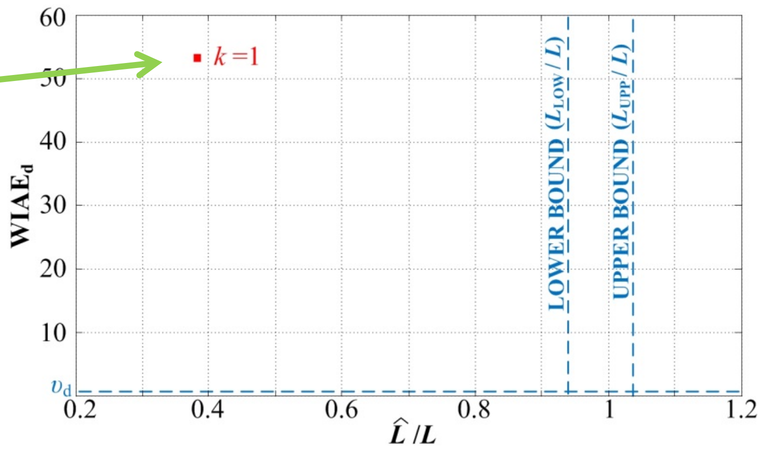

Approach to R 1st bound

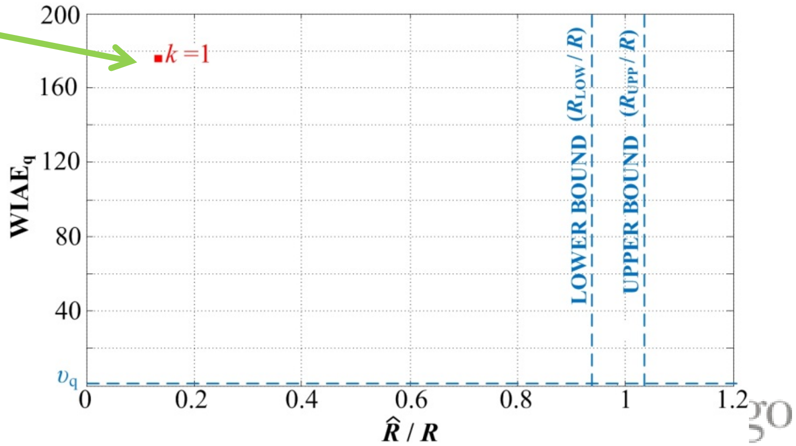

Pag. 67-73

Developed Method

k =17

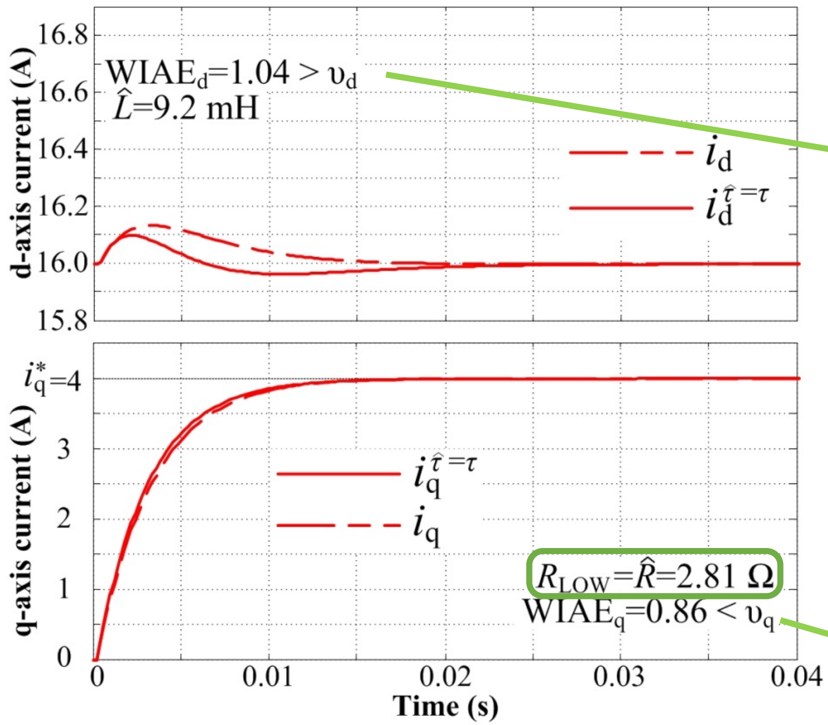

Approach to L 1st bound

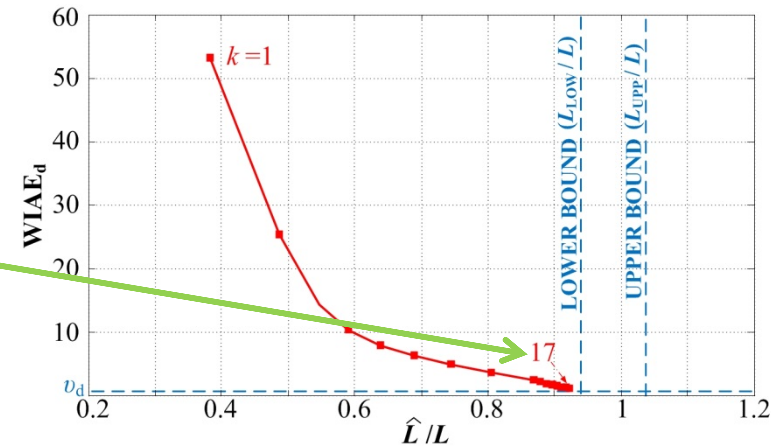

Approach to R 1st bound

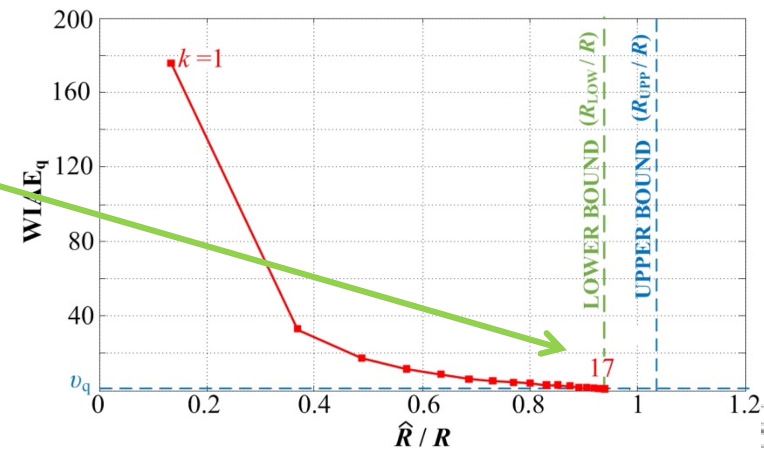

Pag.
67-73

Developed Method

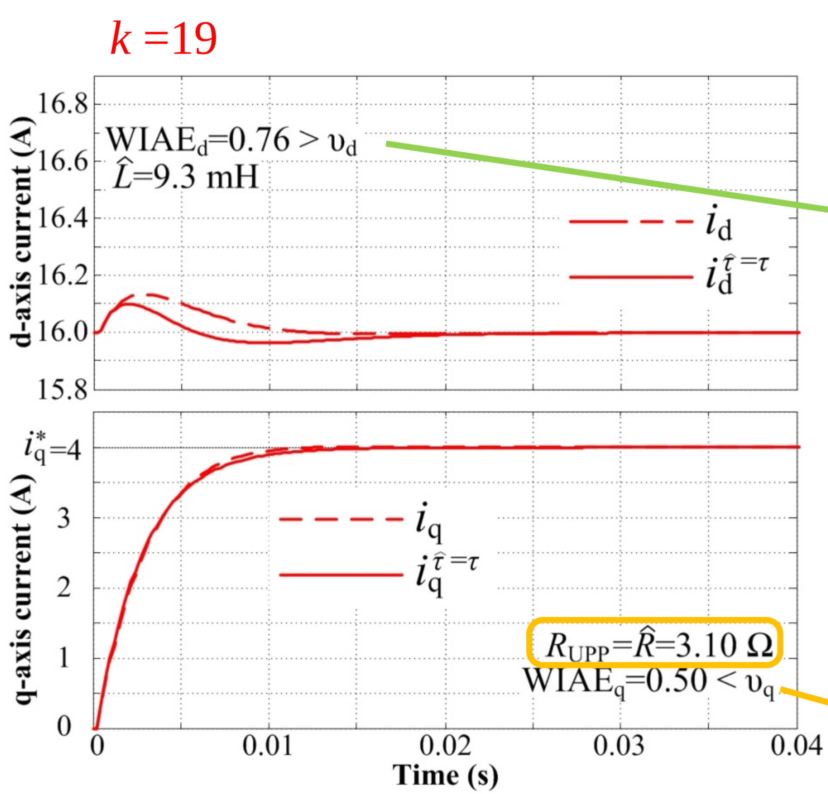

Approach to L 1st bound

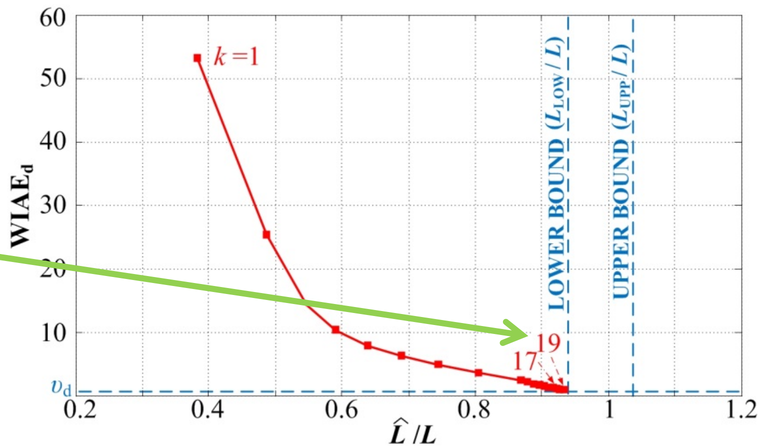

R refinement

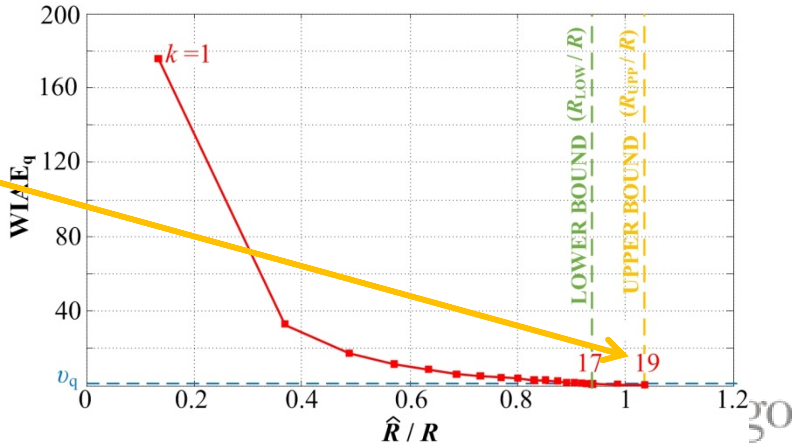

Pag. 67-73

Developed Method

$k = 20$

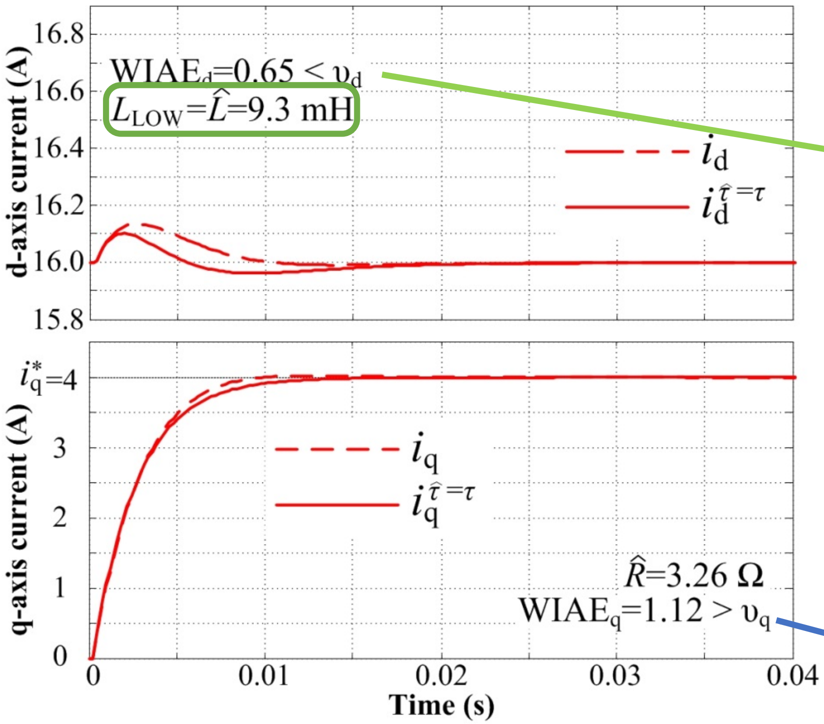

Approach to L 1st bound

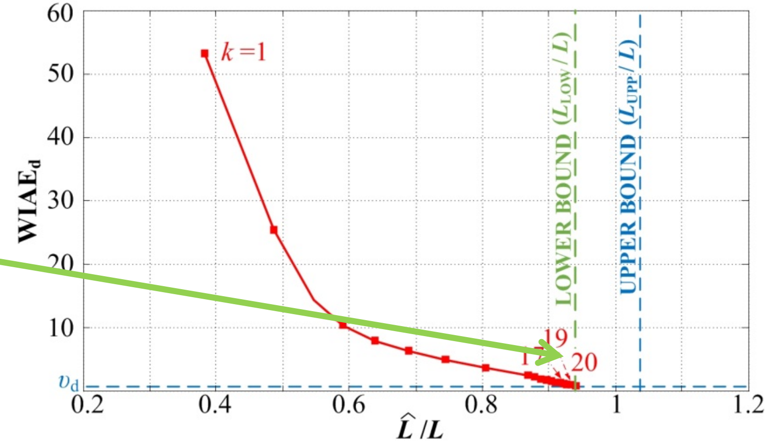

R estimation end

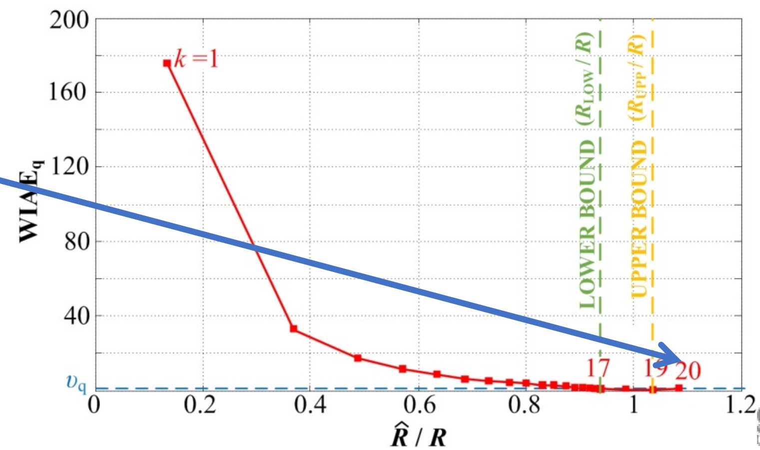

$$R^{met} = (R_{LOW} + R_{UPP})/2 = 2.96\ \Omega$$

Pag.
67-73

Developed Method

$k = 22$

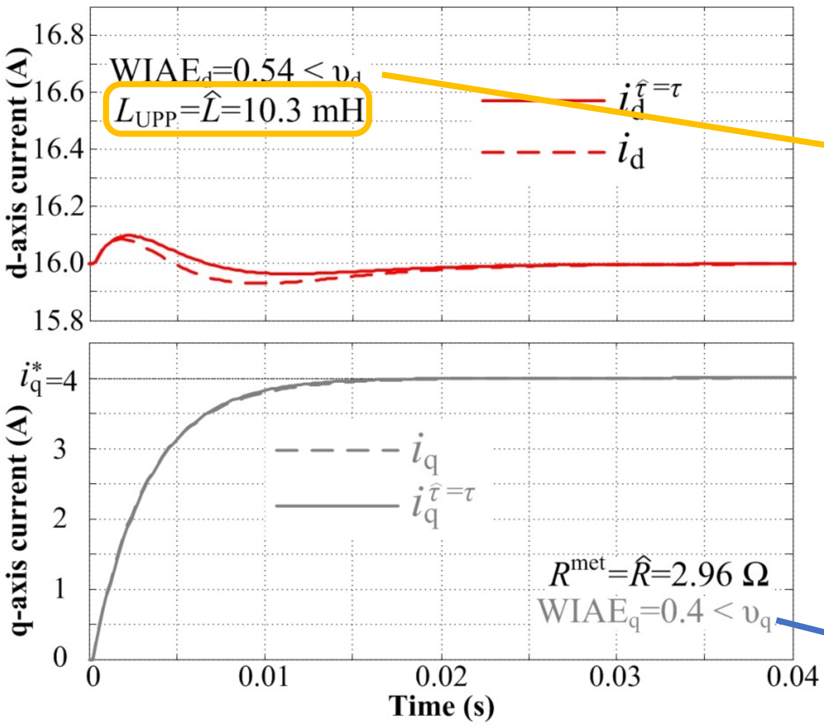

L refinement

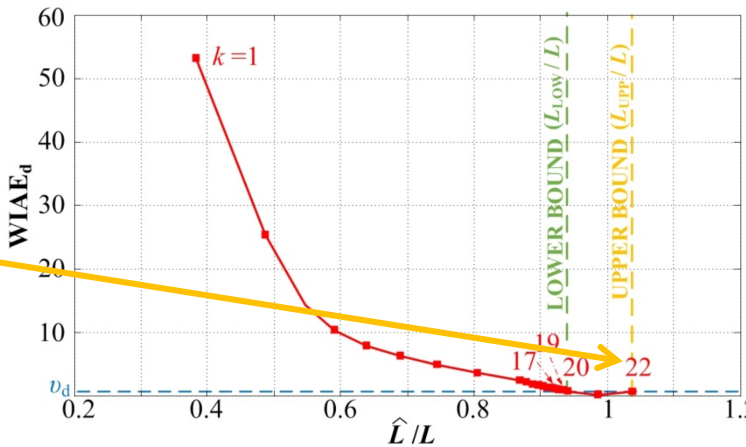

R estimation end

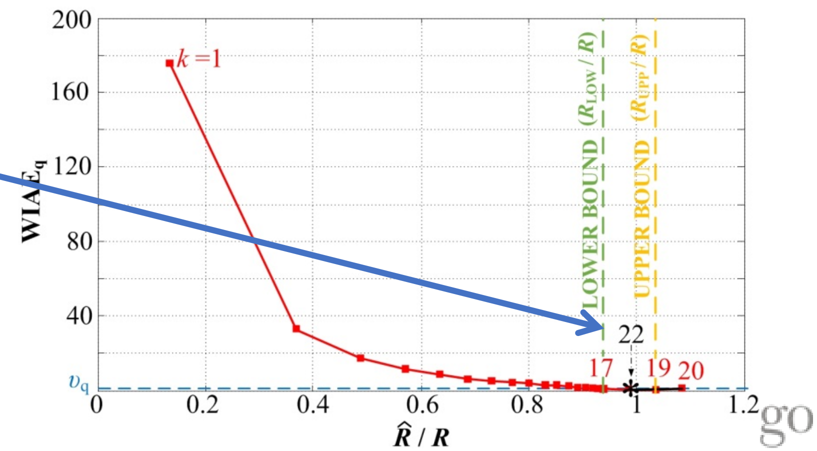

$$R^{met} = (R_{LOW} + R_{UPP})/2 = 2.96\ \Omega$$

Pag.
67-73

Developed Method

$$L^{met} = (L_{LOW} + L_{UPP})/2 = 9.8\text{ mH}$$

Estimation end

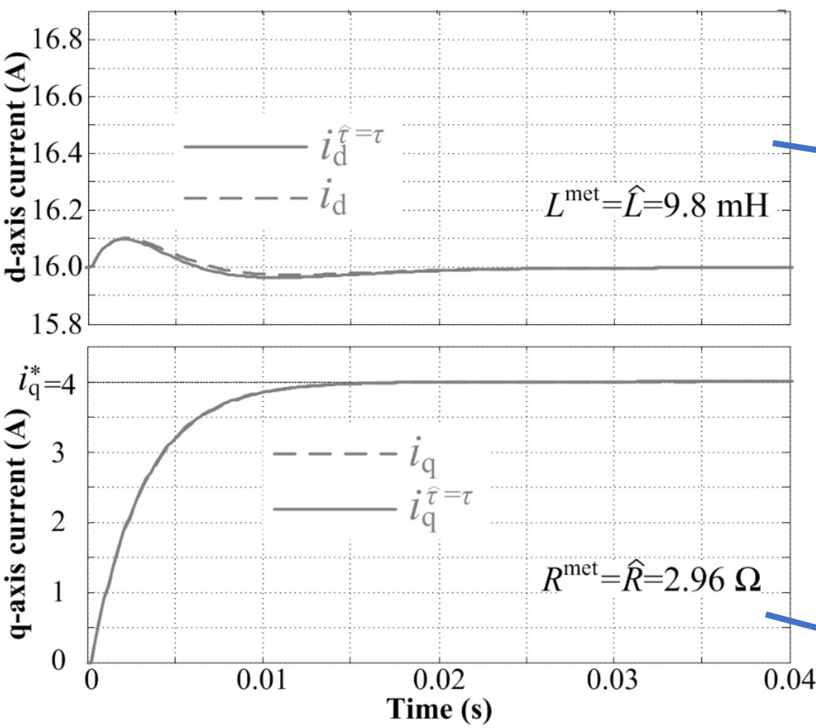

L estimation end

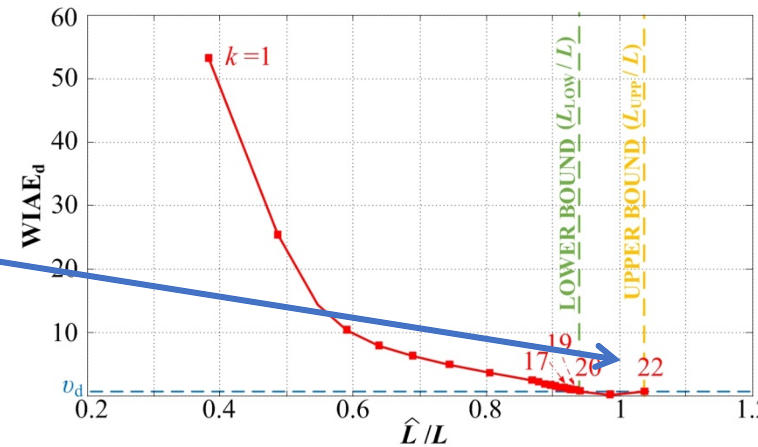

R estimation end

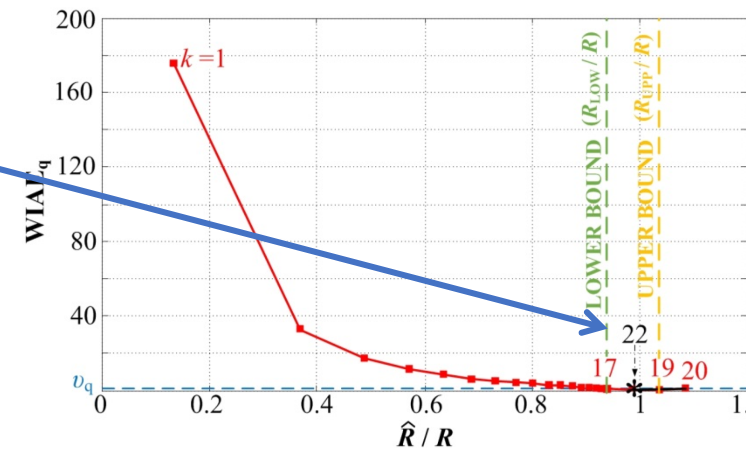

$$R^{met} = (R_{LOW} + R_{UPP})/2 = 2.96\ \Omega$$

Pag. 67-73

Other contents of Chapter 3

- **Analysis** of the **root-locus** diagrams with **L** and **LCL filters.**
  - To evaluate the validity of the **L admittance model for LCL filters**.
  - To study the **loop stability**.
  - To establish a **proper *K*** gain for the method.
  - To corroborate that a **correct estimation** of the plant parameters leads to a **better transient response**, in terms of overshoot and settling time.

Pag. 60-64

- **Parameter tuning guidelines**.

Pag. 73, 74

- **Theoretical examples** of **representative situations** with L and with LCL filters (P_{rated}, $V_{LL_{rated}}$, P_{level}, f_{sw}, f_s, i_q*, L_F, R_F, R_C).
  - For all the cases, R_C matches quite well R_C^{met} in few iterations.
  - **Study** of the **regions of convergence** as a function of the parameter mismatches.

Pag. 75-77

- **Implementation options**:
  - **Offline**, during a precommissioning stage.
  - **Online** → PICCD must be adopted to regulate the positive-sequence fundamental component of the current.

Pag. 74, 75

Experimental Setup

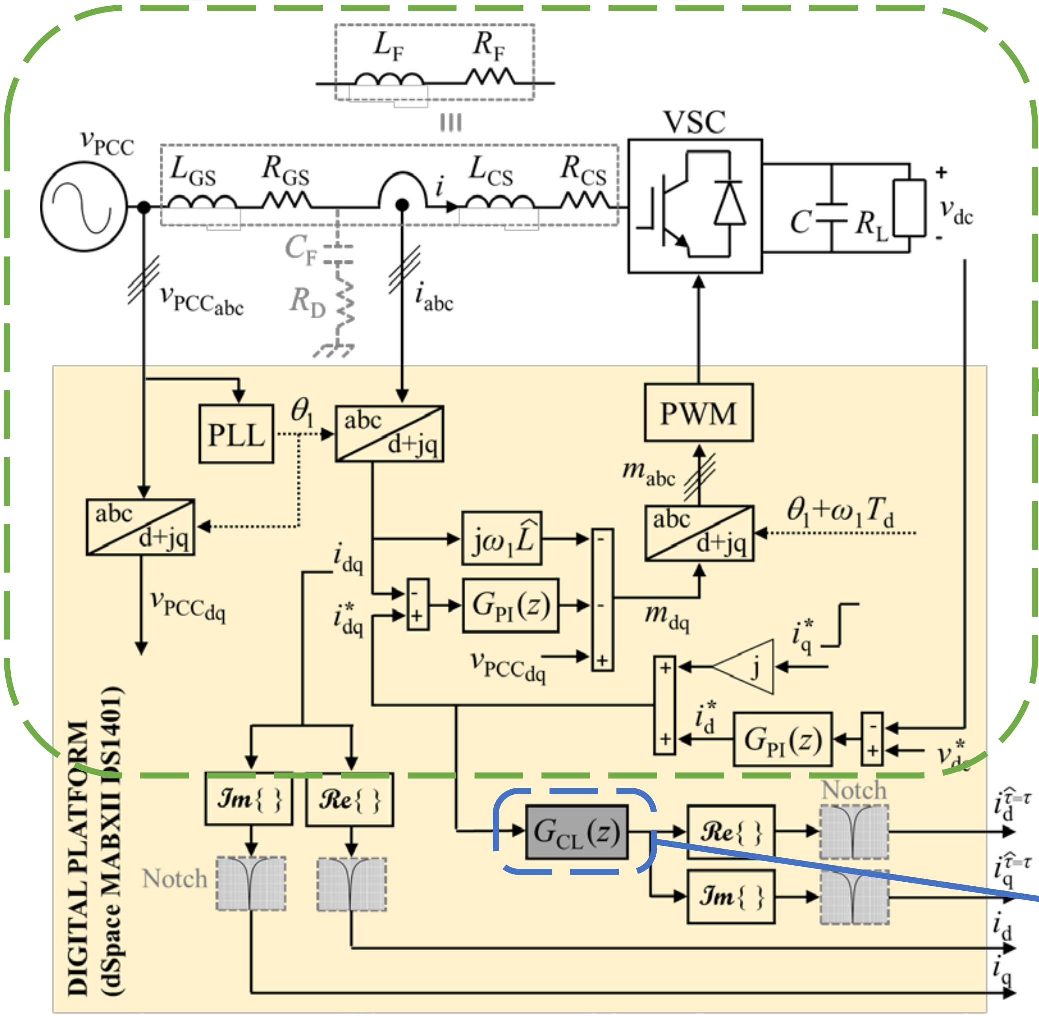

Actual control loop:

- plant → a 3-ph grid-tied VSC
- control → dSpace.

Simulated control loop:

- simulated plant + control → dSpace.

Pag. 77-78

Experimental Tests

Case (filter)	P_{dc}	f_{sw} f_s	L_F ($L_{GS}+L_{CS}$)	R	$\hat{L}(1)$	$\hat{R}(1)=R_F$ ($R_{GS}+R_{CS}$)	L^{met}	R^{met}	k_{max}
A (L)	4.3 kW	10 kHz 10 kHz	5.9 mH	2.3 Ω	$1.6L_F$ = 9.4 mH	0.4 Ω	5.9 mH	2.29 Ω	20
B (LCL)	4.3 kW	5 kHz 10 kHz	10.9 mH (5+5.9)	1.9 Ω	$1.6L_F$ = 17.4 mH	0.45 Ω (0.05+0.4)	11 mH	1.88 Ω	15
C (L)	2 kW	5 kHz 5 kHz	9.5 mH	3 Ω	$0.4L_F$ = 3.8 mH	0.4 Ω	9.8 mH	2.96 Ω	23
C (L)	2 kW	2.5 kHz 2.5 kHz	12.1 mH	1.7 Ω	$0.4L_F$ = 4.8 mH	0.4 Ω	12.6 mH	1.77 Ω	10

Pag. 79-84

APET Universida de Vigo

Test A

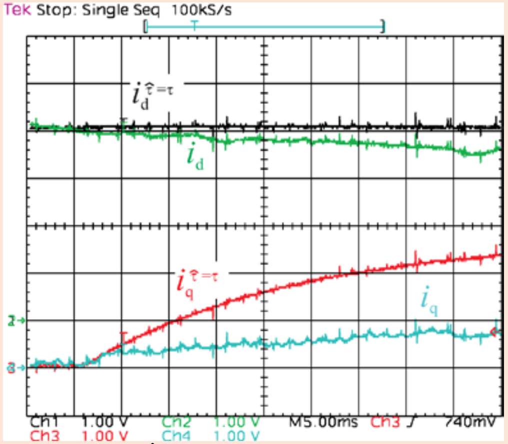

$k = 1$; $\widehat{R} = 0.4\ \Omega$;
$\widehat{L} = 9.4$ mH

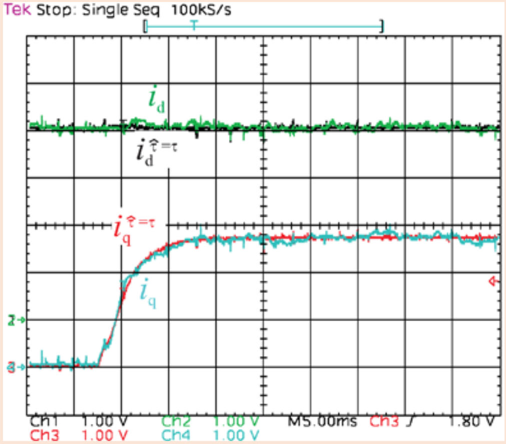

$k = 20$; $R^{met} = 2.29\ \Omega$;
$L^{met} = 5.9$ mH

Test B

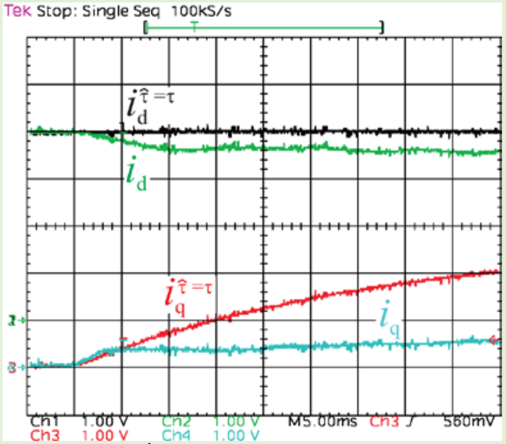

$k = 1$; $\widehat{R} = 0.45\ \Omega$;
$\widehat{L} = 17.4$ mH

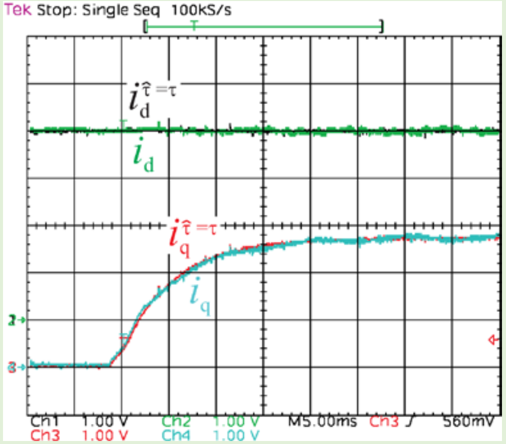

$k = 15$; $R^{met} = 1.88\ \Omega$;
$L^{met} = 11$ mH

Test C

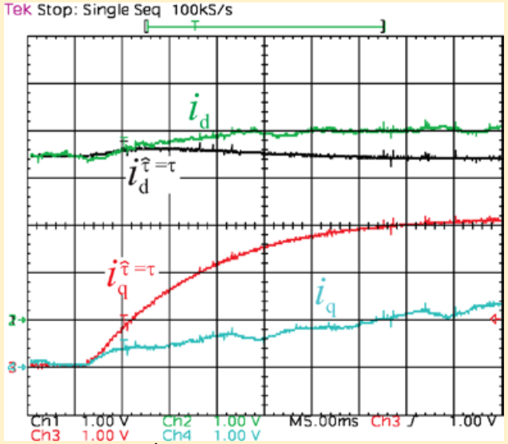

$k = 1$; $\widehat{R} = 0.4\ \Omega$;
$\widehat{L} = 4.8$ mH

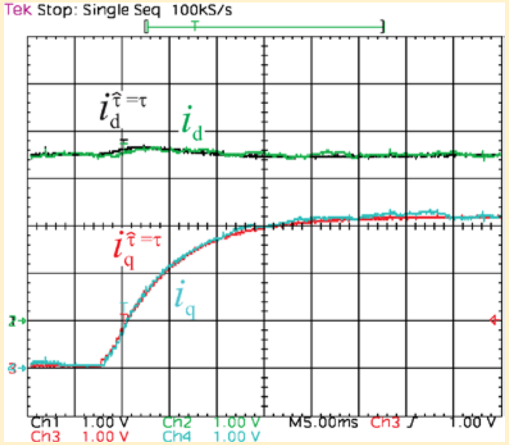

$k = 10$; $R^{met} = 1.77\ \Omega$;
$L^{met} = 12.6$ mH

Conclusions of Chapter 3

- A **method** to **identify** the two parameters of the current loop plant time constant at certain working conditions has been proposed:
  - **the equivalent inductance**
  - **the equivalent resistance**

→ Thus, the **dynamics** of the actual loop **may be properly studied** and the **controller parameters** can be **precisely tuned**.

- The **validity of modeling an LCL filter as an L one** from the viewpoint of the current loop is **analyzed** in detail, as a function of the **gain value**. → It is **demonstrated** that the **method** is also **valid** when **LCL filters** are employed.
- The **developed iterative algorithm** works in **closed loop**, at the same sampling frequency as the rest of the control. It **takes advantage of the current closed loop properties**, and **of the current controller itself** to perform the estimation. Hence, it is **particularly designed** to satisfy **time-domain specifications**.

Pag.
81, 84

APET
Universidade Vigo

Outline

APET
Universidade Vigo

Framework

- In order **to fulfill** the dynamic **GC requirements** (**LVRT** and **grid support**), an **enhanced transient response of the current loop is crucial**, which can be achieved thanks to a **precise tuning of the current controllers**.

- **Resonant regulators** (such as PR ones) have been proved to be a **good choice** for **grid connection**.

- There is a **lack of specific methods** for **PR controller tuning considering this demanding scenario**.

Pag.
85-87

Transient Assessment From the Error Signal Roots

- **Methodology** based on the **root-locus inspection** in the ***z*-domain** of the **current error** signal **caused by transients**:
  - Transients **in the current reference** $\Delta i^*(z)$
  - Transients **in the disturbance** $\Delta v_{PCC}(z)$

1st step:

Discrete-time expression of the global error

$$E(z) = I^*(z) - I(z)$$
$$E(z) = E_{\Delta i^*}(z)\big|_{\Delta v_{PCC}=0} + E_{\Delta v_{PCC}}(z)\big|_{\Delta i^*=0}$$

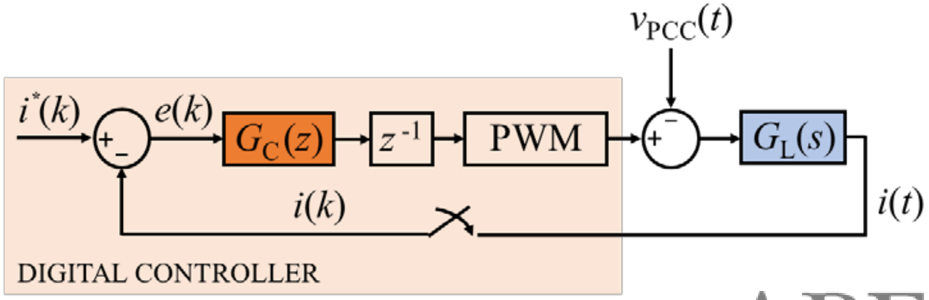

Pag. 89, 90

APET Universidade Vigo

Transient Assessment From the Error Signal Roots

- **Methodology** based on the **root-locus inspection** in the ***z*-domain** of the **current error** signal **caused by transients**:
  - Transients **in the current reference** $\Delta i^*(z)$
  - Transients **in the disturbance** $\Delta v_{PCC}(z)$

1st step: **Discrete-time expression of the global error**

$$E(z) = E_{\Delta i^*}(z)\big|_{\Delta v_{PCC}=0} + E_{\Delta v_{PCC}}(z)\big|_{\Delta i^*=0}$$

$$E_{\Delta i^*}(z)\big|_{\Delta v_{PCC}=0} = \frac{1}{1+G_C(z)z^{-1}G_L^{ZOH}(z)}\Delta i^*(z)$$

Pag. 89, 90

$$\Delta i^*(z) = (A_{new}-A_{old})\underbrace{\frac{1-z^{-1}\cos(\omega_1' T_s)}{1-2z^{-1}\cos(\omega_1' T_s)+z^{-2}}}_{\text{cosine term}} + (B_{new}-B_{old})\underbrace{\frac{z^{-1}\sin(\omega_1' T_s)}{1-2z^{-1}\cos(\omega_1' T_s)+z^{-2}}}_{\text{sine term}}$$

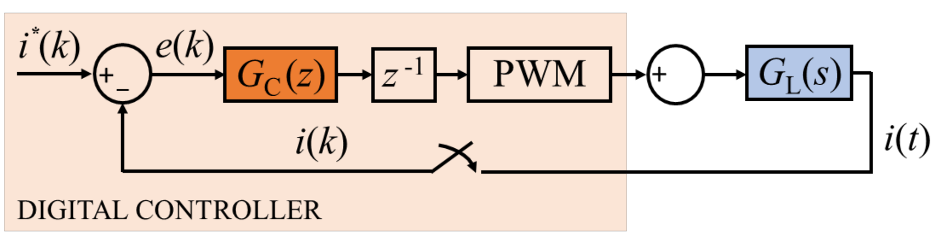

Transient Assessment From the Error Signal Roots

- **Methodology** based on the **root-locus inspection** in the ***z*-domain** of the **current error** signal **caused by transients**:
  - Transients **in the current reference** $\Delta i^*(z)$
  - Transients **in the disturbance** $\Delta v_{PCC}(z)$

1st step: **Discrete-time expression of the global error**

$$E(z) = E_{\Delta i^*}(z)\big|_{\Delta v_{PCC}=0} + E_{\Delta v_{PCC}}(z)\big|_{\Delta i^*=0}$$

$$E_{\Delta v_{PCC}}(z)\big|_{\Delta i^*=0} = \frac{G_L^{\text{Tustin}}(z)}{1+G_C(z)z^{-1}G_L^{\text{ZOH}}(z)}\Delta v_{PCC}(z)$$

Pag. 89, 90

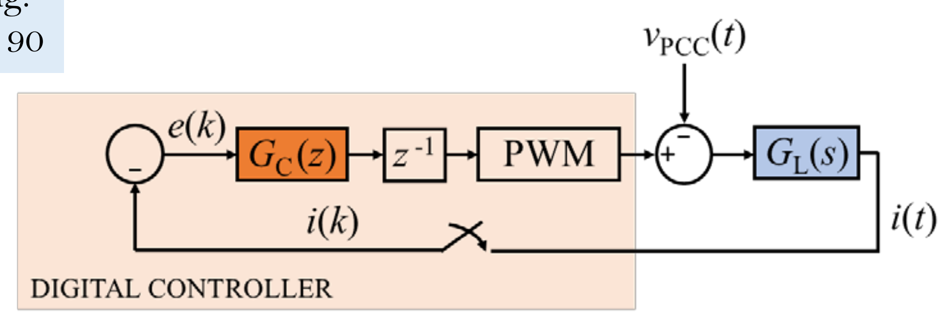

APET
Universidade Vigo

Transient Assessment From the Error Signal Roots

1st step: **Discrete-time expression of the global error.**

- $E(z) = E_{\Delta i^*}(z)|_{\Delta v_{\text{PCC}}=0} + E_{\Delta v_{\text{PCC}}}(z)|_{\Delta i^*=0}$

2nd step: **Graphical representation of the error signal roots as a function of the controller gain → Root loci.**

- Influence on the stability, decay rate, damping.

3rd step: **Accurate prediction of the error waveform.**

- Analysis of the effects of the root position on the transient response.

4th step: **Gain tuning.**

- **Optimization** of the error **transient response** can be achieved:
  - By making the **poles fast** → **large decay rates**.
  - By placing the poles **next to zeros** that cancel their effect → **small residues**

Pag. 89, 90

APET Universida de Vigo

Transient Assessment From the Error Signal Roots

1st step:

Discrete-time expression of the global error.

- $E(z) = E_{\Delta i^*}(z)|_{\Delta v_{PCC}=0} + E_{\Delta v_{PCC}}(z)|_{\Delta i^*=0}$

2nd step:

Graphical representation of the error signal roots as a function of the controller gain → Root loci.

- Influence on the stability, decay rate, damping.

3rd step:

Accurate prediction of the error waveform.

- Analysis of the effects of the root position on the transient response.

4th step:

Gain tuning.

- **Optimization** of the error **transient response** can be achieved:
  - by making the **poles fast** → **large decay rates.**
  - by placing the poles **next to zeros** that cancel their effect → **small residues.**

Pag. 89, 90

APET Universidade Vigo

Transient Assessment From the Error Signal Roots

1st step: **Discrete-time expression of the global error.**

- $E(z) = E_{\Delta i^*}(z)|_{\Delta v_{\mathrm{PCC}}=0} + E_{\Delta v_{\mathrm{PCC}}}(z)|_{\Delta i^*=0}$

2nd step: **Graphical representation of the error signal roots as a function of the controller gain → Root loci.**

- Influence on the stability, decay rate, damping.

3rd step: **Accurate prediction of the error waveform.**

- Analysis of the effects of the root position on the transient response.

4th step: **Gain tuning.**

- **Optimization** of the error **transient response** can be achieved:
  - by making the **poles fast → large decay rates.**
  - by placing the poles **next to zeros** that cancel their effect → **small residues.**

Pag. 89, 90

Transient Assessment From the Error Signal Roots

1st step: **Discrete-time expression of the global error.**

- $E(z) = E_{\Delta i^*}(z)|_{\Delta v_{\mathrm{PCC}}=0} + E_{\Delta v_{\mathrm{PCC}}}(z)|_{\Delta i^*=0}$

2nd step: **Graphical representation of the error signal roots as a function of the controller gain → Root loci.**

- Influence on the stability, decay rate, damping.

3rd step: **Accurate prediction of the error waveform.**

- Analysis of the effects of the root position on the transient response.

4th step: **Gain tuning.**

- **Optimization** of the error **transient response** can be achieved:
  - by making the **poles fast → large decay rates,**
  - by placing the **poles next to zeros** that cancel their effect → **small residues.**

Pag. 89, 90

Transient Assessment From the Error Signal Roots

1st step: **Discrete-time expression of the global error.**

2nd step: **Graphical representation of the error signal roots as a function of the controller gain → Root loci.**

3rd step: **Accurate prediction of the error waveform.**

4th step: **Gain tuning.**

Specific conditions → Design Study

Pag.
89, 90

APET
Universidade Vigo

Tests

1st step: **Discrete-time expression of the global error.**

2nd step: **Graphical representation of the error signal roots as a function of the controller gain → Root loci.**

3rd step: **Accurate prediction of the error waveform.**

4th step: **Gain tuning.**

Three control situations:

- A. PR controller tuned at f_1. High sampling frequency (f_s = 10 kHz).
- B. PR controller tuned at f_1, f_5 and f_7. High sampling frequency (f_s = 10 kHz).
- C. PR controller tuned at f_1. Low sampling frequency (f_s = 2.5 kHz).

Two transients:

- I. Transients in the current reference: a phase change of 90º in i^*. $\Delta i^*(z)$
- II. Transients in the disturbance: a type 'C' sag in v_{PCC}. $\Delta v_{PCC}(z)$

Pag. 89, 90

A. PR Controller Tuned at f_1. High f_s (10 kHz)

2nd step: **Graphical representation of the error signal roots as a function of the controller gain → Root loci.**

Pag. 90-94

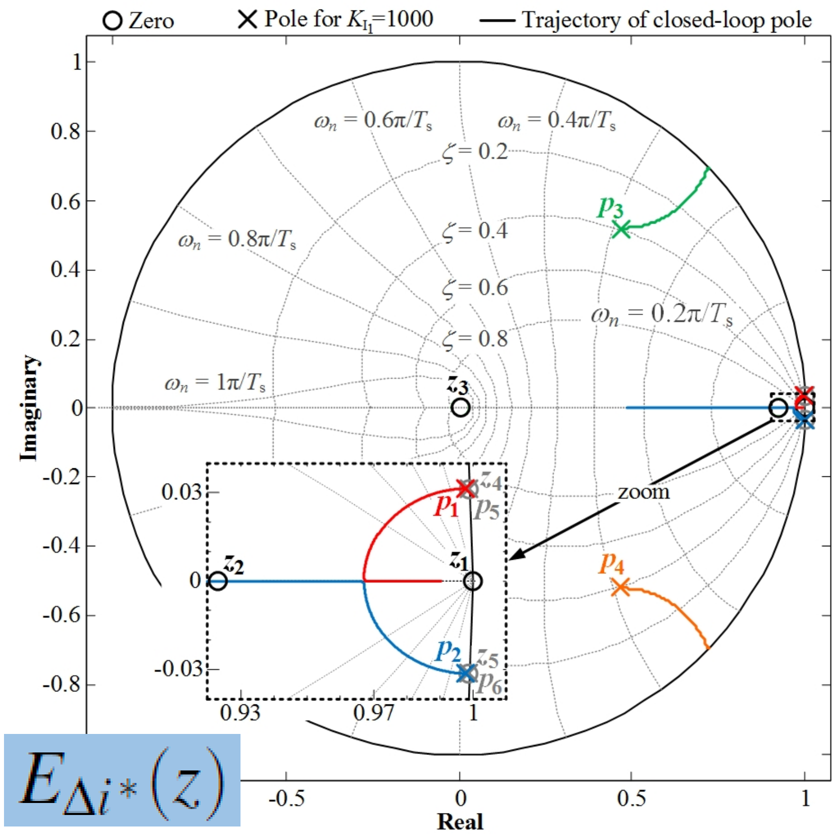

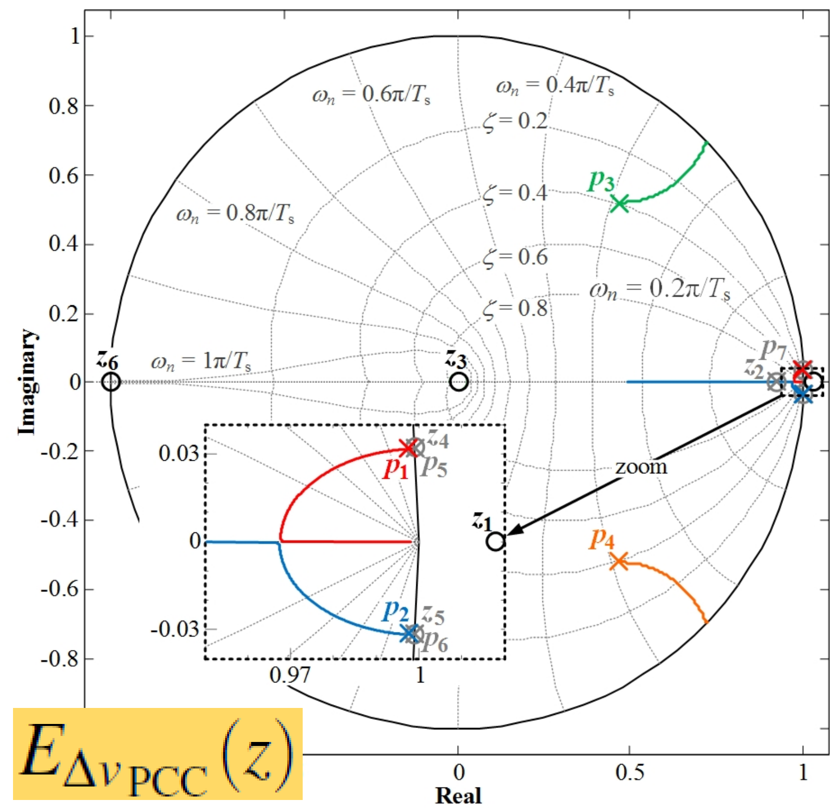

Universidade Vigo

A. PR Controller Tuned at f_1. High f_s (10 kHz)

3rd step: **Analysis of the effects of the root position on the transient response.**

Pag. 90-94

Analysis of four values of K_{I1}.

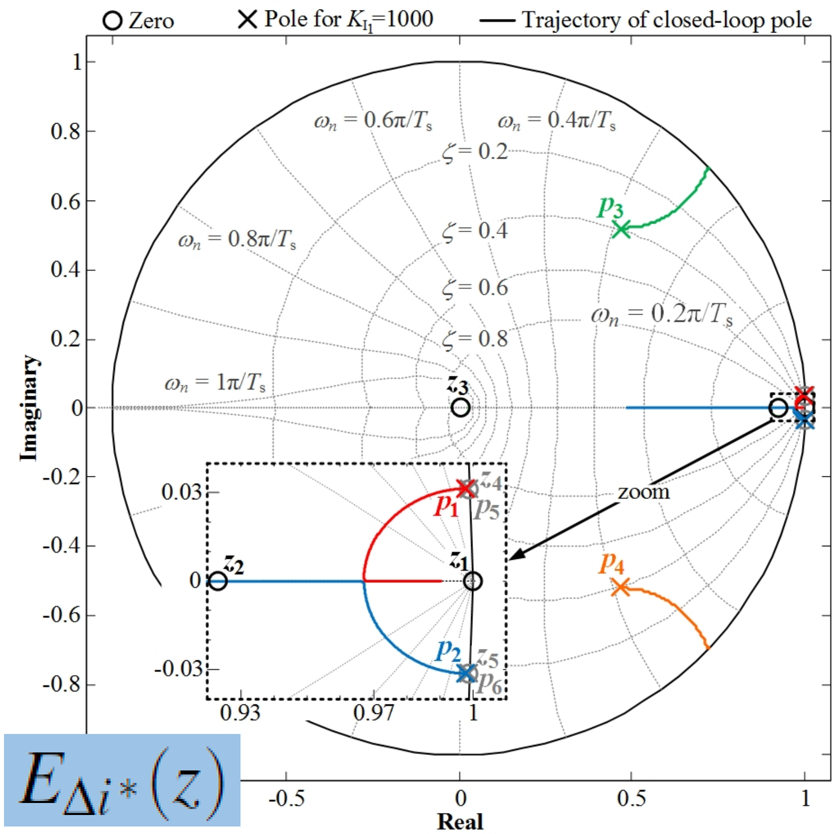

$E_{\Delta i^*}(z)$

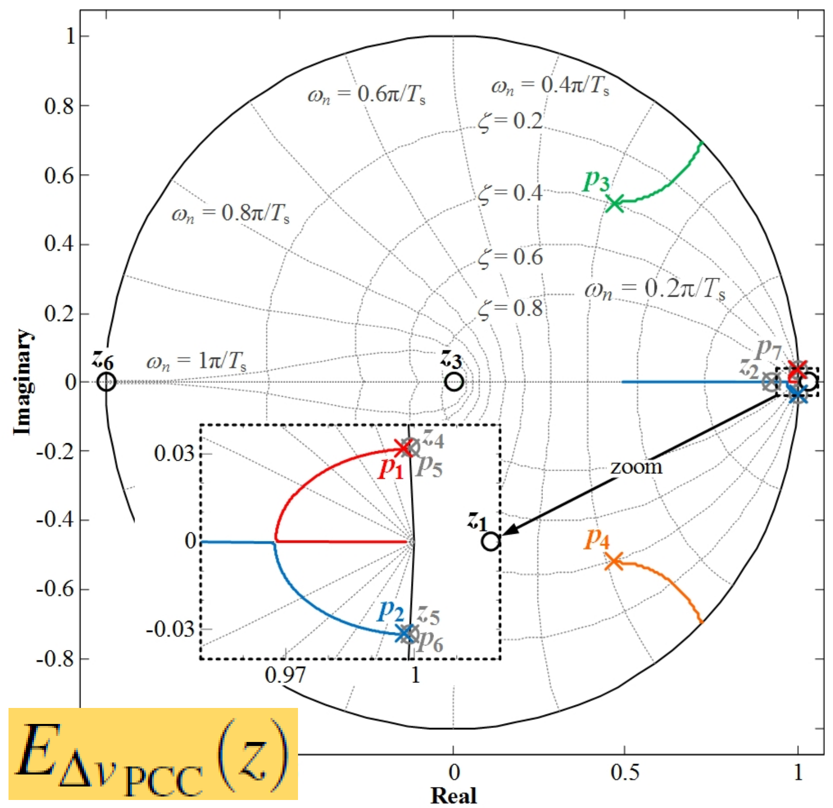

$E_{\Delta v_{PCC}}(z)$

Universidade de Vigo

A. PR Controller Tuned at f_1. High f_s (10 kHz)

Typical value K_{I_1} = 2000:

- $\boldsymbol{p_1}$ **&** $\boldsymbol{p_2}$ **(dominant) slow** and **oscillating**;
- p_3 & p_4 faster than p_1 & p_2, and also oscillating.

→ Not a good choice.

Pag. 93-96

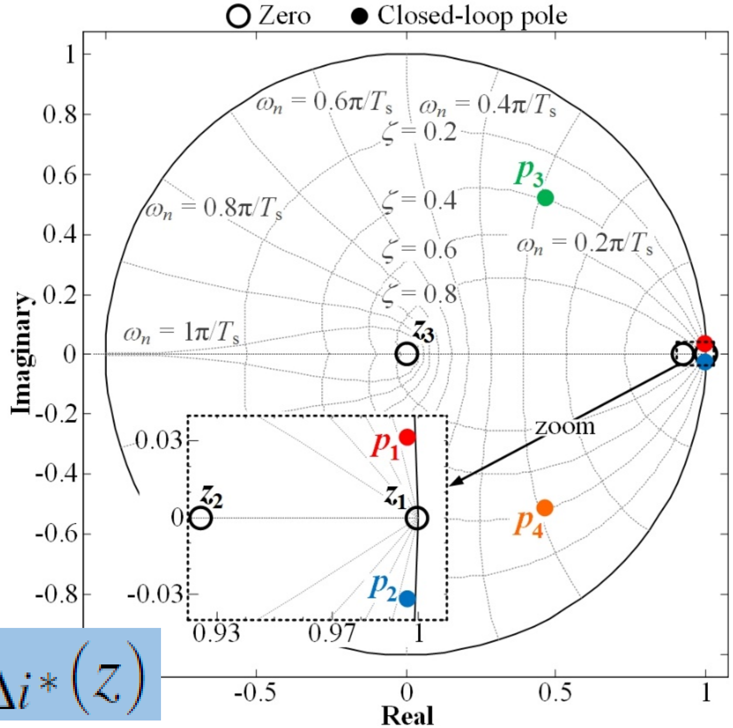

$E_{\Delta i^*}(z)$

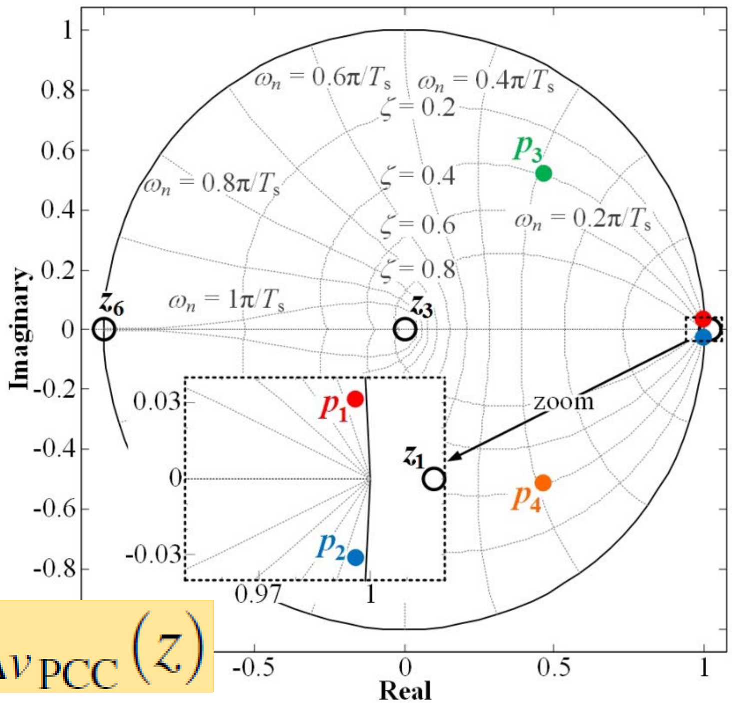

$E_{\Delta v_{PCC}}(z)$

A. PR Controller Tuned at f_1. High f_s (10 kHz)

K_{I_1} = 17645:

- **$p_1 = p_2$ dominant** and **nonoscillating**;
- p_3 & p_4 practically unchanged with respect to those with K_{I_1} = 2000.

+

Not such a big impact of zeros on the dominant poles.

Fastest position of p_1.

→ **Optimal** for changes in the **disturbance.**

Pag. 93-96

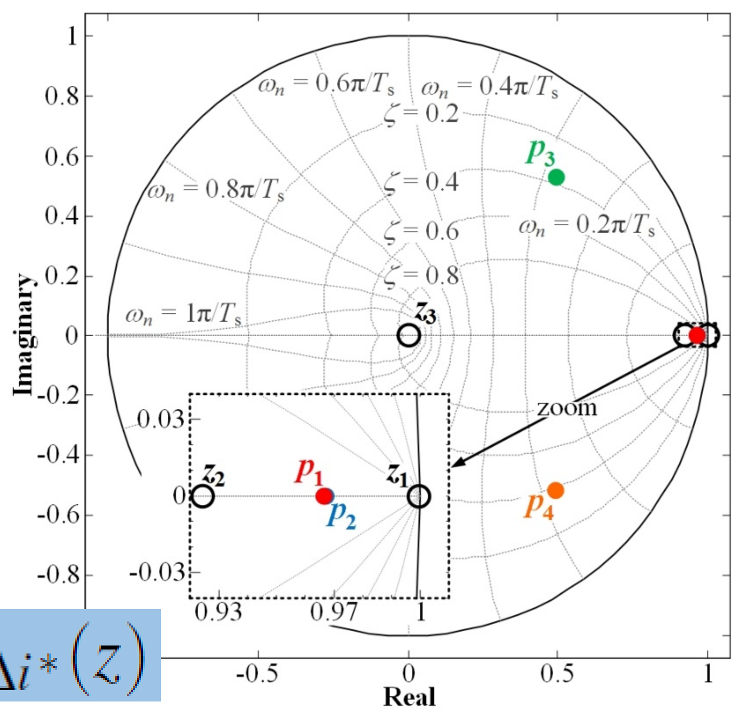

$E_{\Delta i^*}(z)$

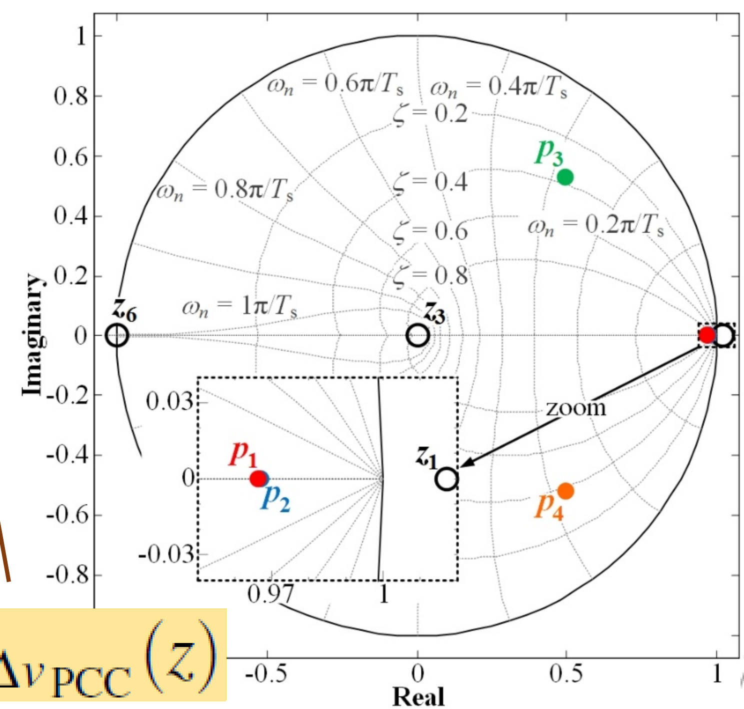

$E_{\Delta v_{PCC}}(z)$

A. PR Controller Tuned at f_1. High f_s (10 kHz)

K_{I_1} = 34000:

- **$p_1 > p_2$ dominant** and **nonoscillating**;
- p_3 & p_4 practically unchanged with respect to those with K_{I_1} = 2000.

\+ **Zeros closer** to the **dominant poles.** → **Optimal** for changes in the **current reference**.

Pag. 93-96

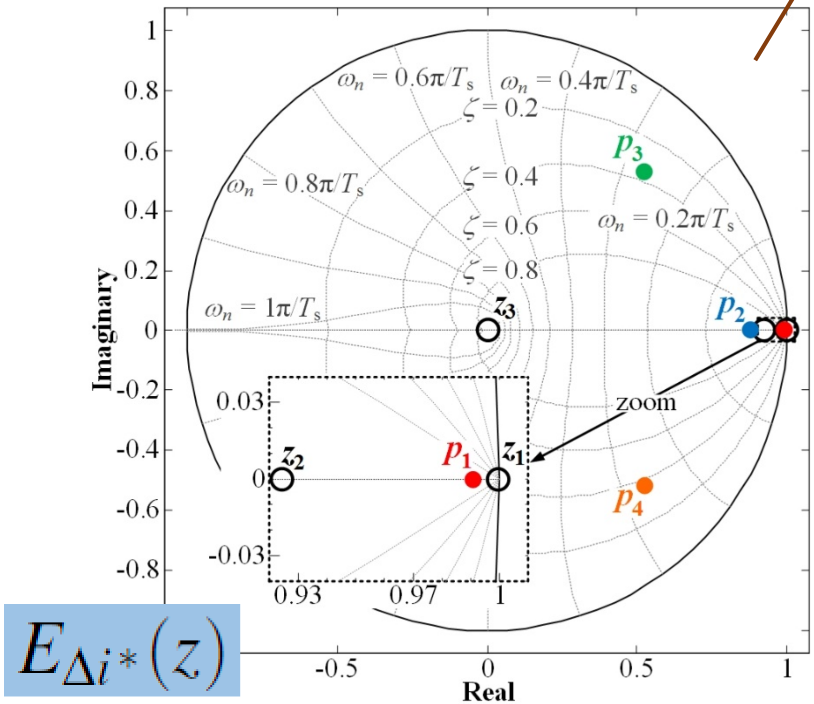

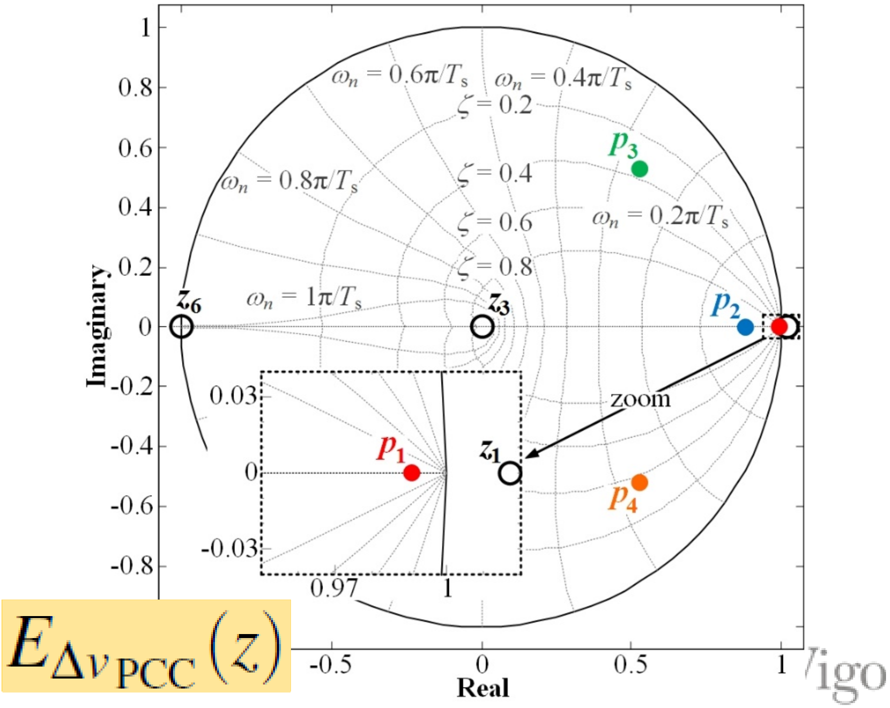

A. PR Controller Tuned at f_1. High f_s (10 kHz)

K_{I_1} = 100000:

- p_1 slower and almost cancelled by a zero;
- p_2 faster and nonoscillating;
- **p_3 & p_4 dominant** and **very oscillating**.

Not a good choice.

Pag. 93-96

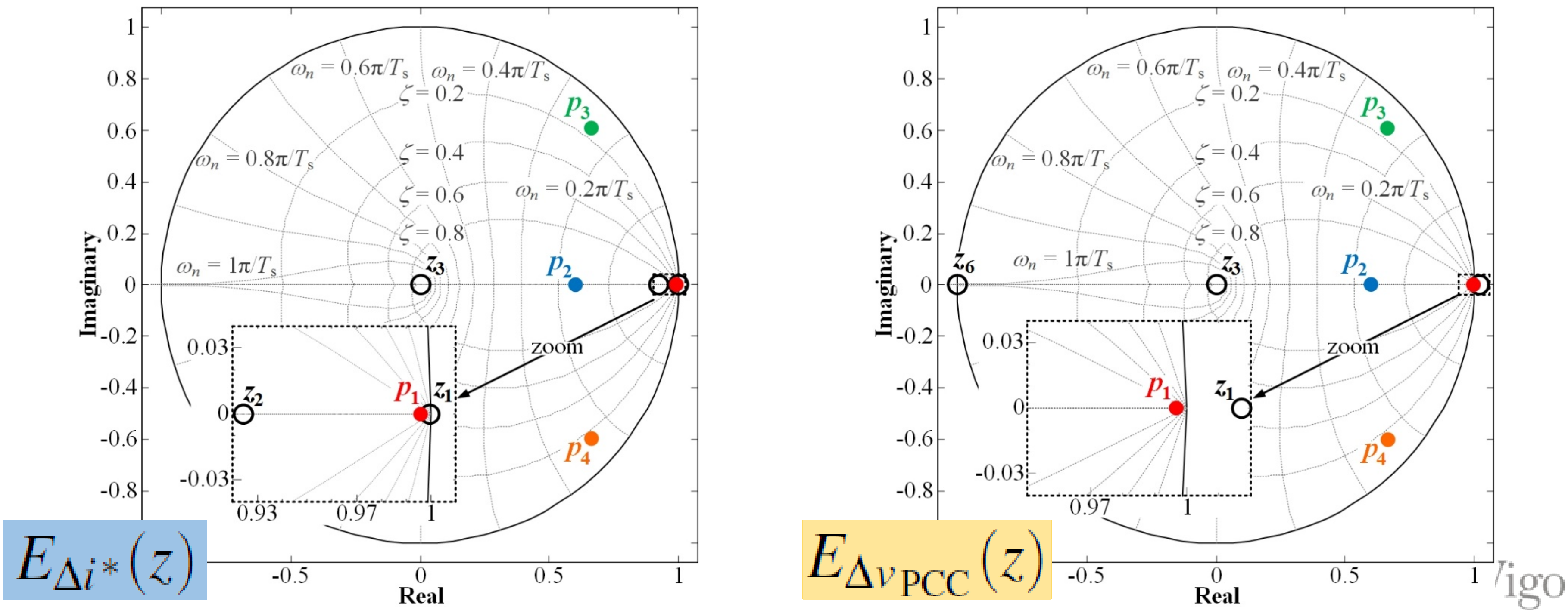

A. PR Controller Tuned at f_1. High f_s (10 kHz)

4th step: **Gain tuning.**

Pag. 93-96

A tradeoff is needed.

	Optimal gain
$E_{\Delta i^*}(z)$	$K_{I_1} = 34000$
$E_{\Delta v_{PCC}}(z)$	$K_{I_1} = 17645$

APET Universidade Vigo

A. PR Controller Tuned at f_1. High f_s (10 kHz)

4th step: **Gain tuning.**

Pag. 93-96

A tradeoff is needed.

	Optimal gain
$E_{\Delta i^*}(z)$	$K_{I_1} = 34000$
$E_{\Delta v_{PCC}}(z)$	$K_{I_1} = 17645$

The disturbance rejection response is usually more critical than the reference tracking one.

APET
Universidade Vigo

B. PR Controller Tuned at f_1, f_5 and f_7. High f_s (10 kHz)

$K_{I5} = K_{I7} = 2000$

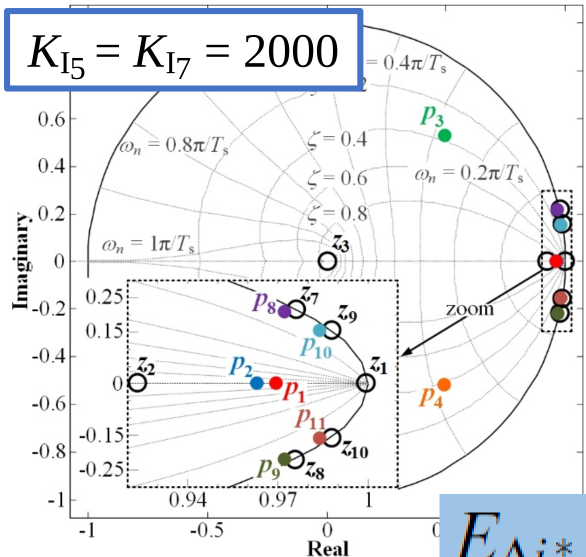

$$E_{\Delta i^*}(z)$$

$K_{I5} = K_{I7} = 17645$

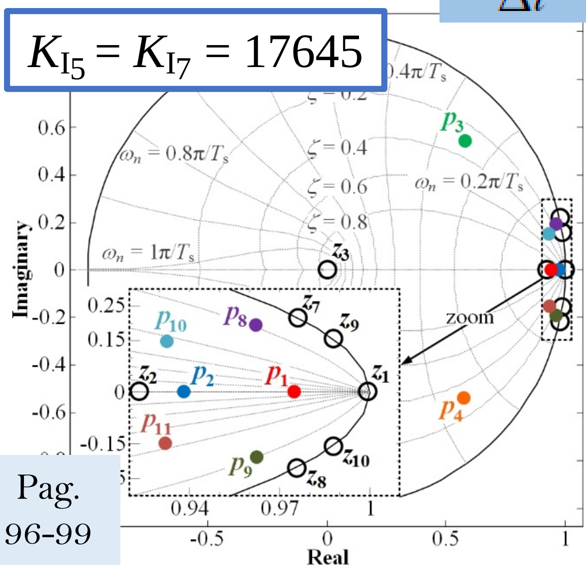

Pag. 96-99

3rd step: Analysis of the effects of the root position on the transient response.

$K_{I1} = 17645$ + two different values of K_{I5} and K_{I7}.

New zeros at the unit circle boundary:

- Impossible to place the new poles far from the unit circle boundary and at the same time, next to those zeros.
- **Difficult to draw conclusions from the root loci.**

Accurate prediction of the error waveform.

Partial-fraction expansions: poles & residues. → Overshoot & settling time. → 4th step: Gain selection.

$K_{I5} = K_{I7} = 17645$

B. PR Controller Tuned at f_1, f_5 and f_7. High f_s (10 kHz)

$K_{I5} = K_{I7} = 2000$

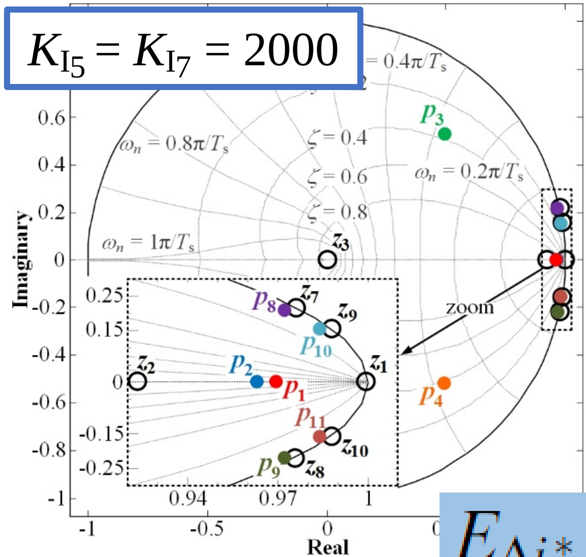

$E_{\Delta i^*}(z)$

$K_{I5} = K_{I7} = 17645$

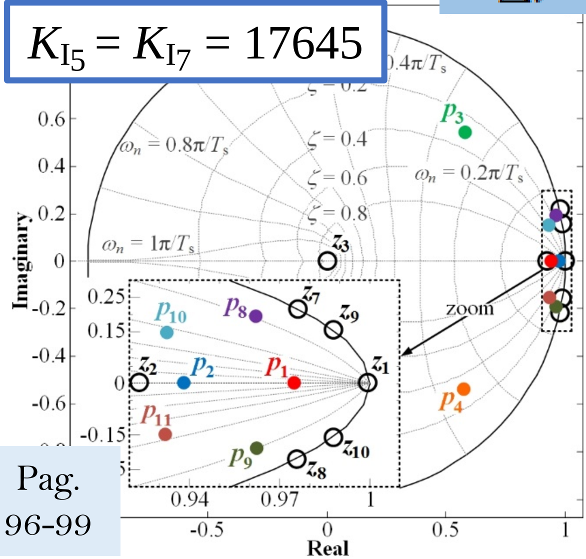

3rd step: **Analysis of the effects of the root position on the transient response.**

$K_{I1} = 17645$ + two different values of K_{I5} and K_{I7}.

New zeros at the **unit circle boundary**:

- **Impossible** to place the **new poles far** from the unit circle boundary **and at the same time, next to those zeros.**
- **Difficult to draw conclusions from the root loci.**

Pag. 96-99

B. PR Controller Tuned at f_1, f_5 and f_7. High f_s (10 kHz)

$K_{I5} = K_{I7} = 2000$

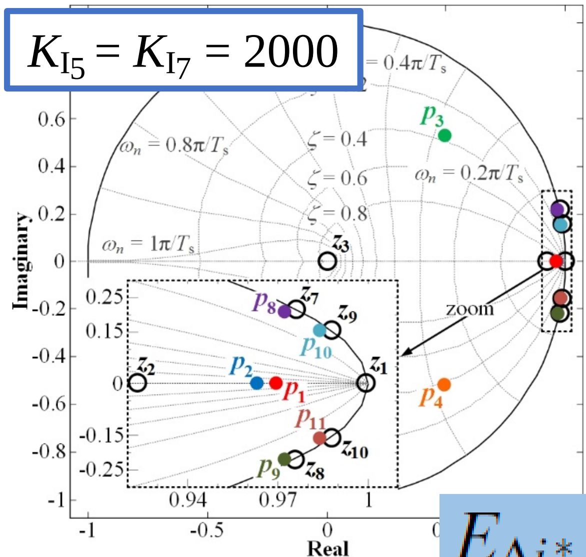

$E_{\Delta i^*}(z)$

$K_{I5} = K_{I7} = 17645$

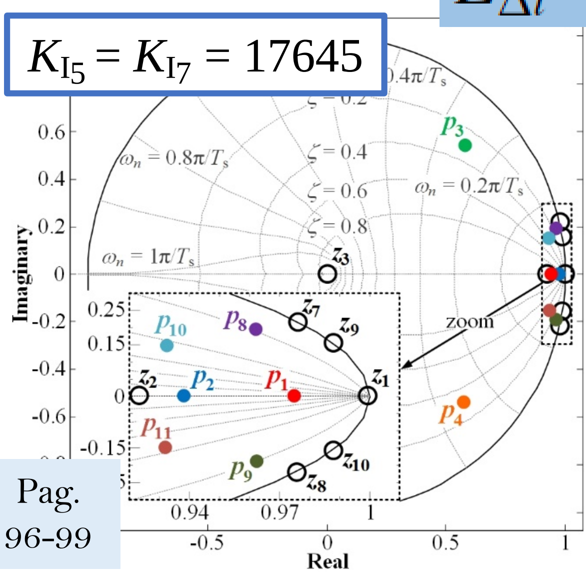

Pag. 96-99

3rd step: **Analysis of the effects of the root position on the transient response.**

$K_{I1} = 17645$ + two different values of K_{I5} and K_{I7}.

New zeros at the **unit circle boundary**:

- **Impossible** to place the **new poles far** from the unit circle boundary **and at the same time**, **next to those zeros.**
- **Difficult to draw conclusions from the root loci.**

Accurate prediction of the error waveform.

Partial-fraction expansions: poles & residues. → Settling time & overshoot. → **4th step:** **Gain selection.**

$K_{I5} = K_{I7} = 17645$

C. PR Controller Tuned at f_1. Low f_s (2.5 kHz)

Gain tuning.

- To favor the settling time of the disturbance rejection response.
- K_{I_1} = 5262 → $\boldsymbol{p_1 = p_2}$ **dominant** and **nonoscillating**.

- Compared to the corresponding ones at 10 kHz, $\boldsymbol{p_3}$ **&** $\boldsymbol{p_4}$ have **more impact at 2.5 kHz**, due to the **delay** effect.

Pag. 96-99

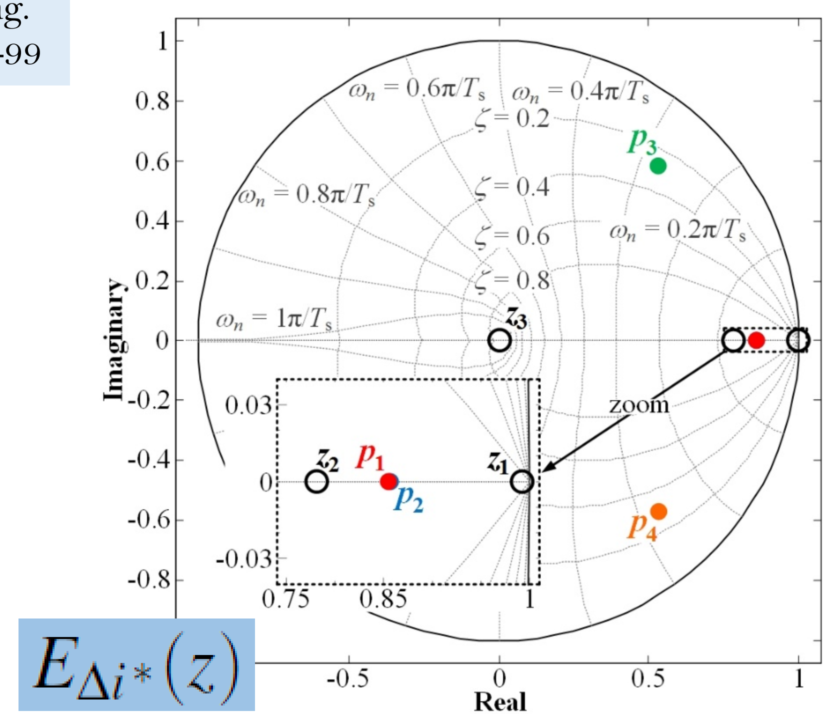

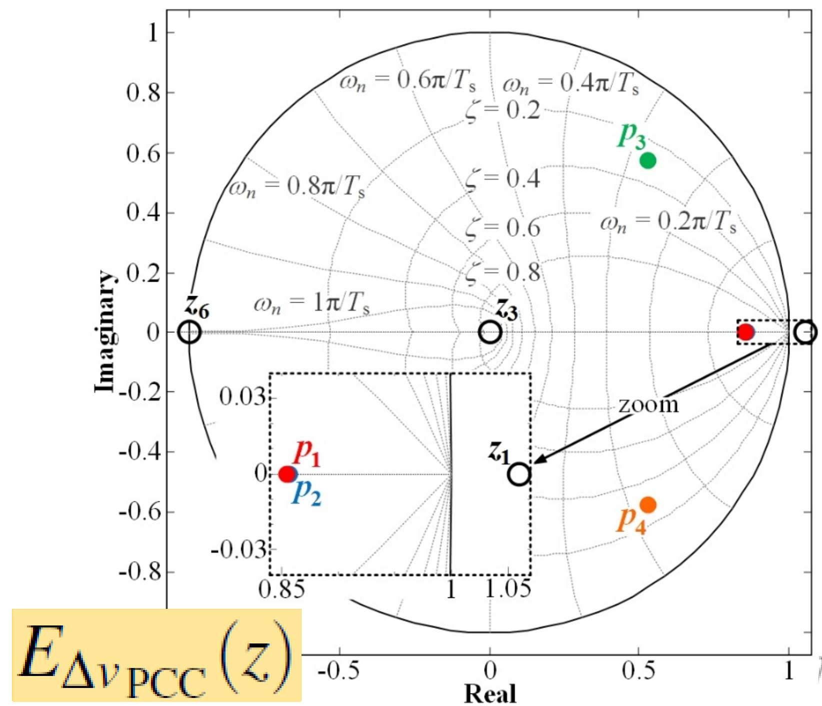

Experimental Setup

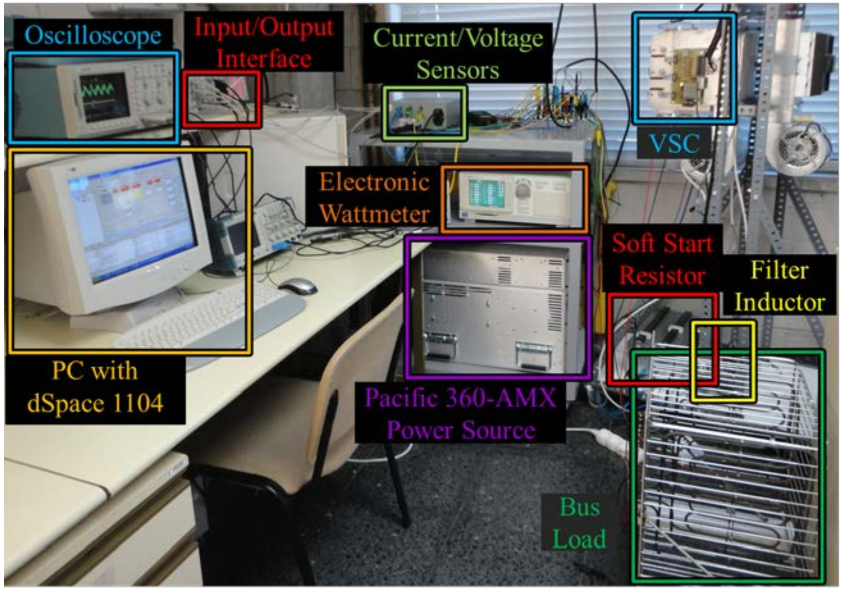

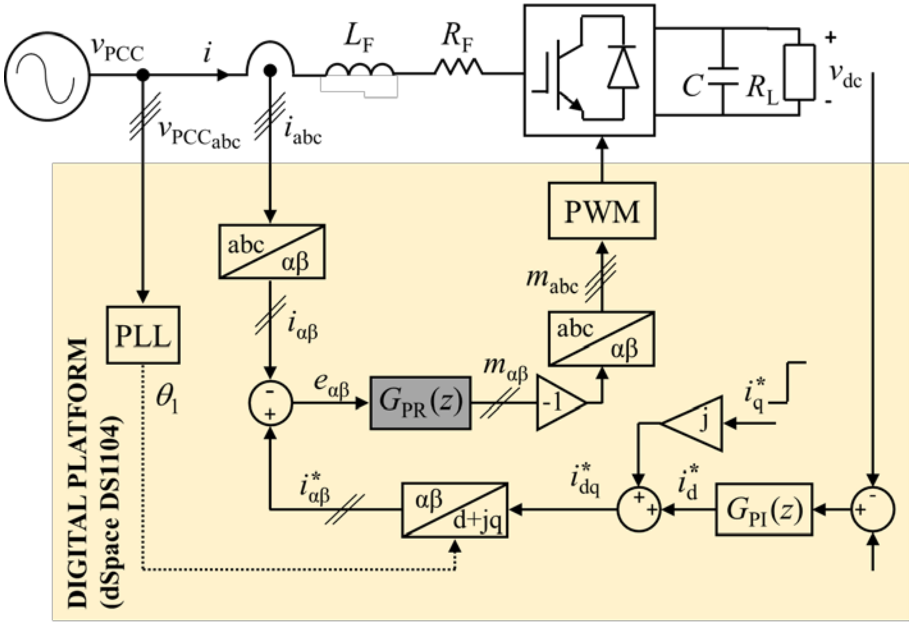

- VSC working as a rectifier.
- Control implemented in dSpace DS1104.
- The Pacific 360-AMX 3-ph linear power source is used to supply the ac voltages and to program the voltage sags.
- i_q^* is set manually to perform transients in the current reference.
- i_d^* is set through an outer loop which controls v_{dc}.

Pag. 100, 101

A. PR Controller Tuned at f_1. High f_s (10 kHz)

$K_{I_1} = 2000$ | $K_{I_1} = 17645$

$E_{\Delta i^*}(z)$

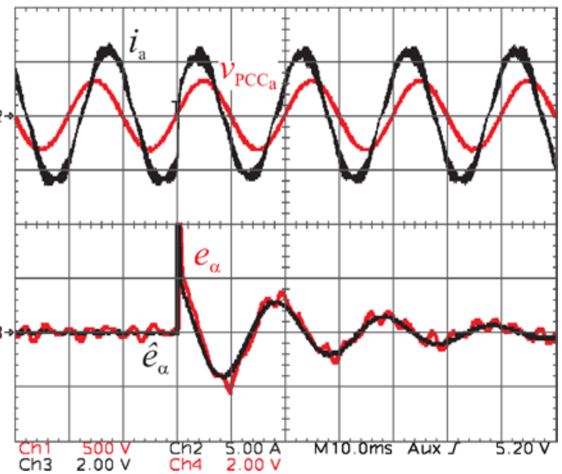

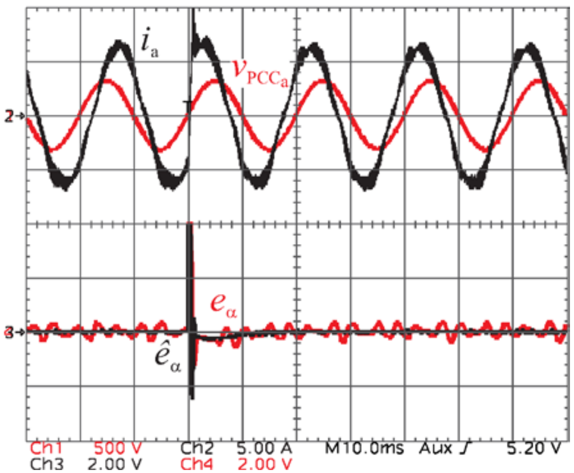

$E_{\Delta v_{PCC}}(z)$

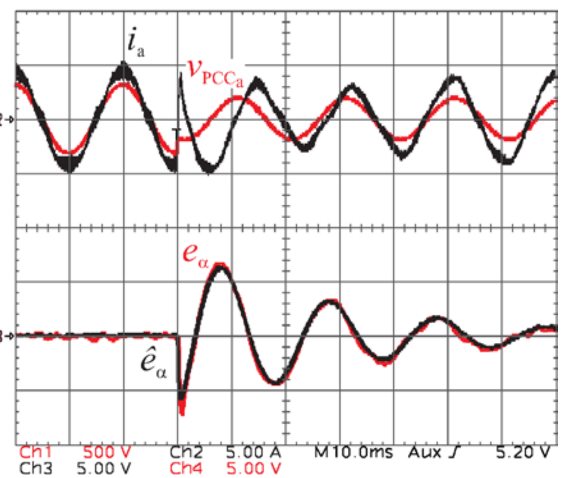

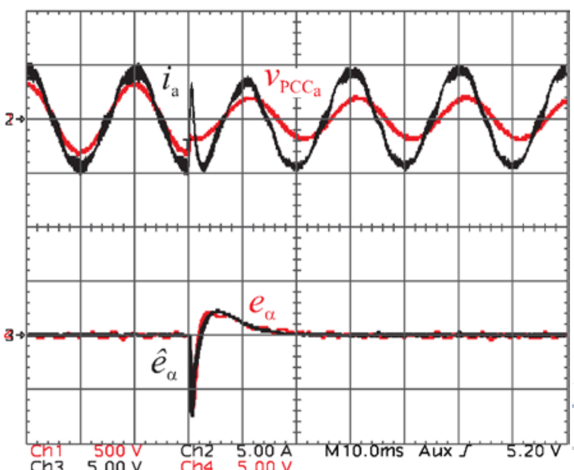

Pag. 101-104

APET
Universidade Vigo

A. PR Controller Tuned at f_1. High f_s (10 kHz)

$K_{I_1} = 34000$ | $K_{I_1} = 100000$

$E_{\Delta i^*}(z)$

$E_{\Delta v_{PCC}}(z)$

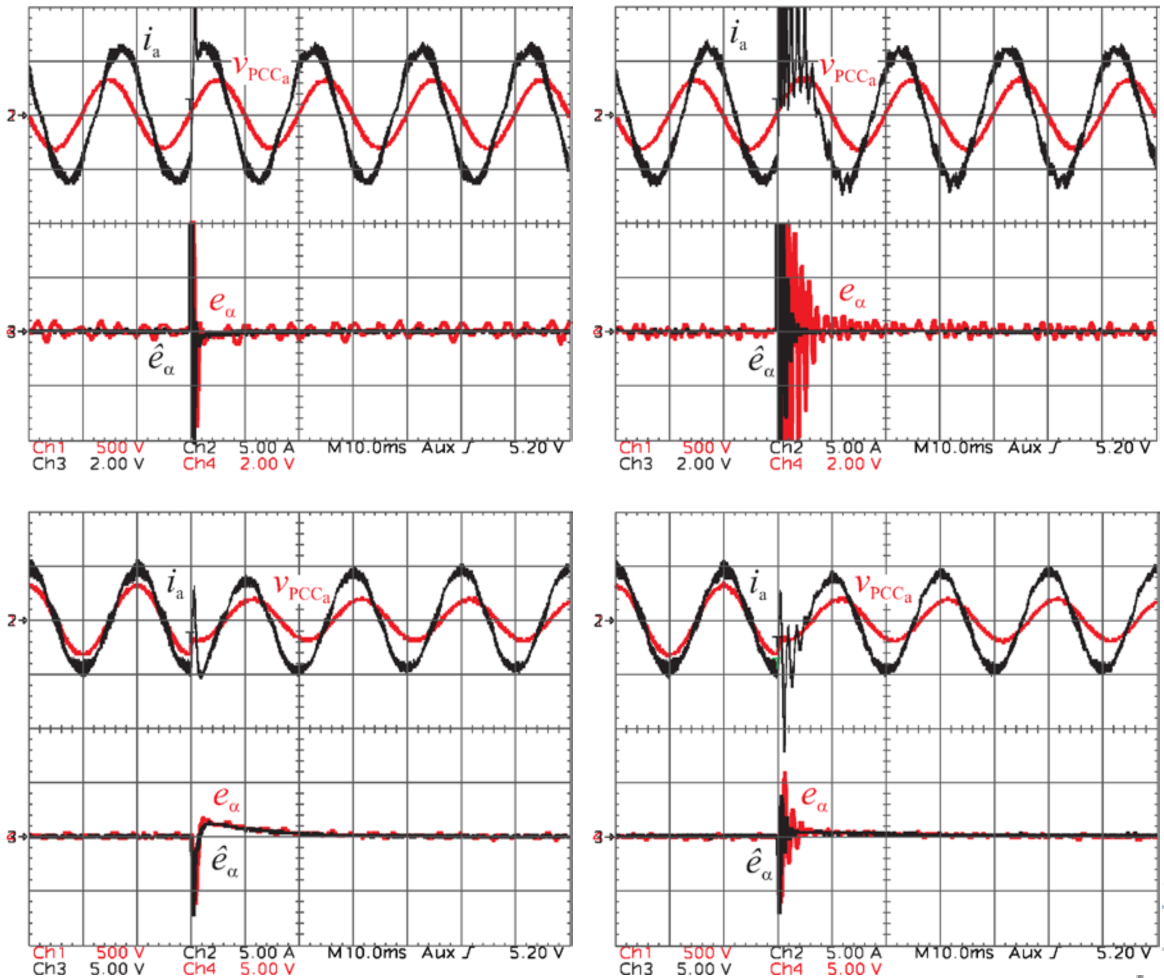

Pag. 101-104

B. PR Controller Tuned at f_1, f_5 and f_7. High f_s (10 kHz)

$K_{I_5} = K_{I_7} = 2000$ | $K_{I_5} = K_{I_7} = 17645$

$E_{\Delta i^*}(z)$

$E_{\Delta v_{PCC}}(z)$

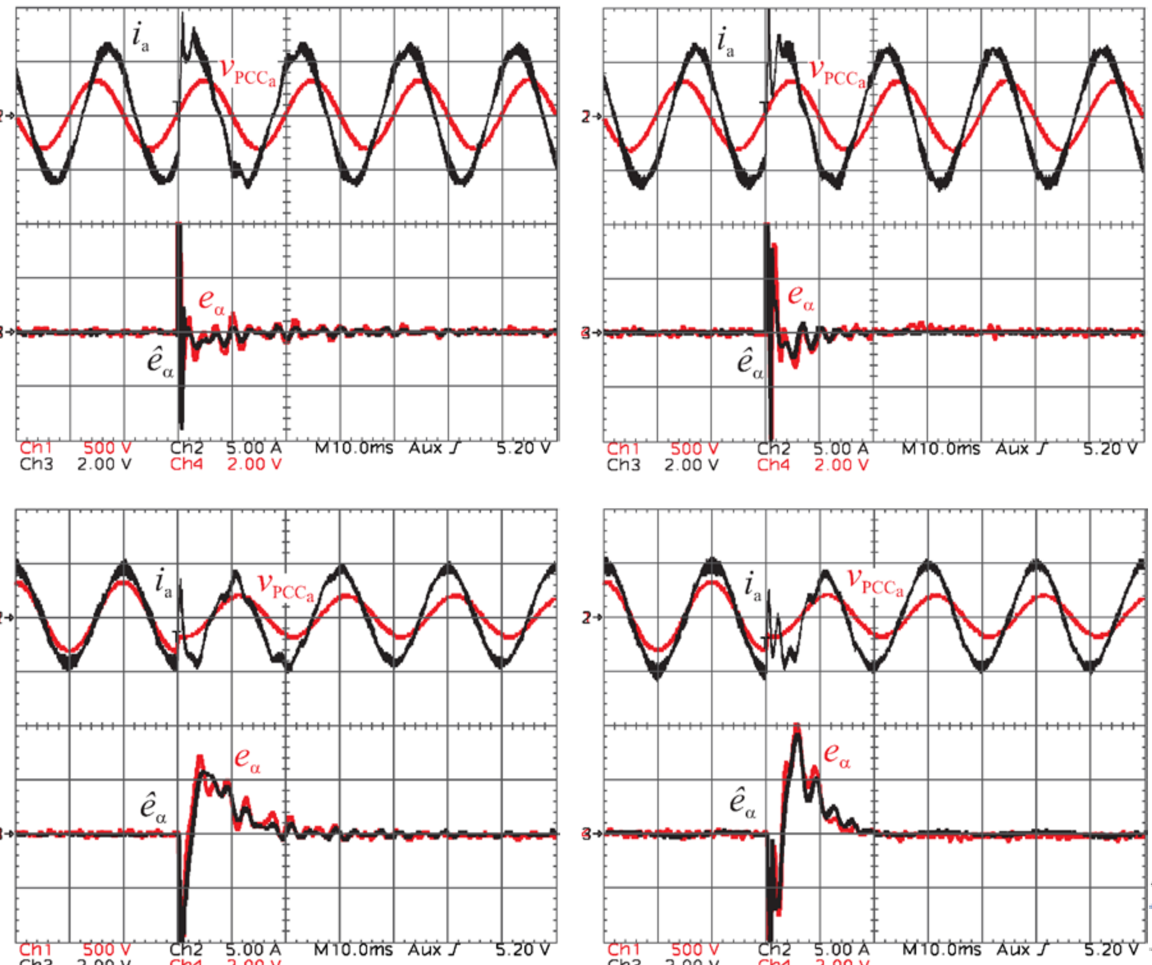

Pag. 105, 106

C. PR Controller Tuned at f_1. Low f_s (2.5 kHz)

$K_{I_1} = 5262$

$E_{\Delta i^*}(z)$

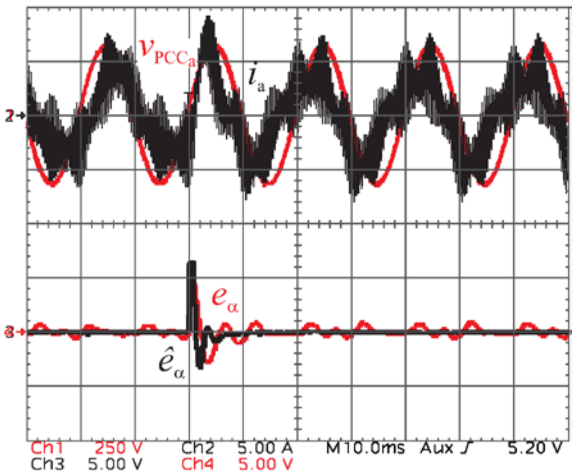

$E_{\Delta v_{PCC}}(z)$

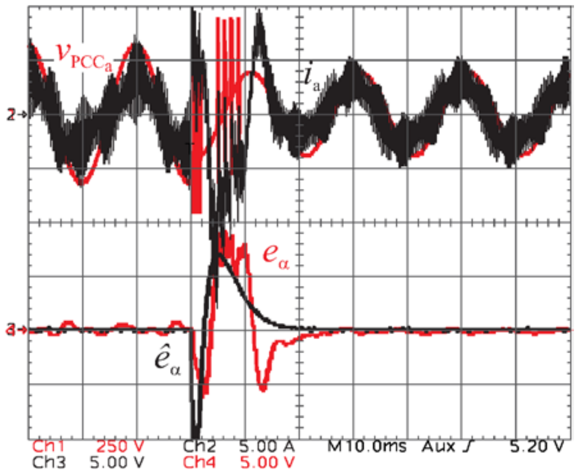

Pag. 106, 107

APET
Universidade Vigo

Conclusions of Chapter 4

- A **methodology to assess** and **optimize** the **transient response** of **PR controllers** has been developed. It is **based on** the **accurate modeling** (including the delay effects) **and study** of the **error** signal **roots caused** either by
  - **Transients** in the **current reference**
  - **Changes** in the **disturbance** (voltage sags at the PCC).
- **Different** significant situations considering very **demanding scenarios** have been **analyzed** and **tested**.
- **Optimal gains** result from a **tradeoff** between the **two types of transients**, in **favor** of the most critical one, which is the **disturbance** one.
- It is concluded that **precisely tuned PR controllers** are a **suitable** option to **fulfill** the **GC** requirements in terms of **transient response.**

Pag. 106-108

Outline

APET
Universidade Vigo

Framework

- **VPI controllers** are **alternative resonant regulators** to PR ones.
- Some works prove **they could provide higher stability margins** than PR ones and hence, **more damped responses**.
- **Studies** about the utilization of **VPI controllers** for **current control** in **renewable energy applications** are **lacking**. There is **not a methodology** for VPI controller **tuning oriented** to the **transient response optimization** of command tracking and disturbance rejection.

APET Universidade Vigo

Framework

- **VPI controllers** are **alternative resonant regulators** to PR ones.
- Some works prove **they could provide higher stability margins** than PR ones and hence, **more damped responses**.
- **Studies** about the utilization of **VPI controllers** for **current control** in **renewable energy applications** are **lacking**. There is **not a methodology** for VPI controller **tuning oriented** to the **transient response optimization** of command tracking and disturbance rejection.

Pag. 109, 110

- **Application to VPI controllers** of the **methodology** described in **Chapter 4.**
- **Comparison between PR and VPI controllers.**

Methodology & Tests

1st step: **Discrete-time expression of the global error.**

2nd step: **Graphical representation of the error signal roots as a function of the controller gain → Root loci.**

3rd step: **Accurate prediction of the error waveform.**

4th step: **Gain tuning.**

Four control situations:

- A. Resonant filters tuned at f_1. High sampling frequency (f_s = 10 kHz).
- B. Resonant filters tuned at f_1, f_5 and f_7. High sampling frequency (f_s = 10 kHz).
- C. Resonant filters tuned at f_1. Low sampling frequency (f_s = 2.5 kHz).
- D. Effect of a feed-forward path.

Pag. 110-112

Two transients:

- I. Transients in the current reference: a phase change of 90º in i^*. $\Delta i^*(z)$
- II. Transients in the disturbance: a type 'C' sag in v_{PCC}. $\Delta v_{PCC}(z)$

A. VPI Controller Tuned at f_1. High f_s (10 kHz)

2nd step: **Graphical representation of the error signal roots as a function of the controller gain → Root loci.**

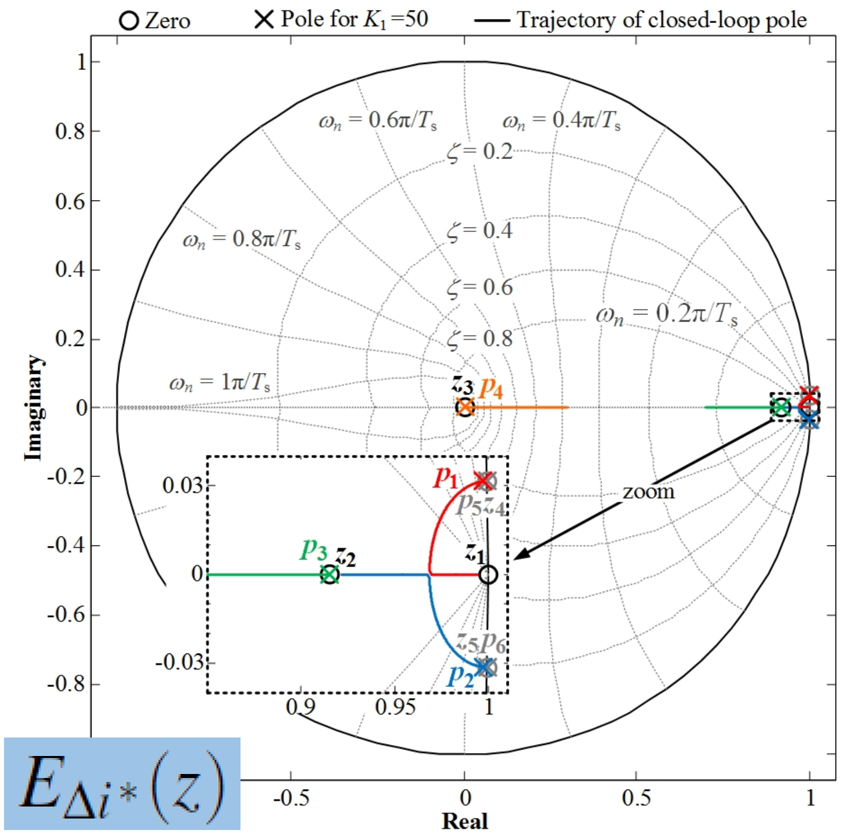

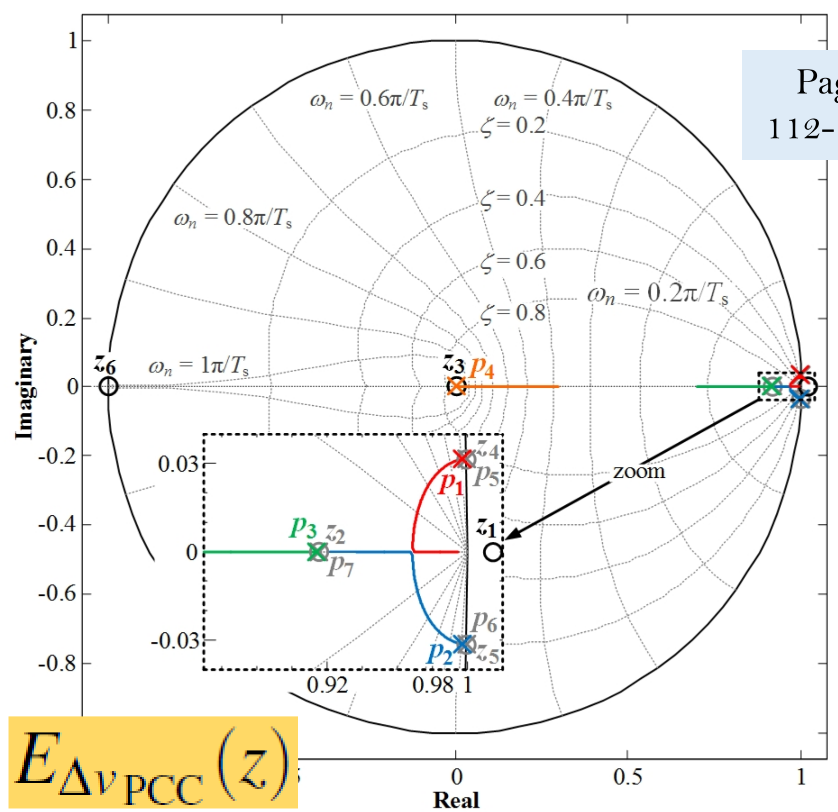

Pag. 112-115

A. VPI Controller Tuned at f_1. High f_s (10 kHz)

3rd step: **Analysis of the effects of the root position on the transient response.**

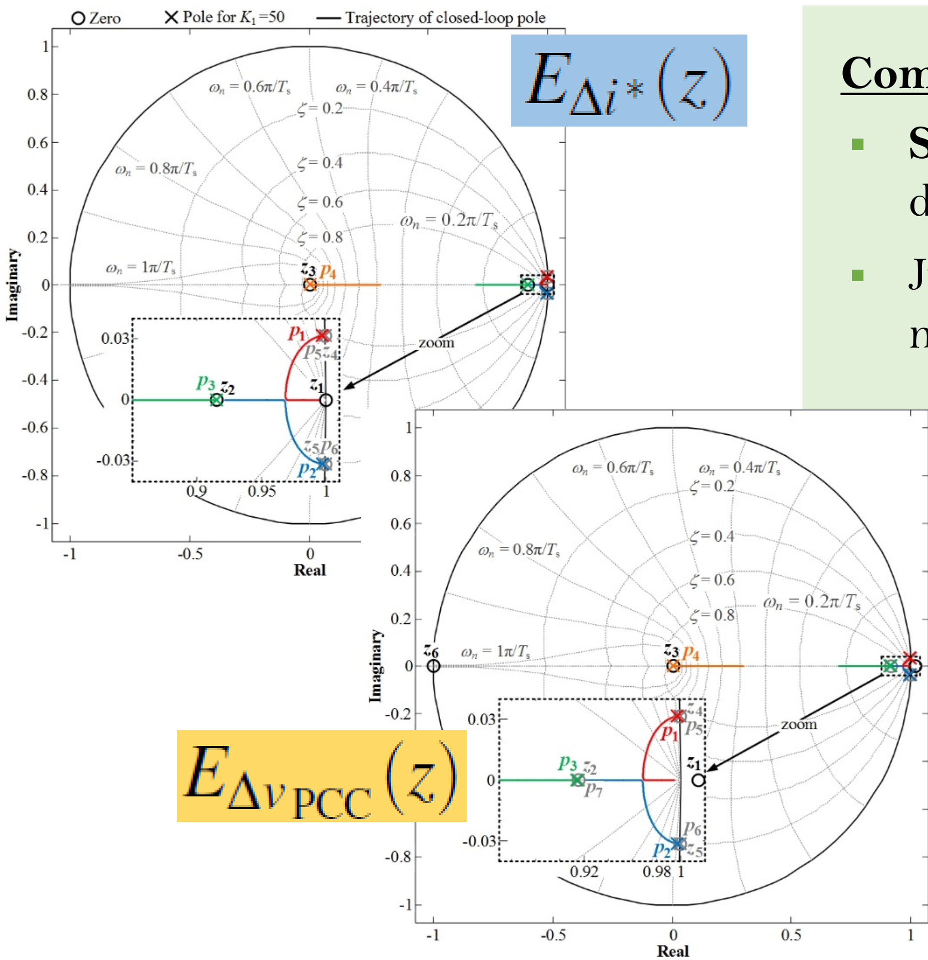

Comparing with the analysis of the PR controller:

- **Same number** of **roots** (numerators and denominators of the same order).
- Just the roots that depend on the controller numerator are different → p_1, p_2, p_3 & p_4
  - **p_1 & p_2 (dominant poles): behave similarly** with an increasing gain.
  - **p_3 & p_4: behave differently**.

PR controller → **Complex**
VPI controller → **Real; plant dynamics cancellation**

Pag. 112-115

$p_3 \leftarrow z_2$
$p_4 \leftarrow z_3$

A. VPI Controller Tuned at f_1. High f_s (10 kHz)

3rd step: **Analysis of the effects of the root position on the transient response.**

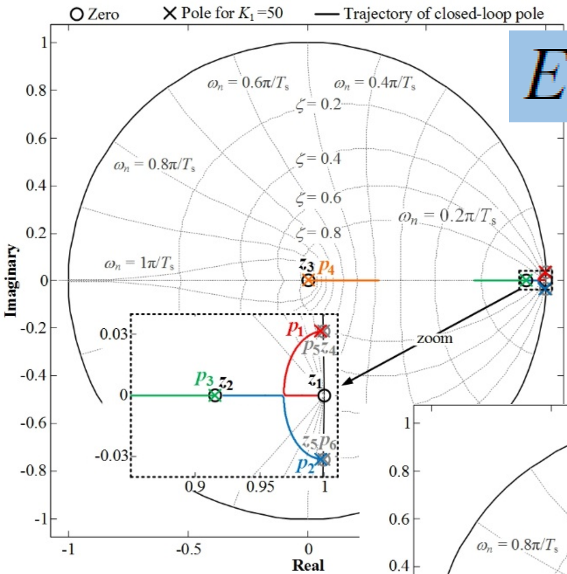

$E_{\Delta i^*}(z)$

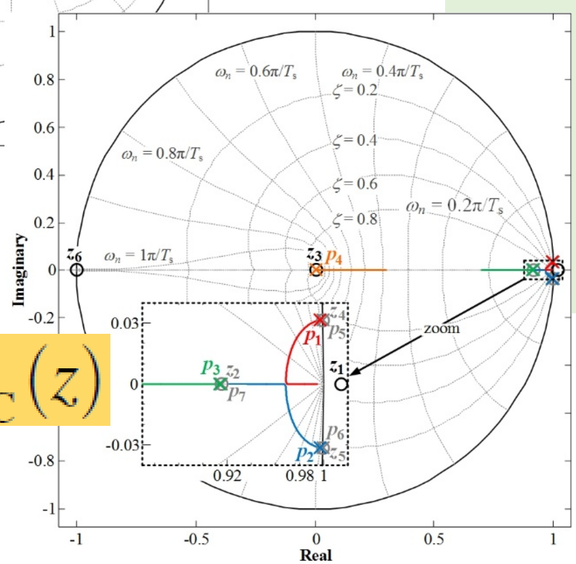

$E_{\Delta v_{PCC}}(z)$

Comparing with the analysis of the PR controller:

- **Same number** of **roots** (numerators and denominators of the same order).
- Just the roots that depend on the controller numerator are different → p_1, p_2, p_3 & p_4
  - p_1 **&** p_2 **(dominant poles): behave similarly** with an increasing gain.
  - p_3 **&** p_4**: behave differently**.

PR controller → **Complex**
VPI controller → **Real; plant dynamics cancellation**

Pag. 112-115

$p_3 \leftarrow z_2$
$p_4 \leftarrow z_3$

4th step:

Gain tuning. → $K_1 \leftarrow p_1 = p_2$

APET Universidade de Vigo

A. Resonant Controllers Tuned at f_1. High f_s (10 kHz)

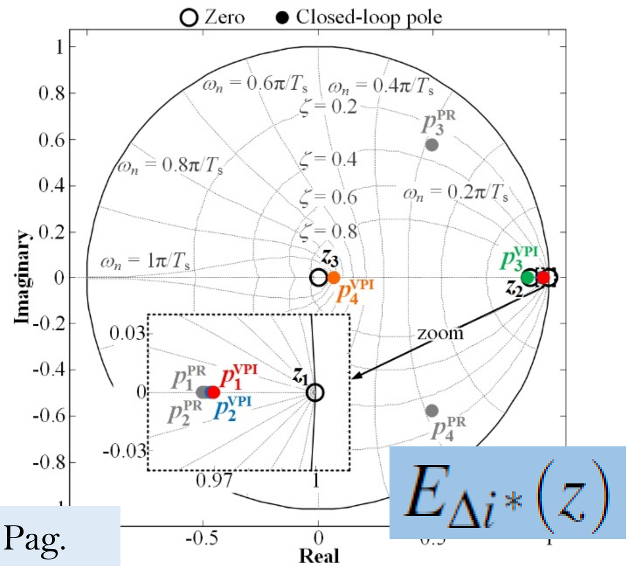

Pag. 112-115

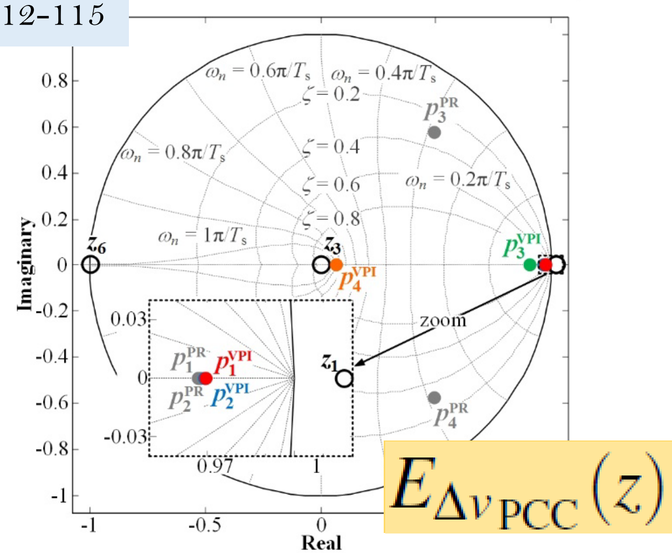

Pole position (decay rate)

- p_1 **&** p_2 **(dominant poles)** → **slower** with the VPI controller
- p_3 & p_4 → p_3 **slower** and p_4 **faster** with the VPI controller

Residues in the reference change (damping)

- p_1 **&** p_2 **(dominant poles)** → **bigger residues** with the VPI controller
- p_3 **&** p_4 → **smaller residues** with the VPI controller

Residues in the disturbance change (damping)

- p_1, p_2 **&** p_3 → **larger residues** with the VPI controller
- p_4 → **smaller residues** with the VPI controller

B. Resonant Controllers Tuned at f_1, f_5 & f_7. High f_s (10 kHz)

- **Adding** more **resonant filters** with high gains **affects the position** of the dominant **poles** p_1 & p_2, as well as those of p_3 & p_4 with both controllers → **Smaller values** of K_{I_1} and K_1 **are needed** to achieve $p_1 = p_2$.
- For p_1, p_2, p_3 & p_4, the conclusions are the same as in the previous case.
- For **the additional poles**, the **differences** are **marginal**.

Pag. 115, 116

C. Resonant Controllers Tuned at f_1. Low f_s (2.5 kHz)

- **As f_s decreases,** the **delay effects** caused by the **discrete-time implementation** become **more noticeable.** The **discretization method** applied to the resonant controllers **affects the system dynamics**. → The **best option** is **assessed**.
- **More similarities** in the root loci of **both controllers at this f_s**.
  - The **dominant poles** p_1 & p_2 are **slightly faster with the PR controller** → slightly faster reference tracking and disturbance rejection responses.
  - **Smaller residues** of the dominant poles with the PR controller → **smaller overshoot**.
  - Initial high-frequency oscillations in the **reference change** with the PR controller (due to **larger residues of p_3 & p_4**) → it will **increase the overshoot**.

Pag. 116-118

B. Resonant Controllers Tuned at f_1, f_5 & f_7. High f_s (10 kHz)

- **Adding** more **resonant filters** with high gains **affects the position** of the dominant **poles** p_1 & p_2, as well as those of p_3 & p_4 with both controllers → **Smaller values** of K_{I_1} and K_1 **are needed** to achieve $p_1 = p_2$.
- For p_1, p_2, p_3 & p_4, the conclusions are the same as in the previous case.
- For **the additional poles**, the **differences** are **marginal**.

Pag. 115, 116

C. Resonant Controllers Tuned at f_1. Low f_s (2.5 kHz)

- **As f_s decreases,** the **delay effects** caused by the **discrete-time implementation** become **more noticeable.** The **discretization method** applied to the resonant controllers **affects the system dynamics.**→ The **best option** is **assessed**.
- **More similarities** in the root loci of **both controllers at this f_s**.
  - The **dominant poles** p_1 & p_2 are **slightly faster with the PR controller** → slightly faster reference tracking and disturbance rejection responses.
  - **Smaller residues** of the dominant poles with the PR controller → **smaller overshoot**.
  - Initial high-frequency oscillations in the **reference change** with the PR controller (due to **larger residues of p_3 & p_4**) → it will **increase the overshoot**.

Pag. 116-118

Experimental Setup

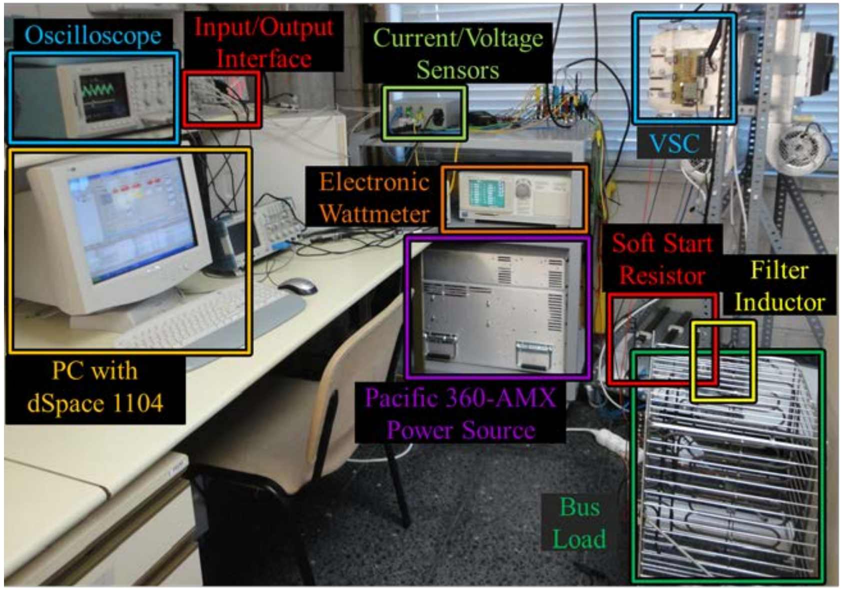

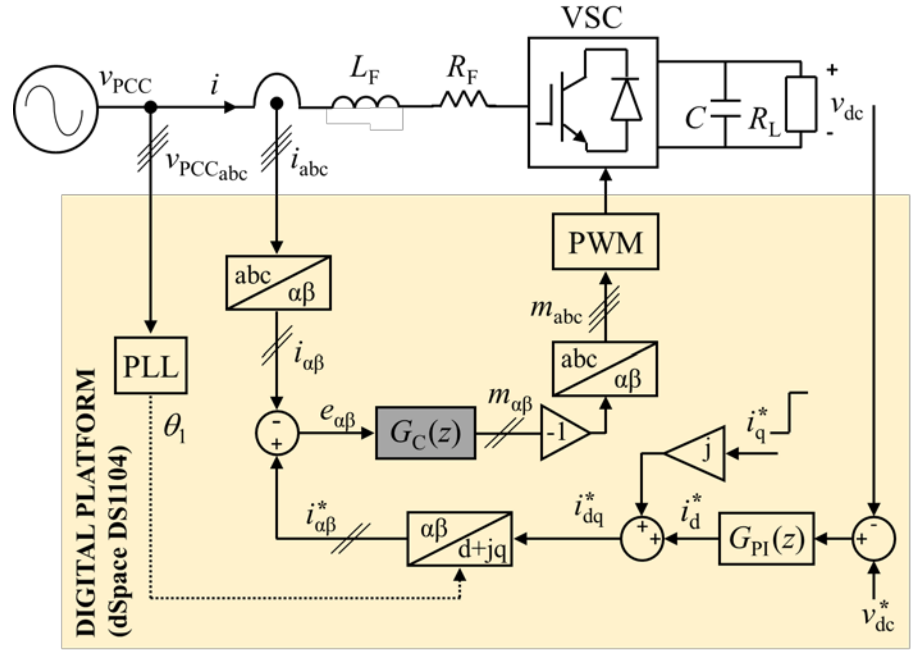

- VSC working as a rectifier.
- Control implemented in dSpace DS1104.
- The Pacific 360-AMX 3-ph linear power source is used to supply the ac voltages and to program the voltage sags.
- i_q^* is set manually to perform transients in the current reference.
- i_d^* is set through an outer loop which controls v_{dc}.

Pag. 119-121

A. Resonant Controllers Tuned at f_1. High f_s (10 kHz)

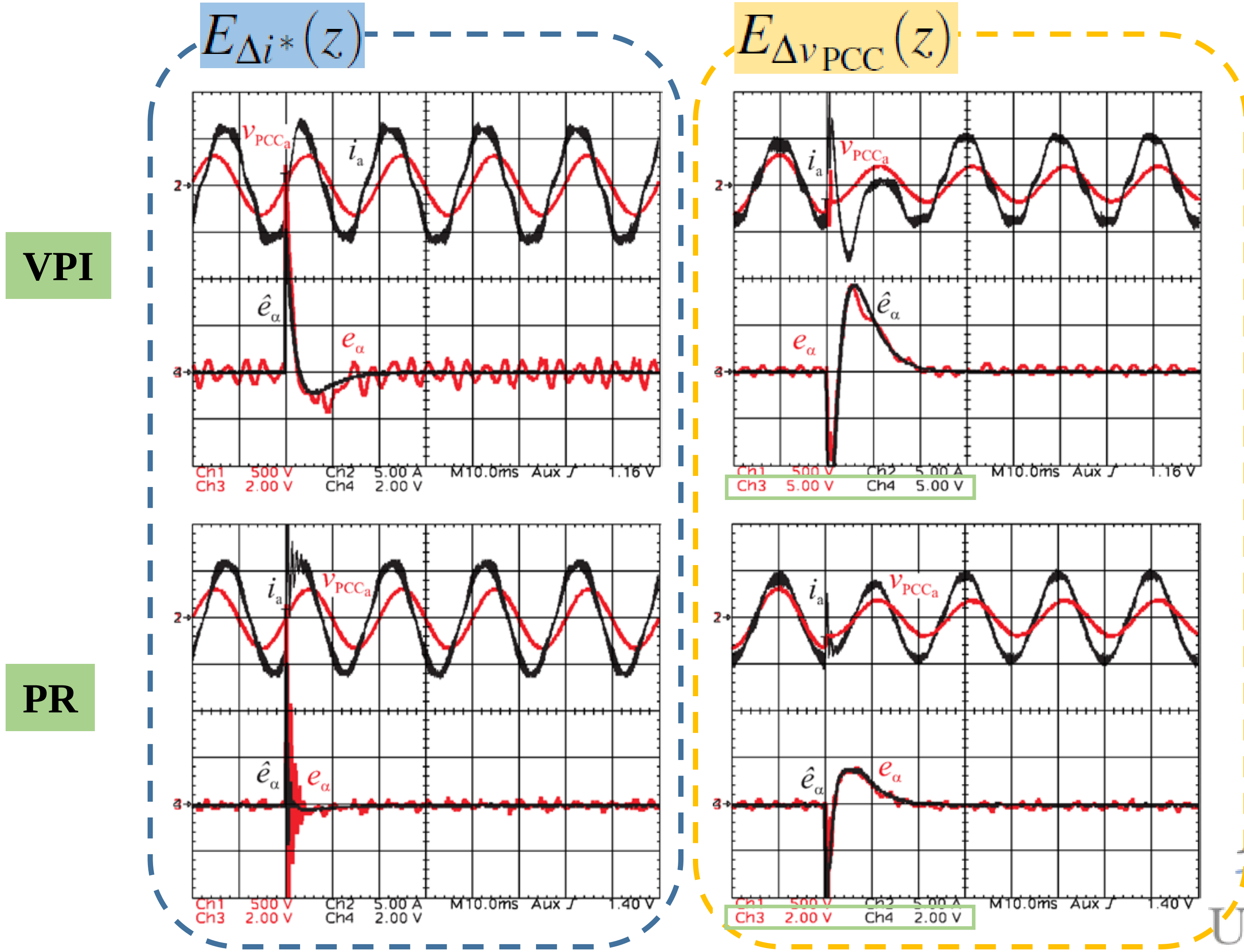

Pag. 121-125

B. Resonant Controllers Tuned at f_1, f_5 and f_7. High f_s (10 kHz)

VPI

PR

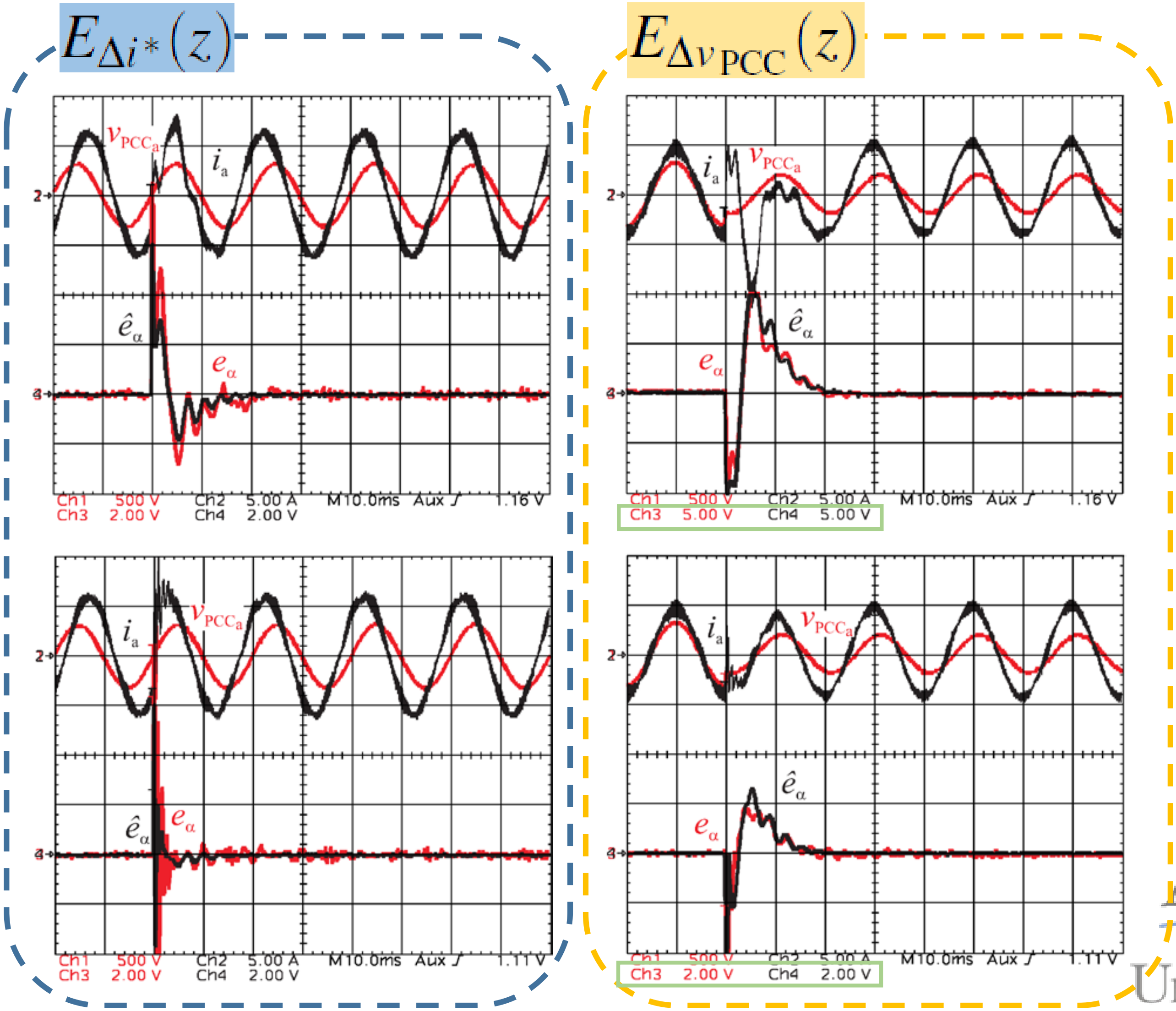

Pag.
121-125

APET
Universidade Vigo

C. Resonant Controllers Tuned at f_1. Low f_s (2.5 kHz)

VPI

PR

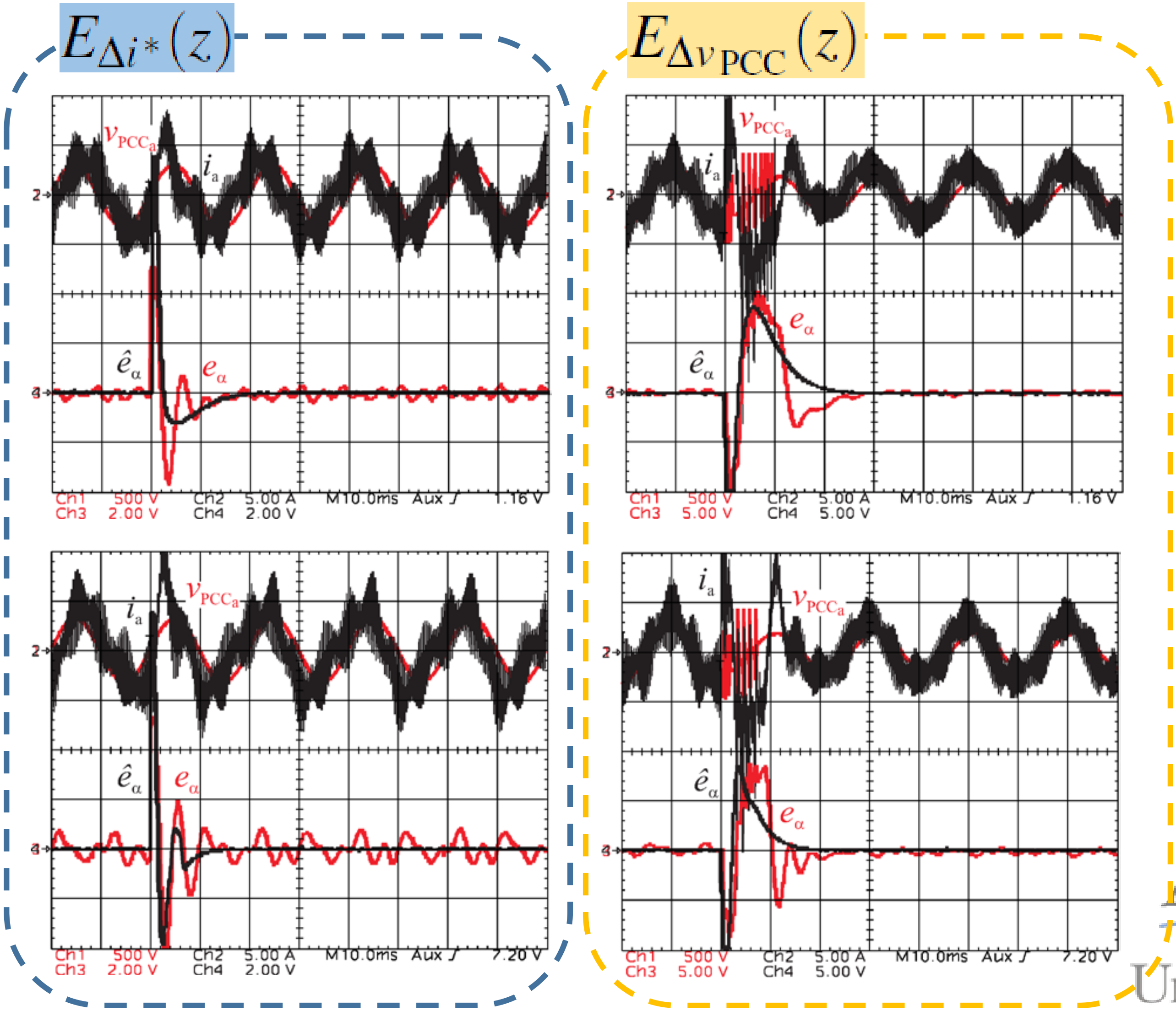

Pag. 121-125

APET Universida de Vigo

D. THD Analysis

A. f_s=10 kHz; without harmonic compensation

B. f_s=10 kHz; with harmonic compensation

C. f_s=2.5 kHz; without harmonic compensation

VPI

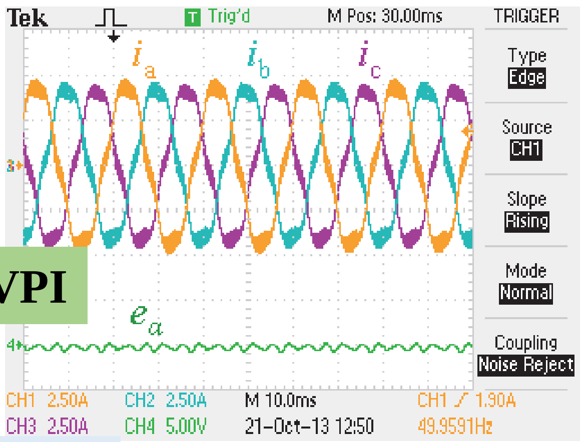

THD = 8.29 %

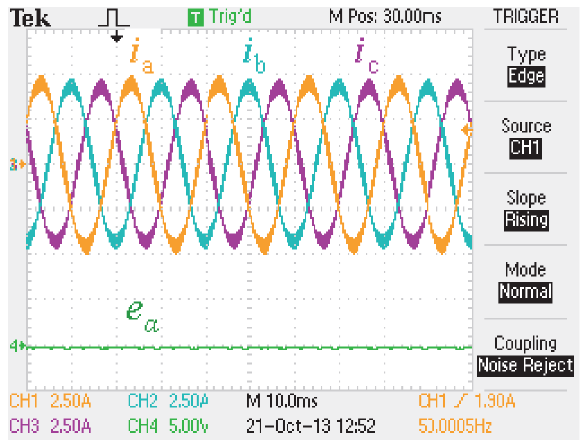

THD = 1.10 %

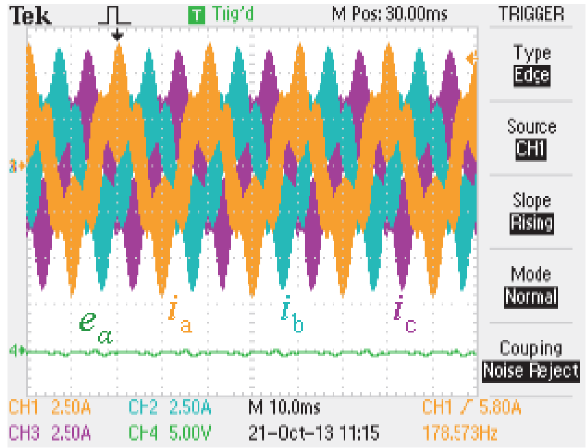

THD = 4.75 %

Pag. 125-128

PR

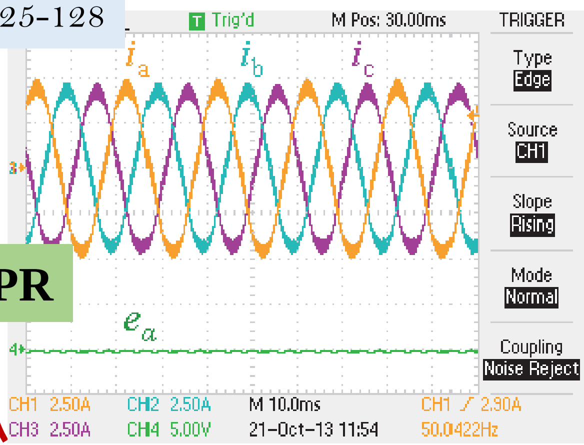

THD = 2.65 %

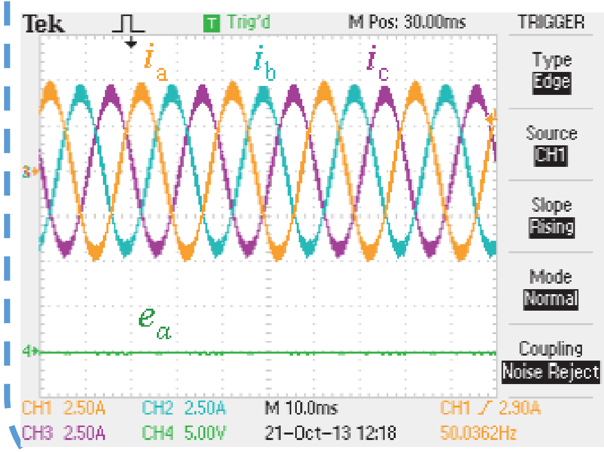

THD = 0.92 %

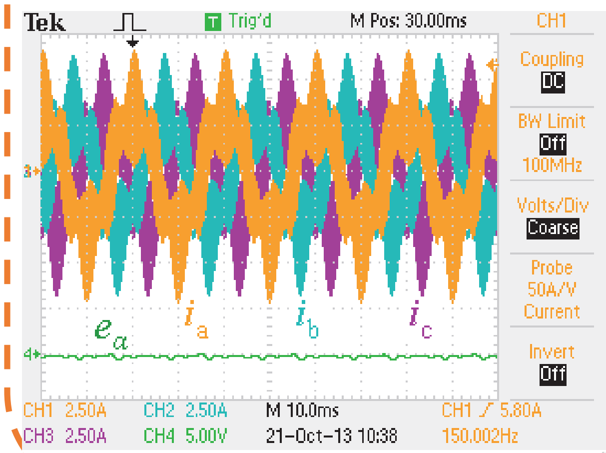

THD = 4.63 %

Controller	f_s	h	THD	Reference change		Disturbance change	
				Overshoot	Set. time	Overshoot	Set. time
VPI	10 kHz	1	8.29 %	14 %	17 ms	8.6 A	27 ms
PR	10 kHz	1	2.65 %	28 %	9 ms	4.4 A	20 ms
VPI	10 kHz	1, 5, 7	1.10 %	49 %	16 ms	8.8 A	26 ms
PR	10 kHz	1, 5, 7	0.92 %	57 %	12 ms	4.4 A	19 ms
VPI	2.5 kHz	1	4.75 %	13 %	16 ms	12.1 A	28 ms
PR	2.5 kHz	1	4.63 %	40 %	10 ms	10.9 A	22 ms

Pag.
121-128

Controller	f_s	h	THD	Reference change		Disturbance change	
				Overshoot	Set. time	Overshoot	Set. time
VPI	10 kHz	1	8.29 %	14 %	17 ms	8.6 A	27 ms
PR	10 kHz	1	2.65 %	28 %	9 ms	4.4 A	20 ms
VPI	10 kHz	1, 5, 7	1.10 %	49 %	16 ms	8.8 A	26 ms
PR	10 kHz	1, 5, 7	0.92 %	57 %	12 ms	4.4 A	19 ms
VPI	2.5 kHz	1	4.75 %	13 %	16 ms	12.1 A	28 ms
PR	2.5 kHz	1	4.63 %	40 %	10 ms	10.9 A	22 ms

Pag.
121-128

APET
Universidade Vigo

Controller	f_s	h	THD	Reference change		Disturbance change	
				Overshoot	Set. time	Overshoot	Set. time
VPI	10 kHz	1	8.29 %	14 %	17 ms	8.6 A	27 ms
PR	10 kHz	1	2.65 %	28 %	9 ms	4.4 A	20 ms
VPI	10 kHz	1, 5, 7	1.10 %	49 %	16 ms	8.8 A	26 ms
PR	10 kHz	1, 5, 7	0.92 %	57 %	12 ms	4.4 A	19 ms
VPI	2.5 kHz	1	4.75 %	13 %	16 ms	12.1 A	28 ms
PR	2.5 kHz	1	4.63 %	40 %	10 ms	10.9 A	22 ms

Pag.
121-128

Controller	f_s	*h*	THD	Reference change		Disturbance change	
				Overshoot	Set. time	Overshoot	Set. time
VPI	10 kHz	1	8.29 %	14 %	17 ms	8.6 A	27 ms
PR	10 kHz	1	2.65 %	28 %	9 ms	4.4 A	20 ms
VPI	10 kHz	1, 5, 7	1.10 %	49 %	16 ms	8.8 A	26 ms
PR	10 kHz	1, 5, 7	0.92 %	57 %	12 ms	4.4 A	19 ms
VPI	2.5 kHz	1	4.75 %	13 %	16 ms	12.1 A	28 ms
PR	2.5 kHz	1	4.63 %	40 %	10 ms	10.9 A	22 ms

Pag.
121-128

Controller	f_s	***h***	**THD**	**Reference change**		**Disturbance change**	
				Overshoot	Set. time	Overshoot	Set. time
VPI	10 kHz	1	8.29 %	14 %	17 ms	8.6 A	27 ms
PR	10 kHz	1	2.65 %	28 %	9 ms	4.4 A	20 ms
VPI	10 kHz	1, 5, 7	1.10 %	49 %	16 ms	8.8 A	26 ms
PR	10 kHz	1, 5, 7	0.92 %	57 %	12 ms	4.4 A	19 ms
VPI	2.5 kHz	1	4.75 %	13 %	16 ms	12.1 A	28 ms
PR	2.5 kHz	1	4.63 %	40 %	10 ms	10.9 A	22 ms

Pag.
121-128

Controller	f_s	h	THD	Reference change		Disturbance change	
				Overshoot	Set. time	Overshoot	Set. time
VPI	10 kHz	1	8.29 %	14 %	17 ms	8.6 A	27 ms
PR	10 kHz	1	2.65 %	28 %	9 ms	4.4 A	20 ms
VPI	10 kHz	1, 5, 7	1.10 %	49 %	16 ms	8.8 A	26 ms
PR	10 kHz	1, 5, 7	0.92 %	57 %	12 ms	4.4 A	19 ms
VPI	2.5 kHz	1	4.75 %	13 %	16 ms	12.1 A	28 ms
PR	2.5 kHz	1	4.63 %	40 %	10 ms	10.9 A	22 ms

Pag.
121-128

APET
Universidade Vigo

Controller	f_s	h	THD	Reference change		Disturbance change	
				Overshoot	Set. time	Overshoot	Set. time
VPI	10 kHz	1	8.29 %	14 %	17 ms	8.6 A	27 ms
PR	10 kHz	1	2.65 %	28 %	9 ms	4.4 A	20 ms
VPI	10 kHz	1, 5, 7	1.10 %	49 %	16 ms	8.8 A	26 ms
PR	10 kHz	1, 5, 7	0.92 %	57 %	12 ms	4.4 A	19 ms
VPI	2.5 kHz	1	4.75 %	13 %	16 ms	12.1 A	28 ms
PR	2.5 kHz	1	4.63 %	40 %	10 ms	10.9 A	22 ms

Pag.
121-128

APET
Universidade Vigo

Controller	f_s	h	THD	Reference change		Disturbance change	
				Overshoot	Set. time	Overshoot	Set. time
VPI	10 kHz	1	8.29 %	14 %	17 ms	8.6 A	27 ms
PR	10 kHz	1	2.65 %	28 %	9 ms	4.4 A	20 ms
VPI	10 kHz	1, 5, 7	1.10 %	49 %	16 ms	8.8 A	26 ms
PR	10 kHz	1, 5, 7	0.92 %	57 %	12 ms	4.4 A	19 ms
VPI	2.5 kHz	1	4.75 %	13 %	16 ms	12.1 A	28 ms
PR	2.5 kHz	1	4.63 %	40 %	10 ms	10.9 A	22 ms

Pag.
121-128

Controller	f_s	h	**THD**	**Reference change**		**Disturbance change**	
				Overshoot	Set. time	Overshoot	Set. time
VPI	10 kHz	1	8.29 %	14 %	17 ms	8.6 A	27 ms
PR	10 kHz	1	2.65 %	28 %	9 ms	4.4 A	20 ms
VPI	10 kHz	1, 5, 7	1.10 %	49 %	16 ms	8.8 A	26 ms
PR	10 kHz	1, 5, 7	0.92 %	57 %	12 ms	4.4 A	19 ms
VPI	2.5 kHz	1	4.75 %	13 %	16 ms	12.1 A	28 ms
PR	2.5 kHz	1	4.63 %	40 %	10 ms	10.9 A	22 ms

Pag. 121-130

- **Effect** of a **Feed Forward** on the **Disturbance Rejection Response**
  - At **high** f_s (10 kHz) → **significant** improvement in overshoot & settling time.
  - At **low** f_s (2.5 kHz) → improvement in overshoot & **insignificant** improvement in settling time.

- **Effect** of the **PLL** on the **Disturbance Rejection Response**
  - In principle, it might have a certain impact: transient in v_{dc} error in the outer loop & transitory increase in the error.
  - Evaluation → **scarce** influence.

Conclusions of Chapter 5

- This chapter **studies** the **convenience of VPI controllers** use when **fast transient responses** are **demanded**:
  - For new **reference tracking**
  - For **disturbance rejection**

Pag. 130-132

- The **transient response** of the current loop is **assessed** by means of the **error signal roots** following the **methodology** proposed in the **previous chapter**.
- Different significant situations considering very **demanding scenarios** have been **analyzed and tested for the VPI controller** and **compared with those obtained with the PR one**.
  - At **high f_s, VPI controllers** lead to **longer settling times** than PR ones**, for both reference and disturbance changes** and also to a **higher THD**.
  - **At f_s = 2.5 kHz**, the root loci of both controllers, and accordingly, their transient responses, present **more similarities**, although the **PR regulator is faster**. The **THD** is **similar**.
- However, **as the sampling frequency decreases**, the **VPI controller** becomes an **interesting alternative** to the PR one: its transient response **can be optimized** at lower sampling frequencies **without risking the stability**.

Outline

1. Introduction
2. Equivalent Loss Resistance Estimation of Grid-Tied Converters for Current Control Analysis and Design
3. A Method for Identification of the Equivalent Inductance and Resistance in the Plant Model of Current-Controlled Grid-Tied Converters
4. Assessment and Optimization of the Transient Response of Proportional-Resonant Current Controllers for Distributed Power Generation Systems
5. Transient Response Evaluation of Stationary-Frame Resonant Current Controllers for Grid-Connected Applications
6. Conclusions and Future Research
   - Conclusions
   - Future Research

APET
Universidade Vigo

Conclusions

- It is demonstrated that **a precise knowledge of *L* and *R*** (which includes the converter losses) **is essential to guarantee the performance of the current loop** (particularly when specifications are stablished in terms of transient response). **Closed-loop identification methods**, able to work either **offline or online**, are developed. These methods are also **valid** when **LCL filters** are employed.
- A **methodology to assess and optimize** the **transient response of PR controllers** is proposed, oriented to **fulfilling** the **LVRT (disturbance rejection)** and **grid-support (command tracking)** requirements **from GCs**. A **criterion** for **gain tuning** is developed according to the observations.
- A **comparison between** the **transient response of PR and VPI controllers** is presented, aimed at evaluating the suitability of the latter in grid-tied applications. Their **THD** is also assessed, as well as the **effects of the feedforward and of the PLL** on the **disturbance rejection response**.

Pag. 133, 134

APET Universidade Vigo

Future Research

- Study of **the VSC equivalent loss resistance at different frequencies**, from the control point of view. Analysis from the control viewpoint of the **correlation between the VSC equivalent loss resistance and the voltage drops** caused by dead times, the voltage drops in the transistors, etc.
- Development of a **tuning method to optimize the transient response of the current loop at very low ratios between the sampling and fundamental frequencies**. The **complete** transfer function of the **plant admittance** in case of **LCL** filters would be employed.
- Analysis of the different **effects** (positive and negative) **of adding an "active resistance"** in order **to improve the disturbance rejection capability.**
- Study of the **interactions between the outer control** of the PCC voltage **and the inner current one**.

Pag.
134, 135

APET
Universidade Vigo

Transient Response Analysis and Design of Current-Controlled Grid-Tied Converters

Author: *Ana Vidal González*

Supervisors: *Jesús Doval Gandoy & Francisco D. Freijedo Fernández*

Applied Power Electronics Research Group,
University of Vigo

15th May 2015

Dissertation submitted for the degree of Doctor of Philosophy at the University of Vigo
"International Doctor Mention"

APET Applied Power Electronics Technology Research Group

Universidade Vigo